Involvement of acid-sensing ion channels in Na^+ uptake in freshwater fish

by

Agnieszka Karolina Dymowska

A thesis submitted in partial fulfillment of the requirements for the degree of

Doctor of Philosophy

in

Physiology, Cell and Developmental Biology

Department of Biological Sciences
University of Alberta

Abstract

The molecular identity of the Na^+ uptake mechanism across the gills of freshwater fish has been the subject of lively debate for decades. Despite the extensive evidence for NHE mediated Na^+ uptake, thermodynamic constraints on the function of NHEs at low ion concentrations and low environmental pHs suggest that other mechanisms may need to exist in fish species inhabiting such environments. An alternative mechanism, whereby Na^+ enters through an epithelial Na^+ channel (ENaC) was previously proposed. However, efforts to identify ENaC homologues in teleost fishes have not been successful and therefore, alternatives to ENaC needed to be explored. In this thesis, I investigated a possible role for acid-sensing ion channels (ASICs), which are close relatives to ENaCs, to serve as epithelial channels for Na^+ uptake by the gill of freshwater rainbow trout and zebrafish. I cloned *asic1* and *asic4* homologues in the rainbow trout and demonstrated that they are expressed in the gills and isolated mitochondrion-rich cells. Moreover, I demonstrated that six *asic* subunits, *asic1.1*, *1.2*, *1.3*, *2*, *4.1*, and *4.2*, are present in the zebrafish gills. Immunohistochemical analysis using a custom made anti-zASIC4.2 antibody was conducted for both zebrafish adult and larvae, and for rainbow trout. In rainbow trout, double staining with anti-ASIC4.2 and anti-NKA antibodies demonstrated that ASIC4 localizes to NKA-rich MRCs in the gill, whereas in zebrafish adult and larvae, staining with anti-ASIC4.2, anti-VHA, and anti-NKA antibodies and ConcanavalinA revealed that ASIC4.2 localizes to HR MRCs. Furthermore, confocal microscopy demonstrated that in both species, ASIC is found in the apical region of the MRCs. Pharmacological inhibitors of ASICs decreased Na^+ uptake in adult rainbow trout and zebrafish in a dose-dependent manner.

Moreover, knock-down of ASIC4.2 with morpholino oligonucleotide resulted in reduced Na^+ uptake in the morphant zebrafish larvae reared in low Na^+ and low pH medium. Based on the findings in my thesis, I present a revised model for Na^+ uptake in freshwater fish, whereby ASIC4 is proposed as one possible mechanism for Na^+ acquisition in rainbow trout and zebrafish.

This is the first demonstration of an apical Na^+ channel in the gills of fishes and resolves a long-standing dispute about the identity of a channel-mediated Na^+ uptake mechanism. Moreover, in a broader context, this is the first demonstration of ASICs being expressed in an epithelia tissue in any vertebrate species, which expands the functional role for this family of channels.

Preface

Most of the Chapters in this thesis have already been published in specialized research journals: Respiratory Physiology and Neurophysiology (Chapter 1), American Journal of Physiology – Cell Physiology (Chapter 2), and The Journal of Experimental Biology (Chapter 3). I am the main contributor to the research described in this thesis and I am the first author of all published articles. I was responsible for the data collection and analysis as well manuscript preparation. All the data presented in this thesis are my original work, except for Figure1.2, which was prepared by my collaborator Dr. Pung-Pung Hwang at Academia Sinica in Taiwan, Figure 2.3 prepared by Sal Blair at the University of Alberta, and Figures 4.6 and 4.7, which were prepared by Dr. Raymond Kwong at the University of Ottawa.

For Zuzia

"…and the zebrafish and rainbow trout lived happily ever after."

Acknowledgements

There are a number of people that helped, aided, advised and supported me in many ways throughout my PhD research. First and foremost, I would like to express my gratitude and thanks to my supervisor, Dr. Greg Goss, for taking me on and letting me become a part of his great lab. I fully appreciate his support, patience and insightful advice. Thank you Greg! Thanks for investing so much into me, for your endless support, and for inspiration. Thank you for all the opportunities to travel and for making my PhD so much fun.

I would also like to express my thanks to many people that contributed to my research as it would have been impossible without their help. First of all I would like to thank the co-authors of my papers: Aaron Schultz, Sal Blair, David Boyle, and the molecular biology wizard Danuta Chamot. I must also thank the staff of MBSU, Troy Locke and Cheryl Nargang for assistance with molecular work. Aquatics Facility staff, Clarence Gerla and Tad Plesowicz are thanked for assistance with setting up rainbow trout experiments. I would like to thank James Ede for help with confocal microscopy and Alex Clifford for advice with phylogenetic analysis.

Part of my research was conducted at the University of Ottawa at Dr. Steve Perry's lab. I would like to thank him for the opportunity to learn new techniques and to gain new research experience. I want to thank Dr. Perry's lab members -Yusuke Kumai and Raymond Kwong for help and support, as well as taking care of me during my stay in Ottawa. Vishal Saxena is also thanked for his assistance with zebrafish and teaching me morpholino technique.

I am also grateful to my fellow Goss' lab mates, as well as friends and colleagues for making my stay in Edmonton and the University of Alberta so enjoyable. Special thanks go to my special friends James Ede, Van Ortega, and Aaron Macri for the endless supply of good times and laughs.

Finally, I would like to thank my family back in Poland, especially my Mom and Gosia, for their support and making my science adventure possible. They've always been encouraging and never doubted me. I love you very much.

Table of Contents

List of Tables

List of Figures

List of abbreviations

AE	anion exchanger
ASIC	acid-sensing sodium channel
BSA	bovine serum albumin
Ca^{2+}	calcium
CBE	chloride-bicarbonate exchanger
CC	chloride cell
cDNA	complementary DNA
Cl^-	chloride
DAPI	4', 6-diamidino-2-phenylindole
DEG	degenerin
DMSO	dimethyl sulfoxide
DNA	deoxyribonucleic acid
ECaC	epithelial Ca^{2+} channel
EIPA	ethyl-iso-propyl-amiloride
ENaC	epithelial Na^+ channel
HCO_3^-	bicarbonate
hpf	hours post fertilization
HR	VHA-rich
K^+	potassium
Kcnj	K^+ inwardly-rectifying channel, subfamily J (non-human)

KS	K^+-secreting
MO	morpholino oligonucleotides
MRC	mitochondrion-rich cell
Na^+	sodium
NaR	NKA-rich
NBC	Na^+/HCO_3^- co-transporter
NCC	Na^+/Cl^- co-transporter
NCX	Na^+/Ca^{2+} exchanger
NH_3	ammonia
NH_3^+	ammonium
NHE	Na^+/H^+ exchanger
NKA	Na^+/K^+-ATPase
PCR	polymerase chain reaction
pH_i	intracellular pH
PMCA2	plasma membrane Ca^{2+}-ATPase
PNA	peanut lectin agglutinin
PVC	pavement cell
RACE	rapid amplification of cDNA ends
Rh	Rhesus
RNA	ribonucleic acid
RO	reverse osmosis

ROMK	renal outer medullary K^+ channel
RT-PCR	reverse transcription PCR
S.E.M.	standard error of the means
SEM	scanning electromicography
SLC	solute carrier (human)
slc	solute carrier (non-human)
SIET	scanning ion-selective technique
TEM	transmission electron microscopy
VHA	vacuolar-type H^+-ATPase

Chapter 1:
General introduction

A version of this chapter has been published previously.

Dymowska, A. K., Hwang, P. P., Goss, G. G. 2012. Structure and function of ionocytes in the freshwater fish gill. *Respiratory Physiology and Neurobiology* 184, 282-292.

Fishes are the most taxonomically diverse group of vertebrates on earth with over 32,400 identified species (www.fishbase.org), of which nearly 40% (~15,000) inhabit freshwater during at least one phase of their life cycle (Bond, 1996). The prevailing theory for evolution of fishes is that they originated from an ancestral marine proto-vertebrate (Evans et al., 2005) that entered into fresh (Smith, 1932) or brackish water (Ditrich, 2007). For ray-finned fishes, there is strong agreement that most species evolved from a common freshwater ancestor (Vega and Wiens, 2012). It has been suggested that whole genome duplications (Panopoulou and Poustka, 2005; Kasahara, 2007) provided the genetic and genomic plasticity necessary for the successful freshwater/seawater transitions. Although the number of invasion events is unknown, we know that transitions of a fish species from freshwater to marine or marine to freshwater environments has likely occurred numerous times (Vega and Wiens, 2012).

The low ion concentration of freshwater environment places numerous challenges on the organism, including the combined problems of net ion loss and osmotic water gain. The problem of osmotic water gain is resolved by reducing drinking (Evans, 1968), decreasing water permeability of the integument (Chasiostis et al., 2012) and production of copious amounts of dilute urine by the kidney (Smith, 1932). The problem of net ion loss is resolved primarily through the combined response of a reduction in diffusive loss by lowering the paracellular permeability (Chasiostis et al., 2012) and an increased capacity to absorb ions from the surrounding water (Evans et al., 2005). To compensate for ions lost through diffusion, fishes use specialized cells located on the gills or skin that accomplish transepithelial uptake of Na^+, Cl^- and Ca^{2+} (Garcia-Romeu and Maetz, 1964; Maetz and Garcia-Romeu, 1964; Hobe et al., 1984; Evans et

al., 2005). In addition to ion regulation, these cells act to control the release of acidic (H^+) or basic (primarily HCO_3^-) equivalents to the water (Goss and Wood, 1990a, 1990b) to achieve pH homeostasis in the blood.

Mitochondrion-rich cells

Transepithelial transport is an energy intensive process, and hence cells involved in ion uptake are characterized by the presence of large numbers of mitochondria in the cytoplasm for ATP production (Figure 1.1B). Based on this feature, ion transporting cells have been collectively termed mitochondrion-rich cells (MRCs). In the recent literature, MRCs have been alternatively termed ionocytes (e.g., Dymowska et al., 2012; Hiroi and McCormick, 2012) in order to distinguish them from other cells abundant in mitochondria but not involved in ionoregulation. Therefore, terms such as mitochondrion-rich cell and ionocyte will be used interchangeably to describe the same cell type throughout my thesis. In addition to high densities of mitochondria, MRCs must also possess a specific complement of transporters or channels on the apical and basolateral membranes that allow for directional movement of ions or acid-base equivalents from the external environment into the animal. It has been initially proposed by Krogh (1938) that uptake of Na^+ is coupled to NH_4^+ extrusion, whereas Cl^- absorption is linked with HCO_3^- secretion (Krogh, 1938). However, despite considerable research efforts, the mechanisms of ion acquisition and identity of the transporters involved in freshwater ion uptake are still not fully understood.

In this introductory Chapter 1, I will first review the historical progression of nomenclature and sub-typing of mitochondrion-rich cells in the most extensively studied

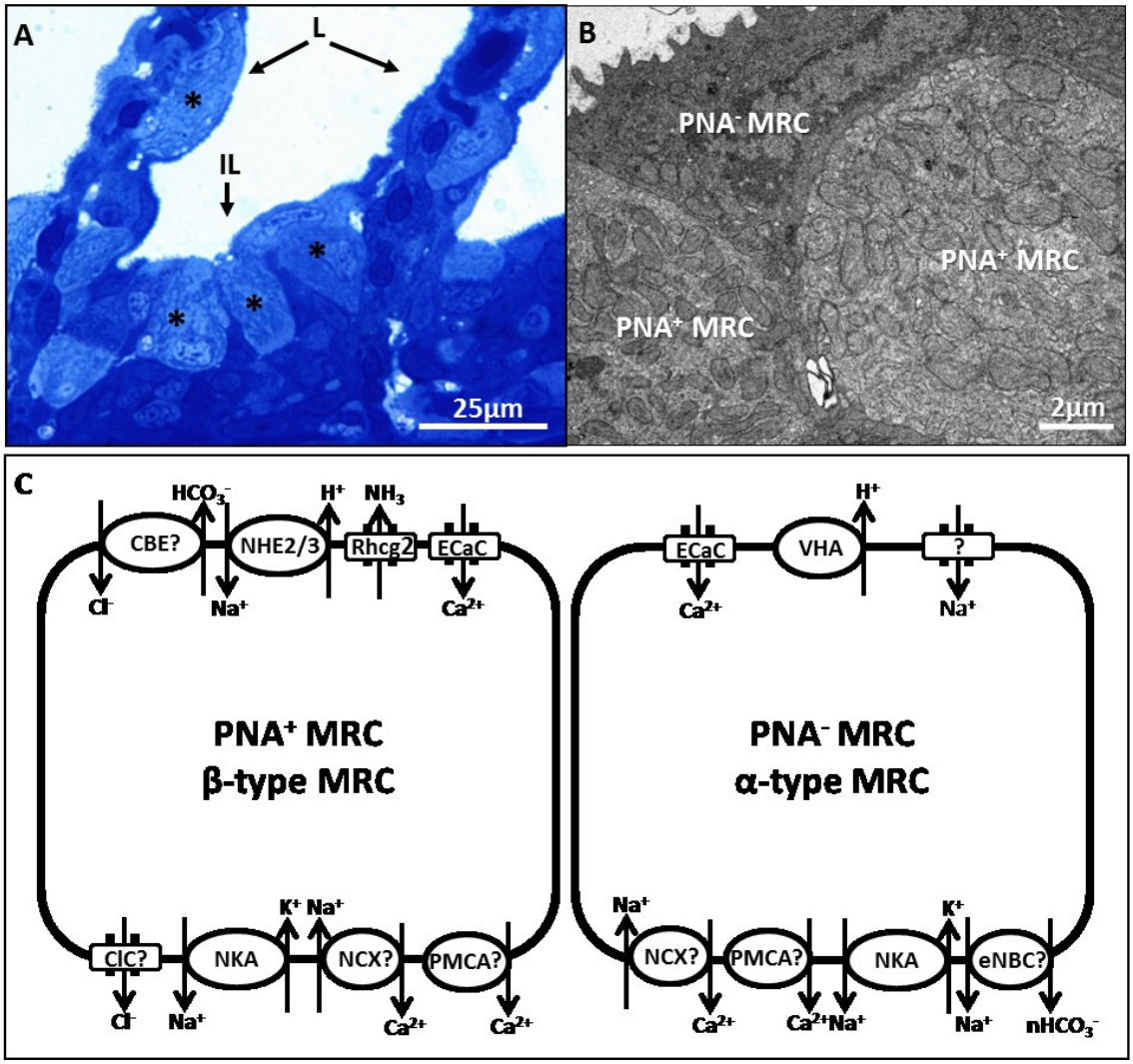

Figure 1.1. Freshwater rainbow trout fish gill ionocytes. (A) Distribution of ionocytes (*) on the lamellar (L) and interlamellar (IL) epithelia. (B) TEM image showing PNA^+ and PNA^- ionocytes (C) Current proposed model for PNA^+ and PNA^- ionocytes. Question marks indicate unidentified transporters.

model fish species for freshwater ion regulation: rainbow trout (*Oncorhynchus mykiss*) and zebrafish (*Danio rerio*). Subsequently, I will highlight both common and distinct components of the molecular strategies for ion and acid-base regulation with the emphasis on Na^+ regulation.

MRCs nomenclature and sub-types

The fish gill epithelium comprises at least five different cell types - MRCs, pavement cells, mucous cells, neuroepithelial cells, and stem cells, with MRCs covering 1-10% of the surface area, depending on the fish species and their environment (Laurent and Dunel, 1980; Evans et al, 2005). Over the past decades, a number of names have been proposed for the MRCs, each unique to the studied species. Given that there were multiple invasions and re-invasions of fishes into freshwater, different species have evolved distinct molecular strategies to accomplish ion and acid-base homeostasis. Therefore, MRCs may be divided into numerous sub-types with different transport functions depending on the species and conditions studied.

Historically, MRCs were first identified as the "chloride secreting cells" or "chloride cells" (CCs) in the gills of seawater European eel (*Anguilla vulgaris* now *Anguilla anguilla*) (Keys and Wilmer, 1932). However, it is now generally accepted that the term chloride cell (CC) should be used in a restricted sense only when referring to MRCs that function specifically in Cl^- secretion in seawater or brackish water fish.

Over the years, researchers have been identifying MRCs in different species and independently assigning names to each sub-type resulting in a proliferation of terms for MRCs with similar functions. For reference, Table 1.1 summarizes the nomenclature for

Table 1.1. Nomenclature of ionocytes for some freshwater fishes.

Species	Ionocyte function			
	Na^+ transporting/ H^+ excreting	Ca^{2+} transporting	Cl^- transporting/ HCO_3^- excreting	Na^+/ Cl^- co-transporting
Killifish	MRC[1] Cuboidal[4]	?	Not present [2]	MRC[3]
Rainbow trout	dark S-cells [5] β-CC[7] α-type MRC[8] PNA^-[9]	PNA^+/PNA^- [6]	light S-cells [5] α-CC[7] β-type MRC[8] PNA^+[9]	?
Tilapia	Shallow basin[10] Concave[12] Type III[13]	Shallow-basin[11]	?	Wavy convex[10] Type II[13]
Zebrafish	HR[14]	NaR[14]	?	NCC[14]
Catfish	MR PVC[15]	?	MR CC[15]	?

1. Patrick et al. (1997) and Patrick and Wood (1999); 2. Patrick et al. (1997); 3. Katoh et al. (2008); 4. Laurent et al. (2006); 5. Doyle and Gorecki (1961); 6. Shahsavarani et al. (2006) and Galvez et al. (2006); 7. Pisam et al. (1987) and Pisam and Rambourg (1991); 8. Galvez et al. (2002); 9. Goss et al. (2001); 10. Lee et al. (1996); 11. Chang et al. (2005); 12. Inokuchi et al. (2009); 13. Hiroi et al. (2005); 14. Hwang and Lee (2007) and Hwang et al. (2011); 15. Goss et al. (1992, 1994)

freshwater fish ionocytes in species where ionocytes and their sub-types have been most characterized. The first ultrastructural study by Doyle and Gorecki (1961) on the gills of freshwater fish demonstrated that there were two types of MRCs (called S-type cells) in the gills of a variety of species. In this study, one MRCs sub-type appeared electron-dense or dark staining and was more abundant in seawater fish while the other sub-type displayed lighter staining and was more abundant in freshwater fish (Doyle and Gorecki, 1961). The subsequent studies by Pisam and collegues (Pisam et al., 1987; Pisam and Rambourg, 1991; Pisam et al., 2000) confirmed the existence of the two sub-types of MRCs in freshwater trout, and termed the electron-dense sub-type as a "β-chloride cell", and the light appearing sub-type as a "α-chloride cell". Simultaneous with the studies by the Pisam research group, studies conducted by Goss and colleagues (1992) demonstrated that in freshwater catfish exposed to hypercapnia, MRCs, collectively termed CCs in that publication, were involved in Cl^- uptake. This study also revealed strong correlation between unidirectional Cl^- uptake and fractional area of exposed MRCs (Goss et al., 1992). Moreover, it was noted that in catfish exposed to hypercapnia, a small sub-population of pavement cells (PVCs) displayed increased number of mitochondria and these mitochondria were concentrated in the sub-apical region of the cell (Goss et al., 1992, 1994). These cells were termed mitochondrion-rich PVCs (MR PVCs) as a means to distinguish them from the PVCs involved in respiration. It is now generally thought that MR PVCs are ionocytes rather than PVCs. The end result of these combined morphological studies further supported that there were different sub-types of ionocytes present in the gills of freshwater fishes.

One of the weaknesses of the morphological arguments for sub-types of ionocytes/MRCs was the lack of evidence for distinct functions. Application of density gradient separation techniques (Hootman and Philpott, 1978, Wong and Chan, 1999) combined with differential peanut lectin agglutinin (PNA) staining (Goss et al., 2001) and magnetic separation (Galvez et al., 2002) allowed characterization of two distinct MRC sub-populations in rainbow trout termed PNA positive (PNA^+) and PNA negative (PNA^-) cells. PNA binding is a key marker of the β -intercalated cell in the mammalian kidney (Lehir et al., 1982). β -intercalated cells are known be involved in base secretion (Kim et al., 2002), and therefore trout PNA^+ cells were proposed to be involved in base secretion. For this reason PNA^+ ionocytes were termed β-type MRCs (Galvez et al., 2002). By corollary, PNA^- MRCs in trout were proposed to match the function of acid-secretion as found for the α-type intercalated cells of the mammalian kidney and were termed α-type MRCs (Table 1.1). Currently, it is thought that gill of freshwater rainbow trout and salmonids in general display only two sub-types of MRCs: PNA^+ (β-type), and PNA^- (α-type) (Hiroi and McCormick, 2012). Both sub-types play different roles in ionoregulation and possess distinct suits of transporting proteins (Figure 1.1; Dymowska et al., 2012). However, both PNA^+ and PNA^- MRCs are characterized by high abundance in Na^+/K^+-ATPase (NKA) on the basolateral side (Perry, 1997). A series of studies using radiolabelled Na^+ uptake (Reid et al., 2003; Goss et al., 2011) demonstrated that in rainbow trout PNA^- cells are the site of acid-stimulated phenamil-sensitive Na^+ uptake (Table1). It has also been suggested that the PNA^+ cell is the site of Cl^- uptake/HCO_3^- excretion (Reid et al., 2003).

Recently, the functions of ionocytes have been extensively studied in zebrafish. The first measurements of Na^+, Cl^-, and Ca^{2+} uptake in zebrafish were performed by Chen and Hwang (2003) and Boisen et al. (2003). These studies demonstrated active and saturable Na^+, Cl^- and Ca^{2+} uptake in embryonic and adult animals. The assumption of these studies was that in zebrafish, ion uptake occurred across the apical membrane of the MRCs but at this time, no sub-types of ionocytes had been identified. An elegant series of experiments using double/triple *in situ* hybridization and/or immunocytochemistry approaches revealed the existence of at least four types of ionocytes on both the skin and yolk sac (Figure 1.2)(Hwang et al., 2011). One population of these ionocytes express high levels of NKA on the basolateral side of the membrane and for this reason are termed NKA rich (NaR) cells (Pan et al., 2005). A separate population of ionocytes is characterised by a high abundance of vacuolar-type H^+-ATPase (VHA) on the apical side, but low abundance of NKA on the basolateral, which differs from trout where both MRCs are NKA-rich. In zebrafish, VHA rich cells have been termed (HR) cells (Lin et al., 2006). Recently, two additional subtypes of ionocytes have been identified in freshwater zebrafish: cells expressing Na^+/Cl^- co-transporter termed NCC cells, and cells secreting K^+ termed KS cells (Wang et al., 2009; Abbas et al., 2011). The functional roles of the ionocytes in zebrafish were characterized by examining the effects of loss- (or gain-) of-function using morpholino or mRNA microinjection into embryos, respectively, combined with either unidirectional fluxes of ions, fluorescent dyes (sodium green) and/or non-invasive scanning ion-selective electrodes (Lin et al., 2006; Esaki et al., 2007; Horng et al., 2007; Yan et al., 2007; Lin et al., 2008; Shih et al., 2008; Liao et al., 2009; Wang et al., 2009;

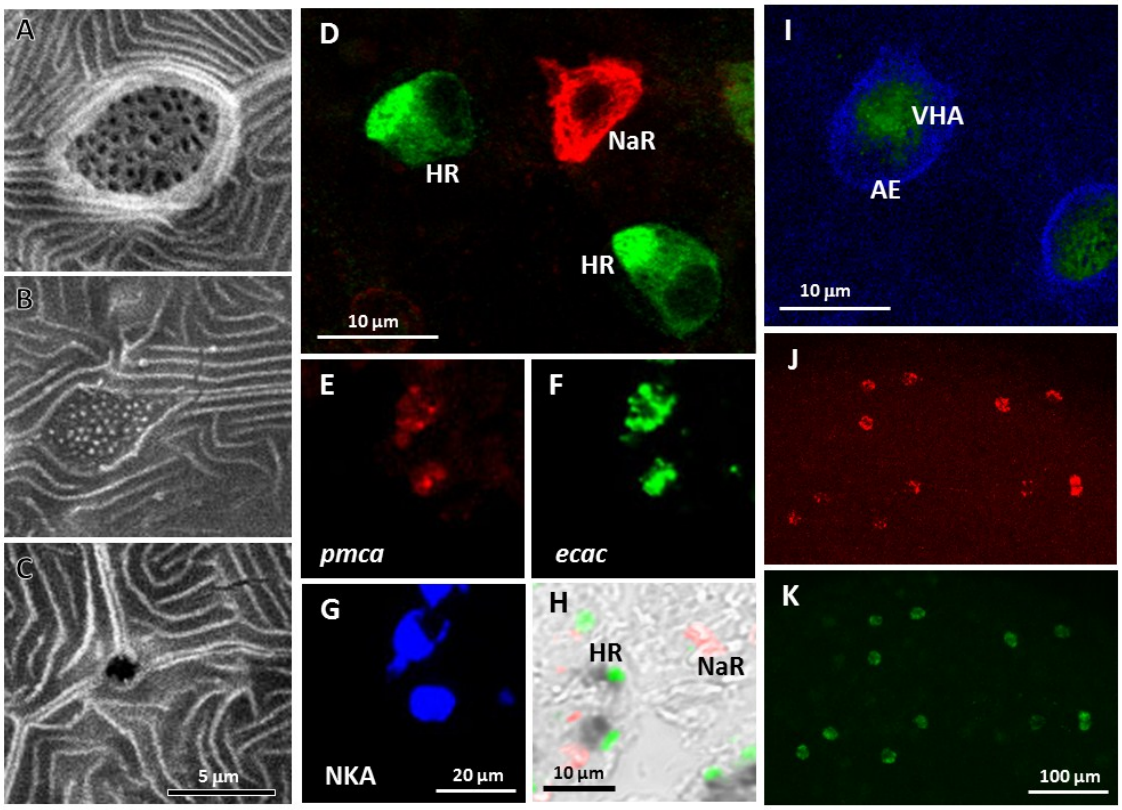
A
B
C
5 µm
D
HR
NaR
HR
10 µm
E
pmca
F
ecac
G
NKA
20 µm
H
HR
NaR
10 µm
I
VHA
AE
10 µm
J
K
100 µm

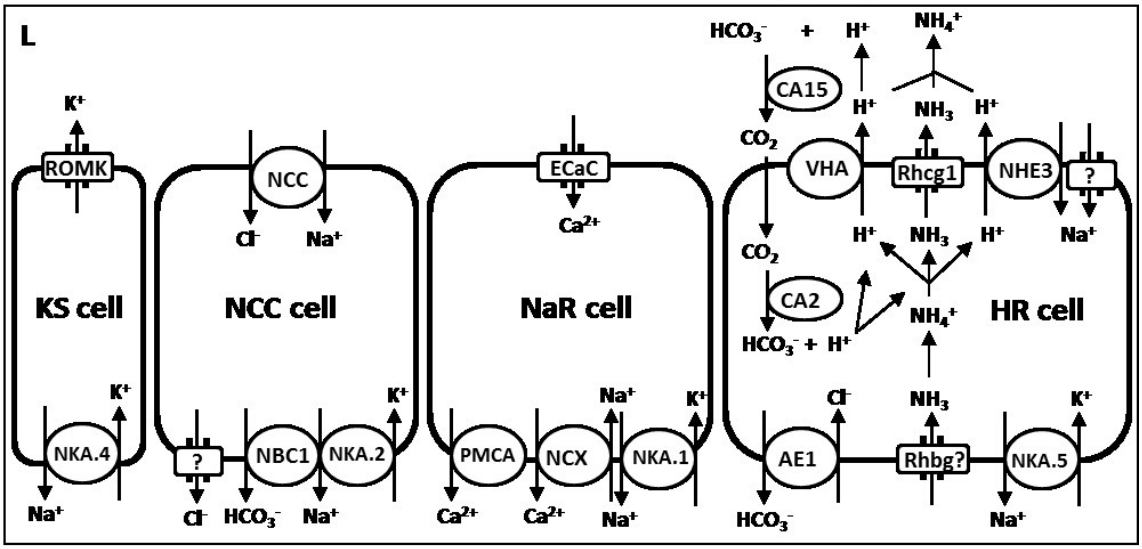
L
K+
ROMK
KS cell
NKA.4
Na+
K+
Na+
NCC
Cl−
Na+
NCC cell
?
NBC1
NKA.2
Cl−
HCO3−
Na+
K+
ECaC
Ca2+
NaR cell
PMCA
NCX
NKA.1
Ca2+
Ca2+
Na+
Na+
K+
HCO3− + H+
NH4+
CA15
CO2
VHA
Rhcg1
NHE3
?
H+
NH3
H+
Na+
CO2
CA2
HCO3− + H+
NH4+
HR cell
Cl−
NH3
K+
AE1
Rhbg?
NKA.5
HCO3−
Na+

Figure 1.2. (previous page) Four different types of ionocytes in freshwater zebrafish skin/gills. Apical surfaces of HR cells (A) and other unidentified cell types (B, C) in embryonic skin identified by SEM (kindly provided by Dr. J. L. Horng). Localization of various ion transporters in different types of ionocytes in zebrafish embryonic skin (D, I, J, K) and adult gills (E, F, G, H). (D) HR cell and NaR cell labeled with anti-VHA (green) and anti-NKA (red) antibodies, respectively. (E, F, G). Co-localization of pmca2 mRNA (red), ncx1b mRNA (green) and NKA in the same NaR cells. (H) nhe3b mRNA (dark grey) co-localized with VHA (green) in HR cells, but not with NKA (red) in NaR cells. (I), co-localization of VHA (green) and AE1b (blue) protein signals in HR cells. (J, K) co-localization of ncc mRNA (red) and nbce1b mRNA (green) in NCC cells. (L) current proposed model of the function of each of the 4 types of ionocytes in zebrafish. Question marks indicate unidentified transporters.

Lee et al., 2011). Based on the differential pattern of transporters expressed on the apical and basolateral membranes, HR cells are proposed to be the main site of Na^+ uptake and acid-base regulation. HR cells have apically expressed Na^+/H^+ exchanger 3 (NHE3b), and VHA, complemented by basolaterally expressed Cl^-/HCO_3^- exchanger (AE1b) (Hwang et al., 2011; Dymowska et al., 2012). NCC ionocytes have been suggested to be the major player in Cl^- uptake (Hwang and Lee, 2007; Hwang et al., 2011), while the NaR cells co-express the cellular machinery necessary for transepithelial Ca^{2+} uptake including ECaC, PMCA2, and NCX1b in addition to NKA (Pan et al., 2005; Liao et al., 2007, 2009; Tseng et al., 2009). KS cells were found to co-express a potassium channel (Kcnj1, an ortholog of mammalian kidney renal outer medullary K^+ channel-ROMK) and were proposed to be associated with K^+ secretion in embryonic skin (Abbas et al., 2011). However, no *in vivo* evidence is available to support this proposed function in zebrafish and the localization of the protein within the cell is not known (Dymowska et al., 2012).

Based on just these two species, it is clear that MRC subtypes in freshwater fishes do not correspond to each other, although they tend to share similar features. The fundamental transporters responsible for regulation of ion uptake and acid/base regulation appear to be relatively similar across the species, but the distribution of ionocytes, their morphology and functional sub-types as expressed by their specific complement of transporters is relatively species-specific. With fishes having historically moved to seawater and then re-invaded freshwater multiple times, this diversity of ionocytes and their mechanistic approaches to ion and acid-base homeostasis should not be surprising.

Mechanisms for Na^+ uptake in freshwater fishes

Fishes living in freshwater must actively take up Na^+ against a steep concentration gradient. Although mechanisms for Na^+ uptake have been a focus of numerous studies for over 70 years, freshwater Na^+ regulation still remains the subject of a lively debate amongst fish physiologists. Currently, it is accepted that in freshwater fish there are present three mechanisms that enable uptake of Na^+: 1) Na^+/H^+ exchanger (NHE), 2) H^+-ATPase assisted Na^+ uptake, and 3) Na^+/Cl^- cotransporter (NCC). It should be noted, however, that the type of employed mechanism may depend on the fish species and environmental conditions.

Na^+ /H^+ exchanger (NHE)

The most favoured current model for Na^+ uptake in freshwater fish gills proposes that one Na^+ ion is exchanged for one H^+ counterion *via* an electroneutral antiporter, NHE, located on the apical membrane of the MRCs (Hwang et al., 2011; Kumai and Perry, 2012). NHE belongs to the SLC9A family of transporters and to date 9 mammalian isoforms have been cloned, *nhe 1-9*, with *nhe1-5* being expressed on the cell membrane and *nhe 6-9* expressed intracellularly (Alper and Sharma, 2013; Donowitz et al., 2013). Since in the mammalian kidney cells, NHE2 and NHE3 are expressed on the apical side of the cell membrane, NHEs were thought to be to be expressed apically in the fish gills. Using anti-rat NHE antibodies, Edwards and colleagues (1997) were the first to report the presence of NHE3 in the gill epithelium of freshwater rainbow trout and blue-throated wrasse (*Pseudolabrus tetrious*). A subsequent study by Wilson et al. (2000) demonstrated expression of NHE2-like protein in the MRCs of freshwater tilapia (*Oreochromis mossambicus*). Since then, the NHE model has been further supported by

empirical evidence from other freshwater fish species including Osorezan dace (*Tribolodon hakenesis*) (Hirata et al., 2003), zebrafish (Esaki et al., 2007; Yan et al., 2007), and goldfish (*Carassius auratus*) (Bradshaw et al., 2012). NHE3 has been localized to the apical side of the PNA^+ MRCs in rainbow trout (Ivanis et al., 2008; Hiroi and McCormick, 2012), and HR cells in zebrafish (Hwang et al., 2011).

The limitation of the NHE model for Na^+ uptake in freshwater is the questionable ability of the electroneutral NHE to function in low Na^+ waters (Na^+ <0.1 mM) and/or low pH (pH<5), where gradients for Na^+ and H^+ would be reversed (Avella and Bornancin, 1989; Parks et al., 2008). Recently, the NHE model has been extended by the addition of an ammonia (NH_3)-transporting Rhesus (Rh) protein (Nakada et al., 2007; Nawata et al., 2007), whereby NHE2/3 and Rhcg1 protein form a metabolon, which locally decreases H^+ concentration in the boundary layer, and facilitates NHE function in acidic environments (Wright and Wood, 2009). In this attractive "ammonia trapping" gill boundary layer alkalinisation model, the Rhcg2 protein transports ammonia (NH_3) to the outside of the MRC. The formation of NH_4^+ in the boundary layer from the reaction of NH_3 (via Rhcg1) and H^+ (from NHE function) would locally increase pH and decrease NH_3 concentration, and thus facilitate NHE activity in thermodynamically unfavourable environments. This is essentially a corollary of the well-accepted "acid-trapping model" used by fish to acidify the boundary layer in alkaline waters to trap NH_4^+ and maintain NH_3 diffusion (Pitts, 1973). However, two points regarding the effectiveness of this model for elevation of boundary layer pH for fish in acidic waters should be noted. The first is that the measured pH in the boundary layer of NHE expressing HR cells in zebrafish embryos is actually slightly acidic compared to the bulk

water pH of 6.8 (Lin et al, 2006) suggesting that boundary layers of NHE expressing ionocytes are acidic rather than alkaline. Although, this may not be true for other species, it would be predicted that the pH of the boundary layer could only rise to a maximum value equal to the equilibrium point where the NH_3 gradients would be reversed, which would result in the net NH_3^+ transport into the animal. In theory, this pH maximal value would be at or very close to the intracellular pH since the total ammonium concentration difference across the membrane would be quite small given the high permeability to ammonia in that area as defined by the expression of the Rh protein. This raises an interesting point that for NHE to function as an electroneutral transporter, the Na^+ gradient would have to be favourable if the intracellular and external medium pHs were in a near equilibrium. Given that some fish take up Na^+ from extremely dilute waters (e.g. < 50 μM), either the ΔpH in the boundary layer must be very large, namely more than 1 pH unit higher in the boundary layer than inside of the cell (Parks et al., 2008), or the intracellular Na^+ concentration must be exceptionally low. Therefore, while this alkalinisation "ammonia –trapping" model does remove the thermodynamic constraints imposed by low pH in the environment, it does not remove all thermodynamic constraints imposed by very low Na^+ concentrations. How Na^+ is transported under these conditions remains the topic of a great deal of interest and debate.

Vacuolar-type H^+-ATPase (VHA) assisted Na^+ uptake

An alternative model for Na^+ uptake, where Na^+ ions enter the gill *via* an epithelial Na^+ channel from the ENaC that works in concert with VHA, was first proposed by Avella and Bornancin (1989) (Figure 1.1C). The ENaC/VHA model is

based on models for Na^+ uptake in the frog skin (Harvey, 1992) and gained popularity among fish physiologists since theoretically it is not limited by external Na^+ concentrations. Support for this model came from studies demonstrating that VHA plays a role in the freshwater fish Na^+ uptake. An early study by Lin and Randall (1990, 1991) reported VHA activity in the gills of rainbow trout and demonstrated that this activity decreased in fish adapted to seawater. Additionally, exposure to bafilomycin, a VHA specific pharmacological inhibitor, has been shown to reduce Na^+ uptake in whole animals (Bury and Wood, 1999) and in isolated rainbow trout MRCs (Reid et al., 2003; Goss et al., 2011). Bafilomycin has been shown to decrease uptake of Na^+ also in other freshwater species including goldfish (Preest et al., 2005), and zebrafish (Boisen et al., 2003; Esaki et al., 2007). Involvement of VHA in Na^+ uptake in zebrafish has been further confirmed by a "loss of function" study using morpholino injections, where VHA knock-down resulted in decreased Na^+ content in whole animals (Horng et al., 2007). In rainbow trout VHA has been localized to the apical surface of the PNA^- MRCs (Sullivan et al., 1996; Reid et al., 2003; Goss et al., 2011), whereas in zebrafish VHA has been detected on the apical side of the HR cells (Lin et al., 2006). Therefore, the model for Na^+ uptake via an epithelial Na^+ channel, presumably ENaC, places the Na^+ channel on the PNA^- MRCs and HR cells (Dymowska et al., 2012).

However, a significant issue with the VHA/ENaC model is that searches of available fish genomes do not find evidence for the ENaC α, β, or γ subunits orthologues in teleost fishes. As a result, this model has received less support from researchers in the recent years. However, the unquestionable role of VHA in Na^+ uptake in freshwater fish gill has not been explained by any other model. A publication by

Wright and Wood (2009) attempted to justify the involvement of VHA in freshwater Na^+ uptake by proposing a NHE/VHA/Rhcg1 metabolon on the MRCs apical side. However there are two major flaws of this model: 1) NHE and VHA do not co-localize to the same MRC in the rainbow trout (Dymowska et al., 2012), and 2) acidification of the boundary layer by H^+ ions pumped outwards by the VHA would impede NHEs function in low Na^+ environments (Parks et al., 2008; Dymowska et al., 2012).

In a previously published PhD thesis emanating from our lab (Parks, 2009), it had been noted that perhaps another channel, a relative to ENaC, performs the function of the epithelial Na^+ channel in freshwater fishes. Parks (2009) found that zebrafish gills express one of the acid-sensing ion channels (ASIC), namely ASIC4.2, which belongs to the same family of channels as ENaCs. My thesis was based on this finding, and investigation of the involvement of ASICs in freshwater fish Na^+ uptake became the main area of my thesis research.

Acid-sensing ion channels (ASICs)

ASICs are Na^+ channels that belong to the epithelial Na^+ channel/degenerin (ENaC/DEG) superfamily of ion channels that was discovered in the mid-nineties (Waldmann et al., 1995). All ENaC/DEG subfamilies share ~15-30% identity at the amino-acid level, with ASICs and ENaCs sharing ~20-25% sequence identity (Grunder et al., 2000, Kellenberger and Schild, 2015). Unlike ENaCs, ASICs are gated by extracellular H^+ and in the continued presence of H^+ they desensitize (Kellenberger and Schild, 2015). In humans, eight different ASIC subunits were identified (ASIC1a, 1b, 2a, 2b, 3a, 3b, 3c, 4), and are encoded by four different genes (Waldmann and Lazdunski,

1998; Grunder et al., 2000). Recently, ASICs have been also identified in several fish species (GenBank and Ensembl). In zebrafish, a fish species with the most extensive functional characterization of ASICs, six ASIC subunits are present (ASIC 1.1, 1.2, 1.3, 2, 4.1, and 4.2) and each subunit is encoded by a different gene (Paukert et al., 2004; Sakai et al., 1999).

ASIC subunits comprise of two transmembrane domains, short intracellular amino and carboxy termini, and a large extracellular loop with H^+-sensing residues that are involved in the ASICs activation (Jasti et al., 2007). Structural arrangement of ASIC subunits has been compared to an upright forearm and a clenched hand, where the forearm corresponds to the transmembrane segments and the hand to the extracellular loop (Kellenberger and Schild, 2015). Despite recent efforts, the exact mechanism of ASIC gating and the location of the residues involved in the activation have still not been resolved (Kellenberger and Schild, 2015; Paukert et al., 2008). As revealed by crystallography, the functional ASIC channels are formed by three ASIC subunits (trimers) of identical (homomers) or different (heteromers) subunits (Jasti et al., 2007; Kellenberger and Schild, 2015). The trimeric structure of ASICs has been verified by direct visualization with atomic force microscopy (Carnally et al., 2008) and oocyte expression of ASIC1a and ASIC2a (Bartoi et al., 2014).

ASICs are evolutionarily conserved and are mostly associated with neuronal expression in the central and peripheral nervous system of mammals, birds and fishes (Paukert et al., 2004; Springauf and Grunder, 2010; Vina et al., 2013; Wemmie et al., 2013). In mammals, ASIC subunits are present in the brain tissue and in neurons innervating heart, muscle, gut and skin (Kellenberger and Schild, 2015), where they are

involved in mechanoreception, sensory transduction of taste and pain (Wemmie et al., 2013). In fish, the expression of ASICs has been demonstrated in the brain tissue from dogfish shark (*Squalus acanthias*) (Coric et al., 2005; Springauf and Grunder, 2010), lamprey (*Lampetra fluviatilis*) (Coric et al., 2005), toadfish (*Opsanus tau*) (Coric et al., 2005), and zebrafish larvae (Paukert et al., 2004). Interestingly, functional characterization of ASIC1 from lamprey and shark by oocyte expression revealed that ASICs in these two species are not activated by external H^+ (Coric et al., 2005). Therefore, it has been suggested that proton gating of ASICs arose in bony fishes (Coric et al., 2005; Springauf and Grunder, 2010). In lower vertebrates the gating ligand is still unknown. ASIC subunits were detected in the peripheral nervous system of adult zebrafish. Using heterologous antibodies, ASIC1, ASIC2, and ASIC4 were localized to the taste buds of the adult zebrafish (Vina et al., 2013). Moreover, ASIC2 protein has been found in the zebrafish intestine, where it most likely acts as a chemo- and mechano-sensor (Levanti et al., 2011). However, in fish no other tissues have been investigated for the presence of ASICs.

Mammalian and zebrafish ASICs are sensitive to amiloride, which has been demonstrated to blocks ASICs currents at the milimolar range (Kellenberger and Schild, 2002; Paukert et al., 2004). However, since amiloride also inhibits other Na^+ transporters such as ENaCs and NHEs, it cannot be used as an ASIC-selective inhibitor (Kleyman and Cragoe, 1988). Recently, Chen and colleagues (Chen et al., 2010) described a group of potent ASIC non-amiloride derived inhibitors, the diarylamidines. Diarylamidines are a class of anti-protozoan drugs that includes more than 30 compounds (Chen et al., 2010). The study by Chen et al. (2010) demonstrated that four diarylamidines including

DAPI, diminazene, hydroxystilbamadine, and pentamidine had high affinity for ASICs, but had no effect on ENaC (Chen et al., 2010). This finding was exploited in my thesis to pharmacologically investigate a potential role for ASIC in Na^+ uptake in freshwater fish.

Na^+/ Cl^- co-transporter (NCC)

The existence of the NCC, a thiazide-sensitive membrane protein that co-absorbs Na^+ and Cl^-, has been first demonstrated in the urinary bladder of winter flounder (*Pseudopleuronectes americanus*) (Renfro, 1975). In mammals, NCC is expressed in distal convoluted tubules in the kidney, where they are considered to be one of the major players in the uptake of Na^+ (Reilly and Ellison, 2000). Recently, NCC has been cloned from the gill/skin of zebrafish, and tilapia (*Oreochromis mossambicus*), and it has been suggested that it plays a role in ion uptake in these two species (Hwang and Lee, 2007; Hiroi et al., 2008). Staining with homologous antibodies revealed that in freshwater tilapia gill and yolk sac NCC localizes to the apical side of the type II MRCs, whereas in zebrafish it is present in the NCC MRC sub-type (Table 1.1) (Hiroi et al., 2008; Hwang et al., 2011). Notably, the type II ionocytes in the euryhaline tilapia appear to be analogous to the NCC cells in the stenohaline zebrafish in terms of ion transporter expression and ion transport functions (Hwang, 2009; Hwang et al., 2011).

It is unclear to what extent NCC is involved in Na^+ uptake in freshwater fish, and it has been suggested that NCC is more important for Cl^- rather than Na^+ uptake (Hwang et al., 2011). However, Wang and colleagues (2009) demonstrated that exposure of zebrafish larvae to metolazone, a potent inhibitor of NCC, decreased uptake of Cl^- and

Na^+, suggesting that NCC may play some role in transport of Na^+ in this species (Wang et al., 2009). Interestingly, it has been showed that knock-down of NCC using morpholino technique increases Na^+ uptake and Na^+ content in the zebrafish larvae, which is accompanied by up-regulation of NHE3b and increase in the HR cell number (Wang et al., 2009; Chang et al., 2013). Moreover, study by Chang et al. (2013) demonstrated that translational knock-down of NHE3b or prevention of HR cell differentiation in zebrafish larvae resulted in increased number of NCC cells and increased Na^+ uptake rates (Chang et al., 2013). It should be noted that since NCC is an electroneutral transporter, in fresh water, gradients for uptake of Cl^- and Na^+ *via* this transporter are unfavorable (Hwang et al., 2011). Hiroi et al. (2008) proposed that the driving force for Na^+ uptake in MRCs may be provided by the basolateral NKA, which would maintain low intracellular Na^+ concentrations (Hiroi et al., 2008). Then again, Hwang et al. (2011) speculated that it is possible that kinetics and/or the stoichiometry of the fish NCC may differ from the NCC found in mammals and thus enable it to operate in low external Na^+ and Cl^+ concentrations (Hwang et al., 2011). Defining how the NCC functions despite apparent thermodynamic limitations is a key challenge for future researchers to solve.

Uptake of other ions

Cl^-

The molecular mechanisms of Cl^- uptake in freshwater fish have not been studied as extensively as those for transport of Na^+, and remain to be elucidated. Since the initial study by Krogh (1938), strong evidence has accumulated showing that in freshwater fish

Cl^- uptake is directly linked to HCO_3^- excretion in a 1:1 equimolar ratio (Kerstetter and Kirschner, 1972; Goss and Wood, 1990a; 1990b). Therefore, it has been proposed that the main mechanism for apical Cl^- transport involves a Cl^-/ HCO_3^- anion exchanger (AE) (Evans et al., 2005; Hwang and Lee, 2007). The likely candidates to play a role as an anion exchanger in Cl^- in freshwater fish are transporters from either the SLC4, or SLC26 family of proteins. While there are reports of S4a1 (AE1) immunoreactivity in MRCs from the rainbow trout (Wilson et al., 2000), these results have been questioned (Tresguerres et al., 2006). In his review on Cl^- uptake in freshwater fishes, Tresguerres et al. (2006) pointed out that the antibody used in the study by Wilson and colleagues (2000) was a polyclonal antibody against a ~100 kDa band from trout red cell SDS-PAGE (band 3), and was likely immunoreactive against other co-migrating proteins. Similarly, reports of Slc4a1 expressed in the ionocytes of rainbow trout using *in situ* hybridization (Sullivan et al., 1996) are unreliable given the lack of specificity of the probes used (Perry et al., 2009). Recently, Boyle and colleagues (2014) cloned SLC26a6 gene from the gills of the rainbow trout, and based on the functional and expression analyses, suggested that SLC26a6 protein was involved in Cl^- transport in this species (Boyle et al., 2014). However, studies investigating SLC26a6 localisation in the MRCs as well as the transport properties are required.

Similar to Na^+ uptake, the thermodynamic constraints on Cl^- uptake in freshwater would seem to negate an electroneutral Cl^-/HCO_3^- exchange at a low environmental concentration of Cl^-. Importantly, Slc26 family members (specifically Slc26a3 and Slc26a6) are known to transport in an electrogenic mode $Cl^-/nHCO_3^-$ which would aid in overcoming these thermodynamics constraints. Another alternatively proposed theory is

that the thermodynamic constraints on Cl^- uptake in dilute freshwater is overcome using a metabolon involving a basolateral VHA driving apical absorption of Cl^- via a Cl^-/HCO_3^- exchange (Tresguerres et al., 2006). However, this requires further investigation.

The mechanisms responsible for the branchial uptake of Cl^- in zebrafish still remain to be precisely determined. Cl^-/HCO_3^- exchanger - *slc26a3*, *slc26a4* and *scl26a6* was expressed at the mRNA level in the adult zebrafish gill and zebrafish embryos, with *slc26a6* being the most abundant (Bayaa et al., 2009; Perry et al., 2009). Slc26a3 was found to be present in a portion of NaR cells, but there was no reported localization for Slc26a6 and Slc26a4. Moreover, exposure of zebrafish adults to the medium containing low Cl^- concentration resulted in increased mRNA expression of all three isoforms of *slc26* (*a3*, *a4* and *a6*)(Perry et al., 2009). The same study reported that knock-down of *slc26a3*,*4*, and *6* reduced Cl^- uptake in low Cl^- containing medium. The abovementioned studies showed that slc26 isoforms are involved in uptake of Cl^-, however the definitive roles of each of the isoforms need to be determined.

Recently, it has been proposed that NCC, which is mentioned above in the Na^+ uptake section 1.2.3., is also involved in branchial Cl^- uptake in tilapia and zebrafish (Hwang and Lee; 2007; Hiroi et al., 2008). Wang and collegues (2009) report that expression of NCC mRNA was up-regulated in zebrafish exposed to media low in Cl^- and translational knock-down of NCC resulted in decrease of both Cl^- uptake and content in zebrafish morphants (Wang et al., 2009). Together, these findings show that NCC plays a role in Cl^- transport in the gills of zebrafish and tilapia. NCC has not been identified in the gill epithelium of other freshwater fish species. Furthermore, the

mechanisms that enable the electroneutral NCC to operate in zebrafish and tilapia despite unfavourable gradients for Na^+ and Cl^- are still unclear.

Ca^{2+}

Early models for Ca^{2+} uptake in freshwater fish gill suggested passive entry of Ca^{2+} *via* voltage-independent Ca^{2+} channel located on the MRCs (Payan et al., 1981; Perry and Wood, 1985; Perry and Flick, 1988; Marshall, 2002). In 2006, Shahsavarani and colleagues cloned an epithelial Ca^{2+} channel (ECaC) from the gills of the rainbow trout and localized it to the apical membrane of gill epithelial cells (Shahsavarani et al., 2006a, 2006b). However, immunostaining with a homologous polyclonal ECaC antibody revealed that the distribution of the channel was restricted not only to the MRCs, as assumed by the earlier models, but also extended to PVCs. This finding was further corroborated by the study of Galvez et al. (2006), who reported that Ca^{2+} uptake occurred in both MRC and PVCs. However, Ca^{2+} uptake was 3-fold higher in the PNA^+ fraction of MRCs than in the PNA^- fraction, and significantly lower in the PVCs. Similar result was observed in cultured trout epithelia, where under symmetrical conditions Ca^{2+} uptake was 4-fold higher in MRCs than in PVCs (Galvez et al., 2008). Further, exposure to low environmental Ca^{2+} concentration (20-40 μM) increased both mRNA and protein expression of ECaC in the gill (Shahsawani and Perry, 2006). It was also reported that uptake of Ca^{2+} increased with elevated cortisol levels in the fish, however this appears to have occurred through MRCs proliferation rather than up-regulation of the ECaC. The export pathway for Ca^{2+} across the MRCs basolateral membrane in the trout gill is unknown. It has been hypothesized to be either a plasma

membrane Ca^{2+}- ATPase (PMCA) or a Na^{+}/Ca^{2+} exchanger (NCX) (Shahsawani and Perry, 2006a). However, this remains to be demonstrated.

Transepithelial Ca^{2+} uptake was measured using $^{45}Ca^{2+}$ radiotracer analysis in developing zebrafish embryos (Chen and Hwang, 2003; Pan et al., 2005). Acclimation to low Ca^{2+} increased the rates of Ca^{2+} uptake and this was associated with an increase of ECaC expression (Pan et al., 2005). Similar to the current mammalian model for transcellular Ca^{2+} transport, Ca^{2+} is absorbed through apical ECaC, while intracellular Ca^{2+} is bound to calbindins that facilitate diffusion to the basolateral membrane, and is extruded *via* the basolateral plasma membrane calcium ATPase (PMCA2) and NCX1b. Basolateral NKA creates a Na^{+} gradient and electrical gradient to drive the exchange by NCX1b (Figure 1.2L).

Thesis goals and objectives

Significant advancements have been made in the past few years in our understanding of the mechanisms of ion transport in fishes. However, despite extensive research efforts, fish physiologists have been unable to identify a transporter that would serve as an epithelial Na^{+} channel in freshwater fish Na^{+} uptake. The goal of this thesis was to examine if other channels could play that role. My general hypothesis was that acid-sensing ion channels are involved in Na^{+} uptake in freshwater fish. I tested my hypothesis on the two most common models used in ionoregulation studies, rainbow trout and zebrafish. The objectives of my thesis were as follows:

1) To clone and sequence ASICs genes from the gill epithelium of rainbow trout (Chapter 2)

2) To verify ASICs expression in the rainbow trout and zebrafish tissues (Chapter 2 and 3)
3) To localize ASICs in the gill epithelium and MRCs of rainbow trout, and zebrafish with the use of anti-ASIC antibody (Chapter 2, 3, and 4)
4) To determine effective concentrations of ASIC inhibiting pharmacological agents, DAPI and diminazene in rainbow trout and zebrafish (Chapter 2, 3, and 4)
5) To compare the effect of ASIC inhibitors on Na^+ uptake with other commonly used Na^+ uptake inhibitors (Chapter 2, and 3)
6) Determination of involvement of ASICs in Na^+ uptake in zebrafish larvae using loss-of-function method employing morpholino antisense oligomers (Chapter 4)
7) To examine effect of Na^+ concentration in external media on ASIC expression and ASIC involvement in Na^+ uptake (Chapter 2, 3, and 4)

Chapter 2:
Acid-sensing ion channels are involved in epithelial Na^+ uptake in the rainbow trout *Oncorhynchus mykiss*

A version of this chapter has been published previously.

Dymowska, A. K., Schultz, A. G., Blair, S. D., Chamot, D., Goss, G. G. 2014. Acid-sensing ion channels are involved in epithelial Na^+ uptake in the rainbow trout Oncorhynchus mykiss. *American Journal of Physiology – Cell Physiology* 307, C255-265.

Introduction

Freshwater rainbow trout are derived from the euryhaline steelhead *Oncorhynchus mykiss*, a species that spends its adult life in the ocean but is born in dilute freshwater, in lakes and rivers flowing to the North Pacific, and to which it returns for spawning (Scott and Crossman, 1998). In contrast to steelhead, rainbow trout are a landlocked strain that spend their entire life in freshwater, yet they retain their ability to migrate to seawater. Freshwater rainbow trout live in oligotrophic mountain lakes and streams that can have extremely low concentration of ions (<50 μM of Na^+ and Cl^-, <25 μM of Ca^{2+}). One of their remarkable features is the ability to actively take up Na^+ and Cl^- from these dilute waters, as measured by unidirectional fluxes (Kerstetter et al., 1970; Kerstetter and Kirschner, 1972). For this reason, they are used as a model species for examination of the mechanisms of ion uptake (particularly Na^+) from waters poor in ions. Despite a long history of using rainbow trout in the study of ion transport, the lack of a sequenced genome has impaired research advances. Only recently has specific molecular information on the mechanisms of ion and acid-base transport emerged. Lately, *nhe2* (*Slc9a2*) and *nhe3* (*Slc9a3*) were cloned from rainbow trout and it was shown that they were present in PNA^+ ionocytes (Ivanis et al., 2008). However, as mentioned in Chapter 1, significant thermodynamic constraints associated with the function of NHEs at very low ion concentrations (Na^+<0.1mM) and low environmental pHs (pH<5) (Avella and Bornancin, 1989; Parks et al., 2008), suggest that fish living in very soft and poorly buffered water would not be able to rely on a NHE-based mechanism for sufficient Na^+ uptake. Recently, the NHE model was revised, whereby the ammonia transporter (Rh protein) present on the apical membrane of MRCs (Nakada et al., 2007; Nawata et al., 2007) forms a functional metabolon with NHE2/3 (Wright

and Wood, 2009). As explained in Chapter 1, the revised model does alleviate the thermodynamic constraints associated with a low environmental pH, but not those imposed by low Na^+ concentrations in the freshwater aquatic environment. Therefore, it is unlikely that this mechanism is the sole contributor to Na^+ uptake by freshwater fishes living in low ionic strength and poorly buffered waters. However, fish physiologists were unable to identify a mechanism alternative to NHE, such as ENaC, since no ENaC homologues have been found in the available teleost fish genomes. Therefore, we hypothesized that other related epithelial Na^+ channels may perform this function.

As described in Chapter 1, ENaC is a member of the amiloride-sensitive ENaC/degenerin (DEG) family of ion channels (Kellenberger, 2008). In vertebrates, the closest relatives to ENaC are the acid-sensing ion channels (ASICs), with which they share ~25% identity (Kellenberger and Schild, 2002). Therefore, we investigated the possibility that ASICs may be responsible for Na^+ uptake in freshwater fishes. Recently, a group of potent ASIC inhibitors has been described in the study by Chen and colleagues (Chen et al., 2010). Diarylamidines are non-amiloride derived ASIC blockers that inhibit ASIC currents at very low concentrations (micromolar range), but do not have an effect on ENaCs. This finding can be exploited to pharmacologically investigate a potential role of ASICs in Na^+ uptake in freshwater fishes.

In this study, we investigated a potential role for ASICs in Na^+ uptake in freshwater fishes using a variety of whole animal, cellular and molecular approaches. We used freshwater rainbow trout as our model organism since their natural habitat includes very low ionic strength waters with Na^+ concentrations and pH below the theoretical limits of the NHE/Rh metabolon model. We identified two trout *asic*

subunits: *asic1* and *asic4* and localized their expression to the gill MRCs. Moreover, using immunohistochemistry, we demonstrated that ASIC protein is located on the apical side of the MRCs.

Materials and methods

Animal holding

Rainbow trout embryos were obtained from Raven brood station (Raven, Alberta) and grown to the appropriate size for experimentation (~ 2 g for flux experiments, 200-500 g as adults for other experiments). Fish were maintained indoors in flow-through 450 l fiberglass tanks supplied with aerated and de-chlorinated city of Edmonton tap water (hardness as $CaCO_3$: 1.6 mM; alkalinity: 120 mg l^{-1}; NaCl: 0.5 mM; pH 8.2; and temp. 15 ˚C). Fish were fed ground dry commercial trout pellets (Purina trout chow) once daily and were kept on a 14 h light:10 h dark photoperiod. All animals used in experiments were approved for use by the University of Alberta Animal Care committee under protocol AUP00000072.

Pharmacological inhibition of Na^+ uptake

For flux studies, juvenile trout were first acclimated to low ionic strength pH 6.0 water for 4 days prior to Na^+ flux experiments. The duration of acclimation was deemed sufficient based on a previous soft water exposure study in rainbow trout (*Salmo gairdneri*) (Spry and Wood, 1985). Fish were transferred to 60 l plastic tubs supplied with aerated re-circulating low ionic strength water (Na^+: 30.0 ± 3.0 μM, Ca^{2+}: 24 μM, Cl^-: 78.0 ± 2.0 μM), and kept at a constant temperature of 15 ˚C. Following acclimation,

two series of flux experiments were completed. The first experiment investigated concentration-dependent effects of two ASIC- inhibiting diarylamidines: 4',6-diamidino-2-phenylindole (DAPI; 0.001, 0.01, 0.1, 1.0 and 10 μM; Sigma) and diminazene (0.0003, 0.003, 0.03, 0.3 and 3.0 μM; Sigma) on Na^+ uptake in juvenile trout. This experiment established the 50% inhibitory concentrations (IC_{50}; Hill function) and optimal concentrations (> 80% inhibition) for both DAPI and diminazene. The second flux experiment compared the effects of two well-known pharmacological Na^+ uptake inhibitors (amiloride: 500 μmol l^{-1}; and phenamil: 50 μmol l^{-1}; Sigma) and the two ASIC inhibitors (DAPI: 1 μM; and diminazene: 3 μM) on Na^+ uptake in juvenile trout.

For all flux experiments, fish were transferred to individual darkened 60 ml flux chambers, supplied with a constant flow of aerated low ionic strength low pH water, and acclimated to the chambers for 24 h prior to experimentation. Unidirectional Na^+ influx was measured using radiolabelled ^{22}Na as described previously (Goss and Wood, 1990). Briefly, flow of water to chambers was turned off, 0.1 μCi l^{-1} of ^{22}Na was added to each chamber and allowed to mix for 5 min, followed by addition to the chambers of either the DMSO control (0.05% DMSO) or pharmacological agents dissolved in DMSO. After a 5 min equilibration period, 6 ml water samples were collected at time 0, 90 min and 180 min as appropriate. At the completion of the experiment, fish were terminally anaesthetized (MS-222 1g l^{-1}) and weighed. Water samples (3 ml) were analyzed for ^{22}Na radioactivity using a Gamma counter (Packard Cobra II, Auto Gamma, Model 5010, Perkin Elmer, MA, USA) and total concentration of Na^+ measured using atomic absorption spectrophotometry (Perkin Elmer, Model 3300, CT, USA). Unidirectional

$^{22}Na^{+}$ influx (μmol kg^{-1} h^{-1}) was calculated for each flux period according to the following equation:

$$JNa_{in}^{+} = \frac{\Delta CPMxV}{SA \cdot t \cdot M}$$

where ΔCPM is the difference between the initial and final radioactivities in the water (cpm ml^{-1}), V is the water flux volume (ml), SA is the average specific activity (CPM μmol^{-1} Na^{+}) as measured at beginning and end of the flux period, t is the time elapsed (h), and M is the mass of the fish (kg).

Tissue collection and preparation

RNA isolation for expression analysis was performed on adult fish. Briefly, fish were euthanized as above, a blood sample withdrawn from the caudal arch and then the brain, head kidney, and trunk kidney were dissected out and immediately freeze clamped in liquid N_2 for later processing. For gill tissue, the animal was first perfused with ice-cold, heparinized (15 mg) phosphate buffered saline (PBS; in mM: 137 NaCl, 2.7 KCl, 4.3 Na_2HPO_4, 1.4 NaH_2PO_4; pH 7.8) and gill tissue or MRCs (as appropriate) obtained according to the protocols described previously by (Galvez et al., 2002). Following perfusion, gill arches were either processed for MRC isolation, freeze clamped in liquid N_2 for RNA isolation, or placed in fixative for immunohistochemistry or SEM (see below).

MRC isolation and cellular imaging.

Following original protocols (Galvez et al., 2002; Parks et al., 2007) adult rainbow trout (~300-500 g) gills were perfused with PBS to remove blood. Subsequently,

gill filaments were removed from the rakers, cut into sections (2-5mm; 3-6 filaments), rinsed in PBS (in mM: 137 NaCl, 2.7 KCl, 4.3 Na_2HPO_4, 1.4 NaH_2PO_4; pH 7.8) and subjected to three (20 min) incubations in 5 ml of 0.05% Trypsin-EDTA with shaking 200 rpm, at room temperature (RT). The subsequent cellular suspensions were passed through a 64-μm nylon mesh filter into 10 ml of ice-cold fetal bovine serum (FBS) and rinsed through with PBS thereby halting trypsin activity. The cells were then centrifuged (5 min at 1,500 x g, 4°C) and washed three times with 25 ml PBS. The final pellet was re-suspended in 2 ml ice-cold PBS and applied to a three-step Percoll density gradient (2 ml 1.09 g ml^{-1}; 2 ml 1.05g ml^{-1}; 3 ml 1.03g ml^{-1}) and centrifuged (45 min, 2000 x g, 4°C, 0-brake). Following centrifugation, the cell layer at the 1.09-1.05 interface was removed and washed three times in ice-cold PBS and re-suspended in 800 μl of ice-cold PBS.

Isolated MRCs (~500,000) in PBS with an additional 2 μl of both $MgCl_2$ (1M) and $CaCl_2$ (1M) to aid in cell attachment, were placed on pre-treated (1M HCl acid washed, 0.1% poly-L-lysine coated, rinsed with ddH2O and 70% ethanol) 15mm round glass coverslips (Warner Instruments; CS-15R) and allowed to attach for 2 h at 4°C. After attachment, coverslips were placed, and following removal of PBS cells were briefly rinsed with Na^+-containing buffer (in mM: 142.5 NaCl, 5.0 $CaCl_2$, 1.0 $MgCl_2$, 4.0 KCl, 15 HEPES, 2.5 $NaHCO_3^-$, pH 7.8). The cells were then incubated for 30 min at 18°C in 200 μl of Na^+-containing buffer with 2 μl of 5mM, pH-sensitive BCECF-AM (50 μg in 16μl DMSO and 20% pluronic acid). Coverslips were placed into a 70 μl imaging chamber (RC-20H; Warner Instruments) for the perfusion experiments. The chamber was then fixed to an inverted fluorescent microscope (Nikon Eclipse TE300) and the cells were subjected to differential interference contrast microscopy and

fluorescent imaging. To allow for BCECF-AM excitation at 495 and 440 nm, the microscope was fitted with a xenon arc lamp (Lambda DG-4; Sutter Instruments, Novato, CA). Images were digitally obtained at both 440 and 495 nm on a mono 12-bit charge-couple device camera (Retiga EXi; QImaging, Burnaby BC, Canada) every 1.7 s during perfusion experiments. The 495/440 nm ratios were digitally compiled using Northern Eclipse software (Mississauga, ON, Canada).

Cell pHi perfusion

Solutions were perfused across the attached MRCs in the holding chamber by gravity feed. Using a six-input manifold (Mp-6; Warner Instruments) attached to 60-ml syringe holder blocks controlled by pinch valves (VE-6; Warner Instruments) monitored manually with VC-6 valve controllers (Warner Instruments), the solutions were perfused at a rate of ~0.5ml min^{-1}. Cells were monitored from original resting state for changes in pH_i when exposed to Na^+-free and Na^+- containing solutions. Starting in Na^+- free conditions (in mM: 142.5 *N*-methyl-D-glucamine-Cl, 2.5 $C_5H_{14}NO{\cdot}HCO_3^-$, 5 $CaCl_2$, 1 $MgCl_2$, 4 KCl, 15 HEPES, pH 7.8), followed by replacement with a Na^+- containing solution, we monitored the activity of the NHE present in trout MRCs following a pH_i disturbance. An identical transition between Na^+-free and Na^+-containing solutions was made but this time in the presence of either 1μM DAPI or 100 μM ethyl-iso-propyl-amiloride (EIPA). EIPA was used in this experiment, since it potently inhibits NHE, but has a low affinity for Na^+ channels (Kleyman and Cragoe, 1988). Perfusion solutions were bubbled with 0.3% CO_2 balanced with O_2 throughout the experiments. At the end of each experimental perfusion, cells were subjected to a final high K^+ solution

calibration protocol (in mM: 120 potassium gluconate, 20 KCl, 2 $MgCl_2$, 20 HEPES) in which four solutions were adjusted to pH levels (~8.40, 7.80, 7.20, 6.60) by the addition of the ionophore nigericin (5 μM) in order to equilibrate pH_i and extracellular pH. The 495/440nm ratios at each step of the pH calibration were used to form a regression equation for each individual cell trace. This equation was then extrapolated to the raw ratio data obtained over the entire time course, yielding a calibrated pH_i for each individual cell monitored during the perfusion experiment. Data was collected and analyzed for each calibrated individual cell by comparing the rate of alkalinization ($\Delta pHi/\Delta t$) under the control parameters with that in the presence of the drug to determine % inhibition.

Preparation of total RNA

Total RNA was extracted from frozen tissues using TRIzol® reagent (Invitrogen, Carlsbad, CA, USA) according to the manufacturer's instructions. RNA was treated with DNase I (Ambion, Austin, TX, USA) according to the manufacturer's protocol, followed by an on-column cleanup using RNeasy Mini Kit (Qiagen, Mississauga, ON, Canada). The quality of the extracted RNA was assessed by either a 2100 Bioanalyzer (Agilent Technologies, Palo Alto, CA, USA) or by visualization on a formaldehyde gel. The RNA concentration was measured with a NanoDrop® ND-1000 UV-vis Spectrophotometer (NanoDrop Technologies, Rockland, DE, USA).

Molecular cloning and phylogenetic analysis

RACE-ready cDNA was synthesized from gill RNA using a SMARTer RACE cDNA Amplification Kit (Clontech, Mountain View, CA, USA) as per manufacturer's instructions. cDNA solutions were diluted 1:10 with Tricine-EDTA buffer provided in the kit and stored at -20°C.

Oligonucleotides for cloning of ASIC1 and ASIC4 genes were designed with PrimerQuest (Integrated DNA Technology) (Table 2.1) based on conserved regions in available *asic* mRNA sequences from zebrafish, tilapia, pufferfish, stickleback, and cod (NCBI, Ensembl). Sequences were aligned with GeneDoc (version 2.6.0.2, http:/www.psc.edu/biomed/genedoc) and ClustalX (version 1.81) software. DNA sequences encoding the 5' and 3' termini of ASIC1 and 5' terminus of ASIC4 genes were obtained using Advantage® 2 PCR Kit (Clonetech) with RACE ready cDNA templates generated from gill RNA. *asic4* 3' terminus was obtained using degenerate primer (Table 2.1). Resulting PCR products were excised from the gel and purified with a QIAquick® Gel Extraction Kit (Qiagen). Subsequently, amplicons of interest were either sequenced directly or ligated into pJET 1.2 vector using CloneJET kit (Thermoscientific) for verification. Recombinant plasmids were transformed into competent cells (One Shot® TOP 10 Chemically Competent *E.coli*, Invitrogen). Colonies were screened for plasmids containing inserts of the correct size by agarose gel electrophoresis and sequenced with pJET1.2 specific primers provided in the CloneJET kit.

The amino acid sequences derived from our cloned trout *asic4* and *asic1* genes (accession numbers KF964646- ASIC1 and KF964645- ASIC4, respectively) together

Table 2.1. Primer sets for cloning and tissue distribution of ASICs

Procedure	Gene	Primer Sequence
Cloning	*asic1*	
	5’	5’ TCACCCAGCAACCCTGCGAACTCGT 3’
	3’	5’ ACACCCTGCAACATGACGCGCT 3’
	asic4	
	5’	5’ GATGTCCCGTCCGGTTGAAGATGTC 3’
	F	5’ CCCAGTAACATCAAGTGTGTCG 3’
	R	5’ YYARCANGCRAARTCYTC 3’
RT PCR	*asic1*	
	F	5’ AAGTCCACTCCCATAGA 3’
	R	5’ CAGCCAGGTTATTCCTT 3’
	asic4	
	F	5’ CTTTCGTTTCTCTGCTCTCACC 3’
	R	5’ CAAGACCAGGAAGTTGTCTCTG 3’
	gapdh	
	F	5’ AAGGGTGAGGTGAGCATGGA 3’
	R	5’ GCTTTACCCCATGGGATCTCAT 3’

5’, 5’ RACE primer; 3’, 3’ RACE primer; Y=C +T; R=A+G; N=A+G+T+C

with the previously annotated amino acid sequences of ASIC1, 2, 3, and 4 from various fish species and other taxa were aligned and analyzed using Seaview software (v. 4; http://pbil.univ-lyon1.fr/software/seaview). A rooted phylogenetic tree showing evolutionary relationships between the different ASIC proteins was generated using maximum likelihood method and LG model and 700 bootstrap re-samplings.

Reverse-transcription polymerase chain reaction (RT-PCR)

Tissue specific cDNA templates utilized for RT-PCR were synthesized from 3µg of RNA from either gill, MRCs, kidney, brain, or blood using SuperScript III Reverse Transcriptase (Invitrogen) according to protocols provided by the manufacturer. ASIC4 and ASIC1 amplicons were obtained using primers designed with PrimerQuest (Table 2.1). PCR conditions were as follows: 98°C for 1 min of initial denaturation followed by 35 cycles of denaturation at 98°C for 10s, annealing at 62°C for 30s, elongation at 72°C for 40s, with the final elongation at 72°C for 10min. PCR products were visualized by 1% agarose gel electrophoresis followed by ethidium bromide staining.

Immunoprecipitation of ASIC4 and western blot analysis

An anti-zebrafish ASIC4.2 (zASIC4.2) polyclonal antibody was custom made (21^{st} Century Biochemicals, Marlboro, MA) against two peptides corresponding to regions near A) the N-terminal (aa 146-160; PKSRKGHRPSELQYP) and B) the C-terminal (aa 519-533; CFEEVKVKAANDVAQP) of zASIC4.2 protein (accession no. Q708S3.1). The polyserum was then affinity-purified against each of these peptides independently and this study used the N-terminal peptide purified antibody exclusively.

Immunoprecipitation was performed according to the technique described by Goss and colleagues (Goss et al., 1996). Briefly, trout gills were perfused with heparinized ice cold PBS (Ca^{2+} free), and the second and third gill arches were dissected out and washed three times in ice cold PBS. Gill rakers were removed and the remaining gill arches were cut into 200-300 mg sections. Each section was lysed for 30 min in 2-3 ml of lysis buffer (100mM NaCl, 4mM KCl, 50mM HEPES, 5mM EDTA, pH 7.4, and 1% of Triton-X) containing protease inhibitors (Complete mini, EDTA-free protease inhibitor tablets; Roche Diagnostics GmbH, Mannhein, Germany). After centrifugation to remove the debris (5000g for 5 min at 4°C), the lysates were incubated with 2-4 µl of anti-zASIC4.2 antibody at 4°C over night on an end-over-end rotator. The next day, 60 ul protein A - Sepharose CL4b beads (Sigma Chemical Co., St. Louis, MO) pre-swelled in IP buffer (100mM NaCl, 4mM KCl, 50mM HEPES, 5mM EDTA, pH 7.4) and pre-blocked with 1% bovine serum albumin (BSA fraction V; Sigma) were added to the lysates and incubated at 4°C for 4-6h on the rotator. Following the incubation, the supernatant was removed and the beads were washed 3 times with 1ml of IP buffer. After the washes, the beads were incubated in Laemmli buffer for 15min at 65°C, centrifuged and the supernatant retained for western analysis as described previously (Tresguerres et al., 2006). Briefly, the samples were separated on a 7.5% polyacrylamide mini-gel and transferred to a nitrocellulose (NC) membrane using a wet transfer system (Bio-Rad Laboratories, Hercules, CA). The NC membrane was blocked in 5% BSA in Tris-buffered saline with Triton X-100 (0.2%) (TBST) for 30 min and incubated with rabbit anti-zASIC4.2 antibody (1:1000 dilution) on a rocker at 4°C overnight. The membrane was washed four times for 15 min each with TBST, blocked again with 5% BSA for 15

min and then incubated with a secondary horseradish peroxidase-conjugated goat anti-rabbit antibody (Santa Cruz Biotechnology, Dallas, TX) at 1:50,000 dilution, at room temperature for 1 h. The NC membrane was washed four times in TBST and the immunoreactive bands were visualized using a SuperSignal West Pico Chemiluminescent Substrate kit (Thermoscientific) following the manufacturer's instructions.

Scanning electron microscopy (SEM) and immunohistochemistry

For examination of the surface of the gill by SEM, filaments were fixed in 3% glutaradehyde, 2% paraformaldehyde in 0.15mM sodium cacodylate buffer (pH 7.4, 290 mOsM) for 1 h at 4 °C, dehydrated in a graded series of ethanol and critical point dried. Samples were then mounted on an SEM stub, sputter-coated with gold and examined with a SEM (Joel Model JSM-6301FXV).

For immunohistochemistry, gills were excised from adult rainbow trout, fixed in 4% paraformaldehyde in PBS (pH 7.4) overnight at 4˚C, dehydrated in a graded series of ethanol and embedded into paraffin blocks. Serial sections (5 μm) were cut and rehydrated in a decreasing ethanol series followed by double distilled water. Rehydrated sections were incubated in 10 mM citrate buffer, at 70°C, for 1h for epitope retrieval. After incubation, slides were washed in PBS and then blocked with 6% milk powder in a humidified chamber for 1h. Sections were then incubated overnight at 4°C simultaneously with the anti-zASIC4.2 antibody (1:400) and anti-Na^+/K^+-ATPase monoclonal antibody (1:400) (NKA; anti-chicken alpha-5 subunit; Developmental Studies Hybridoma Bank, University of Iowa) followed by secondary FITC conjugated

anti-mouse antibody (1:500, Invitrogen, Oregon, USA) and TRITC conjugated anti-rabbit antibody (1:500, Invitrogen, Oregon, USA). Slides incubated with pre-immune serum from the anti-zASIC4.2 antibody production in place of primary antibody were used as a negative control. Slides were viewed with a laser scanning confocal microscope (Zeiss LSM 710, Germany) at the Cross Cancer Institute Cell Imaging Facility, Edmonton, Alberta. Images were processed with LSM Image Browser (v. 4.2.0.121; Carl Zeiss). Surface rendering and three-dimensional (3D) reconstruction of Z-stack images were performed using Imaris software (v. 6.2.2, Bitplane, Zurich, Switzerland).

Statistical analysis

Na^+ flux data were subjected to statistical analysis and are reported as the mean ± S.E.M. All pharmacological experiment data sets were tested for homogeneity of variance and compared using a one-way ANOVA (SigmaPlot ver. 11, Systat, Chicago, IL, USA). If significant differences ($p \leq 0.05$) were found, a post-hoc multiple comparisons Tukey test was applied to determine these differences. A paired t-test ($p \leq 0.05$) was used in the imaging experiments to compare the relative inhibition of $\Delta pHi/\Delta t$ in isolated cells under control conditions and after addition of each pharmacological inhibitor.

Results

Pharmacological inhibition

Exposure of juvenile rainbow trout to increasing concentrations of DAPI resulted in a concentration-dependent decrease of Na^+ uptake with > 90% inhibition observed at concentrations at or above 1 μmol l^{-1} (Figure 2.1A). The concentration at which there was a 50% inhibition of Na^+ uptake (IC_{50}) was calculated to be 0.12 μmol l^{-1} DAPI. Exposure to diminazene also resulted in a concentration-dependent decrease in Na^+ uptake in juvenile trout with a maximum reduction of Na^+ uptake from 303 ± 43 μmol kg^{-1} h^{-1} (control) to 51 ± 19 μmol kg^{-1} h^{-1} (79%) after exposure to 3.0 μmol l^{-1} diminazene (Figure 2.1B). The IC_{50} for diminazene was calculated to be 0.96 μmol l^{-1}.

Sodium uptake rates in juvenile rainbow trout were all significantly lower in the first 90 min flux time period after exposure to 500 μM amiloride (17 ± 18.5 μmol kg^{-1} h^{-1}), 1 μM DAPI (29 ± 18.9 μmol kg^{-1} h^{-1}), and 3 μM diminazene (41 ± 33.4 μmol kg^{-1} h^{-1}) when compared to the control (539 ± 170.9 μmol kg^{-1} h^{-1};Fig. 2.2); while 50 μM phenamil (299 ± 107.9 μmol kg^{-1} h^{-1}) did not significantly reduce Na^+ uptake rate. However, during the second consecutive flux period between 90 and 180 min of exposure to the pharmacological agents, the inhibition was less pronounced but still significant for amiloride (104 ± 33.4 μmol kg^{-1} h^{-1}) and DAPI (141 ± 62.7 μmol kg^{-1} h^{-1}), while diminazene (297 ± 41.5 μmol kg^{-1} h^{-1}) was no longer significantly different from control (393 ± 44.1 μmol kg^{-1} h^{-1}; Figure 2.2).

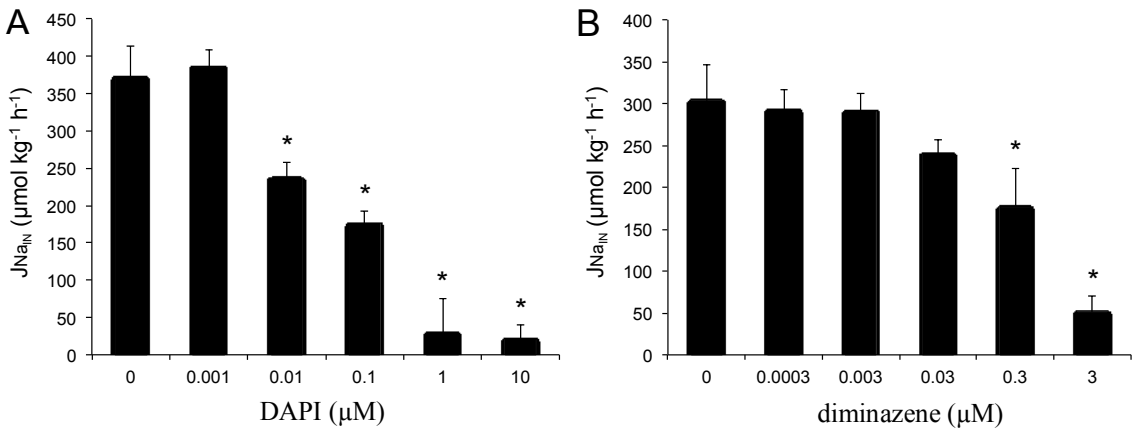

Figure 2.1. Dose-dependent decreases in Na^+ uptake rates in juvenile trout acclimated to low Na^+ (30 μM) and low pH (pH=6.0) water and in the presence of increasing concentrations of diarylamidines, A) DAPI and B) diminazene. Values are mean ± S.E.M. (n = 6). Asterisk (*) denotes significant differences between treatments and control ($p < 0.05$).

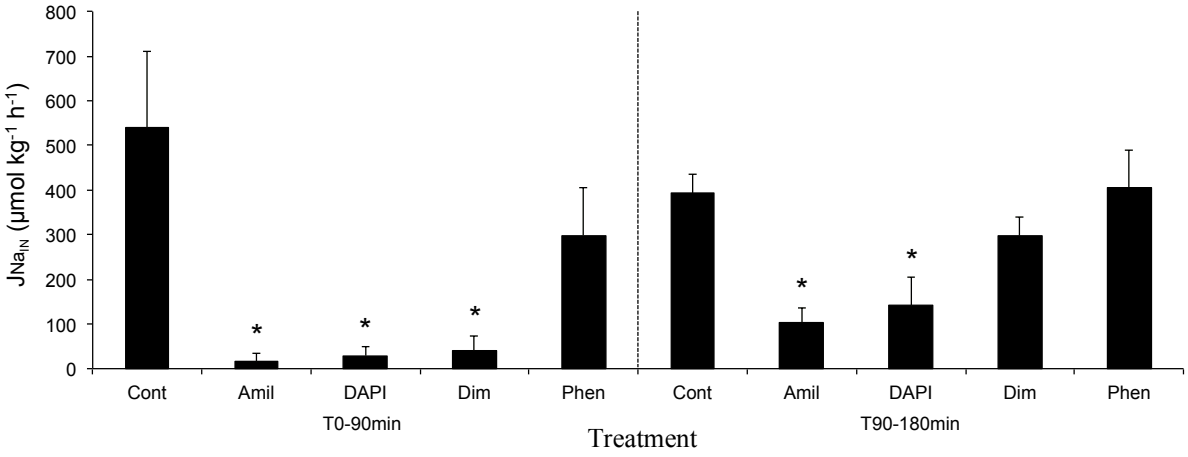

Figure 2.2. Effects of pharmacological agents during consecutive 90 min measurements of Na^+ uptake in juvenile trout exposed to low Na^+ (30 µM) and low pH (pH=6.0). Values are mean ± S.E.M. (n = 6). Asterisk (*) denotes significant differences between treatments and control ($p < 0.05$).

MRC pH_i imaging

Results presented from the whole animal flux experiments showed that administration of DAPI at various concentrations significantly inhibited Na^+ uptake (Figure 2.1A). In order to demonstrate that this inhibition was in fact due to DAPI blocking ASIC type of Na^+ channels rather than affecting NHE activity, we conducted experiments using intracellular pH (pH_i) imaging. NHE activity was measured by examining the rate of pH_i alkalization ($\Delta pHi/\Delta t$) upon exposure of MRCs to a Na^+ containing medium (145mM) in the absence or presence of the either DAPI (1 μM) or EIPA (100 μM).

A representative trace (Figure 2.3A) shows Na^+-dependent alkalization following application of Na^+-containing medium (first rise), while addition of EIPA significantly decreased the rate of alkalization (second rise). The combined results (n=19) show a control of 0.642 ± 0.040 $\Delta pH_i/\Delta min$ while the alkalization rate was reduced 62% by the presence of the EIPA (0. 240 ± 0.036 $\Delta pH_i/\Delta min$) ($p<0.001$) (Figure 2.3B). For DAPI, Na^+ dependent alkalization following Na^+ application was similar in the presence or absence of DAPI (Figure 2.3D). There were no noted differences in $\Delta pHi/\Delta t$ between control (0.542 ± 0.042 $\Delta pH_i/\Delta min$) and DAPI treated cells (0.578 ± 0.047 $\Delta pH_i/\Delta min$) ($p=0.149$, n =22) (Fig. 2.3D).

Phylogenetic analysis and tissue distribution of asic1 and asic4

Two distinct DNA fragments whose derived amino acid sequences exhibit similarity to the ASIC family were cloned from the gill of rainbow trout. To determine their identity, we conducted a phylogenetic analysis by comparison to known ASIC homologues from

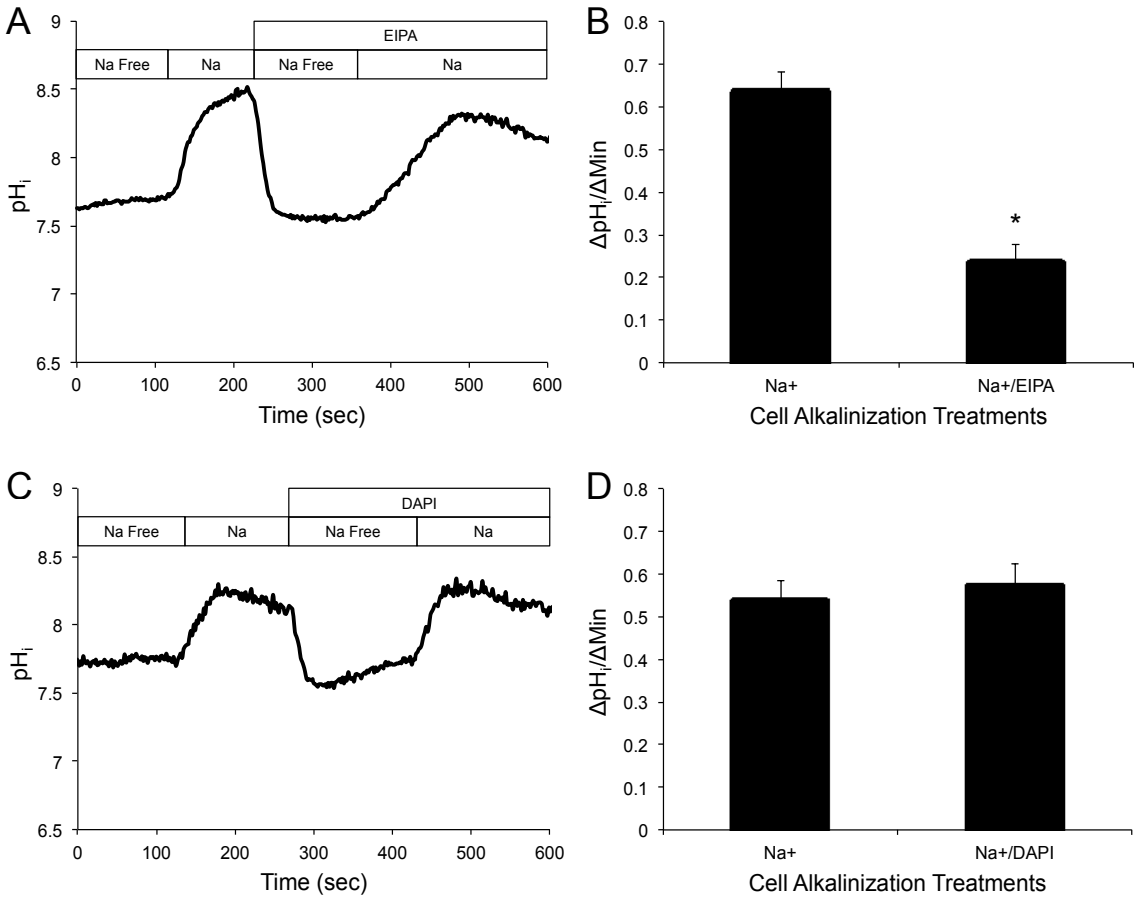

Figure 2.3. Effect of EIPA and DAPI on the Na+-induced alkalinization of the PNA^+ cells following the Na^+-free exposure at resting pH (pHi). A) Representative trace demonstrating inhibition of cell alkalinization by EIPA (100µM), B) Quantitative analysis of cell alkalinization in the absence and presence of EIPA (~62% inhibition; *$p < 0.001$, paired t-test, n=19 cells). C) Representative trace demonstrating lack of effect on cell alkalinization in the presence of DAPI (1µM), D) Quantitative analysis of cell alkalinization in the absence and presence of DAPI (*$p > 0.05$, paired t-test, n= 22).

a variety of species. The generated phylogenetic tree (Figure 2.4) showed that the two cloned rainbow trout *asic* genes (*tasics*) were members of the *asic1* and *asic4* subunits, respectively. The *tasic1* (partial clone) grouped most closely with *asic1* from Salmon (*Salmo salar*), while the *tasic4* grouped with other identified *asic4* family members from other fish and mammal species.

Further, we conducted a tissue distribution analysis of *tasic1* and *tasic4* by RT-PCR. We observed mRNA expression of *tasic1* in all tested tissues: gill, MRCs, head and trunk kidney, brain, and blood. *tasic4* had a slightly different distribution whereby it was present in the perfused gill, MRCs, brain, and trunk kidney, but absent in head kidney and blood tissues (Figure 2.5).

Immunoprecipitation and immunostaining with anti-zASIC4.2.

To determine if ASIC4 was present in the fish gill and to validate our antibody for later immunocytochemistry, we performed an immunoprecipitation (IP) using an antibody raised against zASIC4.2 based on sequence similarly of ~60% between zASIC4.2 (aa 146- 60: PKSRKGHRPSELQYPP) and the cloned tASIC4 (aa 142-156: PKNREGHKPTDLDYPA). We analyzed the precipitates for the presence of ASIC4 using Western blotting (Figure 2.6A) and found a single band of ~65 kDa, which approximates the predicted size for tASIC4 (60.4 kDa). The strong band at ~ 55kDa corresponds to the IgG heavy chain.

To determine the location of ASIC4 protein within the rainbow trout gill tissue, fixed sections were double labelled with anti-zASIC4.2 antibody (Figure 2.6B) and anti-NKA, and then counterstained with the nuclear stain DAPI. Immunoreactivity was

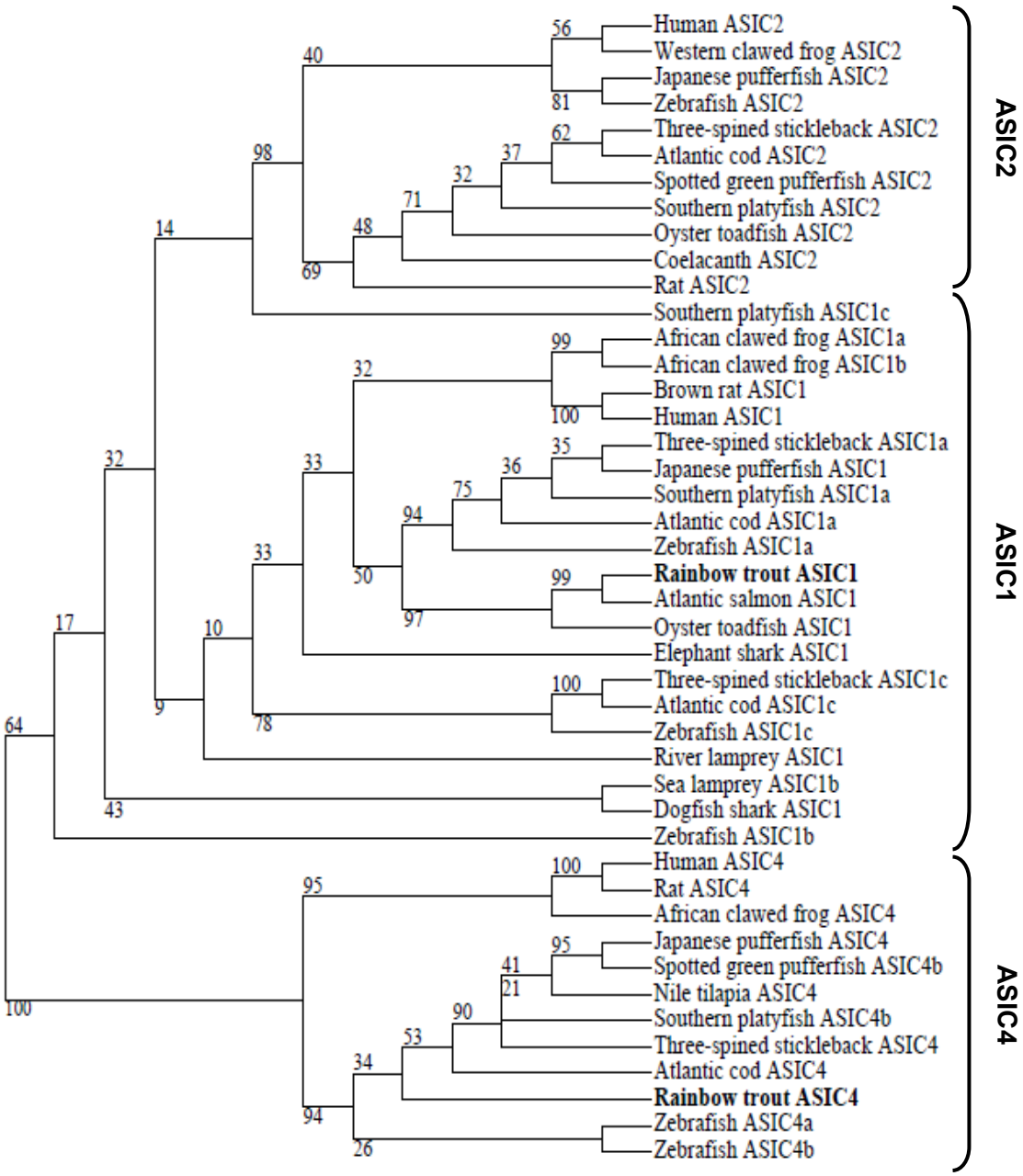
Human ASIC2
Western clawed frog ASIC2
Japanese pufferfish ASIC2
Zebrafish ASIC2
Three-spined stickleback ASIC2
Atlantic cod ASIC2
Spotted green pufferfish ASIC2
Southern platyfish ASIC2
Oyster toadfish ASIC2
Coelacanth ASIC2
Rat ASIC2
Southern platyfish ASIC1c
African clawed frog ASIC1a
African clawed frog ASIC1b
Brown rat ASIC1
Human ASIC1
Three-spined stickleback ASIC1a
Japanese pufferfish ASIC1
Southern platyfish ASIC1a
Atlantic cod ASIC1a
Zebrafish ASIC1a
Rainbow trout ASIC1
Atlantic salmon ASIC1
Oyster toadfish ASIC1
Elephant shark ASIC1
Three-spined stickleback ASIC1c
Atlantic cod ASIC1c
Zebrafish ASIC1c
River lamprey ASIC1
Sea lamprey ASIC1b
Dogfish shark ASIC1
Zebrafish ASIC1b
Human ASIC4
Rat ASIC4
African clawed frog ASIC4
Japanese pufferfish ASIC4
Spotted green pufferfish ASIC4b
Nile tilapia ASIC4
Southern platyfish ASIC4b
Three-spined stickleback ASIC4
Atlantic cod ASIC4
Rainbow trout ASIC4
Zebrafish ASIC4a
Zebrafish ASIC4b
ASIC2
ASIC1
ASIC4

Figure 2.4. (previous page) Phylogenetic analysis of amino acid sequenced of cloned rainbow trout asic1 and asic4 and asics from various fish species**.** Phylogenetic tree was constructed using maximum likelihood method, and numbers indicate bootstrap values for 700 re-saplings. The GenBank or ENSEMBL accession numbers are as follows: Human *asic2*, NP_001085.2; Western clawed frog *asic2*, XP_002933086.2; Japanese pufferfish *asic2*, XP_003964871.1; Zebrafish *asic2*, NP_999953.1; Three-spined stickleback *asic2*, ENSGACG00000009558; Atlantic cod *asic2*, ENSGMOT00000019145; Spotted green pufferfish *asic2*, ENSTNIG00000014943; Southern platyfish *asic2*, ENSXMAG00000008283, Oyster toadfish *asic2*, AAP45633.1; Coelacanth *asic2*, ENSLACG00000007191; Rat *asic2*, NP_037024.2; Southern platyfish *asic1c*, ENSXMAG00000018841; African clawed frog *asic1.1*, AEC48665.1; African clawed frog *asic1.2*, AEC48667.1; Brown rat *asic1*, NP_077068.1; Human *asic1*, NP_064423.2; Three-spined stickleback *asic1a*, ENSGACG00000003075; Japanese pufferfish *asic1*, XP_003963520.1; Southern platyfish *asic1a*, XP_005801801.1; Atlantic cod *asic1a*, ENSGMOG00000009659; Zebrafish *asic1.2*, NP_999955.1; Rainbow trout *asic1*, KF964646; Atlantic salmon *asic1*, NP_001133456.1; Oyster toadfish *asic1*, Q7T1N4.1; Elephant shark *asic1*, AEC48668.1; Three-spined stickleback *asic1c*, ENSGACG00000017974; Atlantic cod *asic1c*, ENSGMOG00000003105; Zebrafish *asic1.3*, NP_999954.1; River lamprey *asic1*, AAY28983.1; Sea lamprey *asic1b*, ENSPMAG00000003813; Dogfish shark *asic1*, AAY28985.1; Zebrafish *asic1.1*, NP_999956.1; Human *asic4*, NP_878267.2; Rat *asic4*, NP_071570.2; African clawed frog *asic4*, AEC48666.1; Japanese pufferfish *asic4*, XP_003962127.1; Spotted green pufferfish *asic4b*, ENSTNIG00000010994; Nile tilapia

asic4, XP_003445446.1; Southern platyfish *asic4a*, ENSXMAG00000003624; Three-spined stickleback *asic4a*, ENSGACG00000007052; Atlantic cod *asic4a*, ENSGMOG00000012740; Rainbow trout *asic4*, KF964645; Zebrafish *asic4.1*, NP_999952.1; Zebrafish *asic4.2*, NP_999951.1.

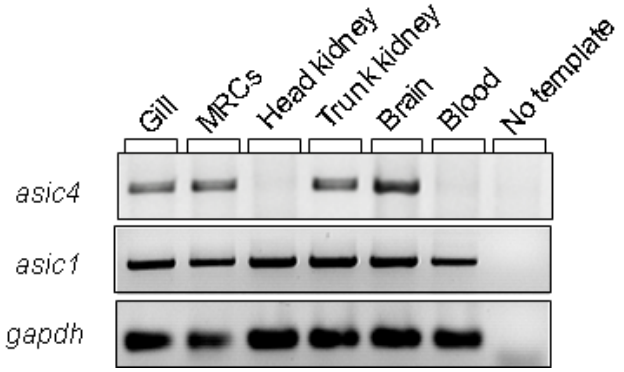

Figure 2.5. Tissue distribution analysis of asic4 and asic1 genes in adult rainbow trout as determined by PCR. GAPDH was used as a reference gene.

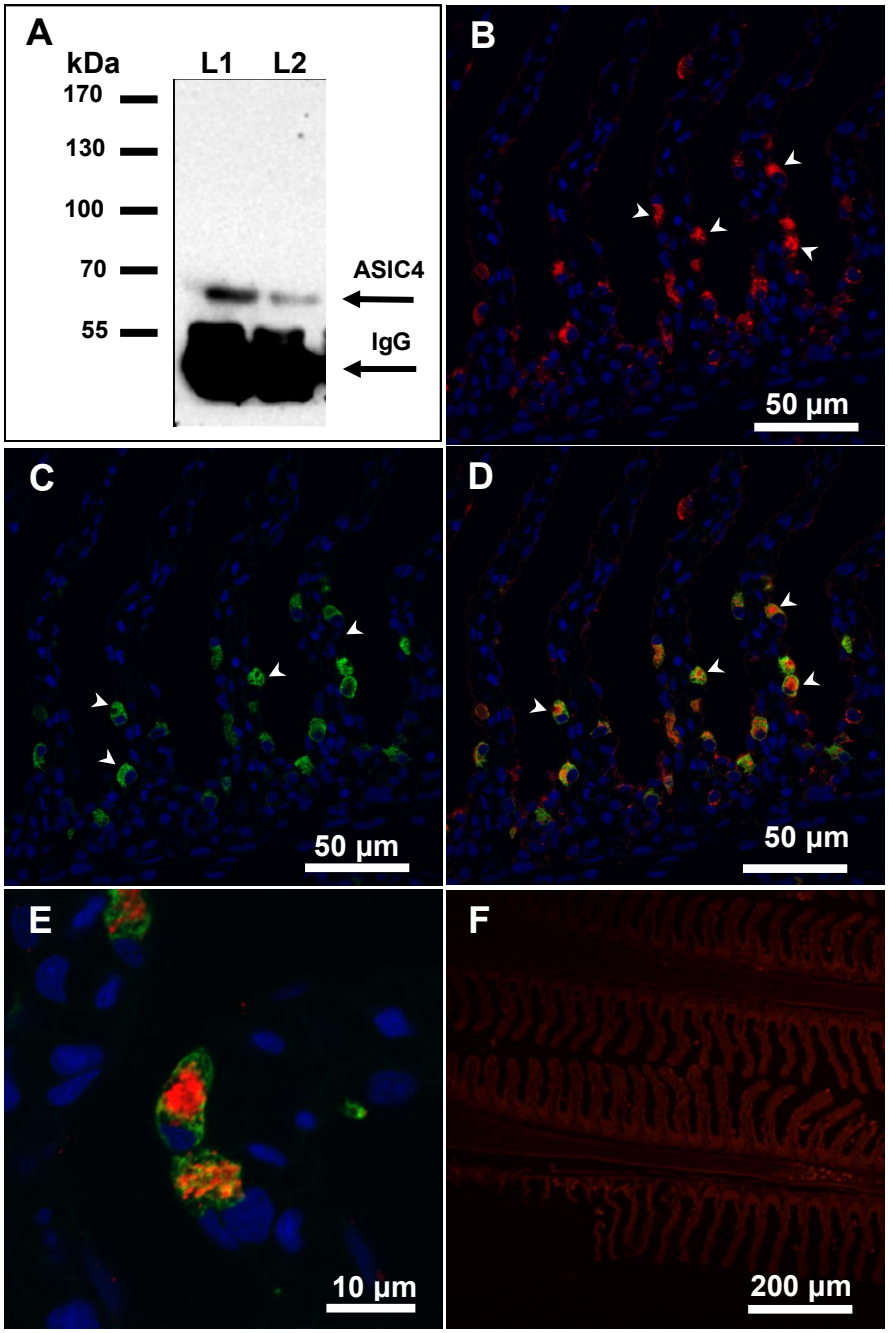
A
kDa
L1
L2
170
130
100
70
55
ASIC4
IgG
B
50 μm
C
50 μm
D
50 μm
E
10 μm
F
200 μm

Figure 2.6. (previous page) Immunoreactivity of the anti- zebrafish ASIC4.2 (zASIC4.2) antibody in the gill of rainbow trout. A) Western blot from whole gill homogenates with zASIC4.2 showing a distinct band of ~65kDa. Lane 1 (L1) contains 300 mg of gill tissue and lane (L2) contains 200 mg of gill tissue. Confocal images of gill sections (*B-E*) labelled for ASIC4 and NKA proteins. Double labelling with B) DAPI and anti-zASIC4.2, and C) DAPI and anti-NKA, D) merged image of B) and C). E) Higher magnification image of mitochondrion-rich cell (MRC) showing that ASIC4 and NKA are present in distinct regions within the MRC. F) Control micrograph with DAPI and no primary antibody. Arrowheads (*B-D*) indicate positive staining as appropriate.

observed in cells located in the lamellae and interlamellar region (Figure 2.6B; arrowhead). Moreover, the majority of cells positive for zASIC4.2 also co-localized with NKA protein (Figure 2.6C,D; arrowhead) a known marker of MRCs, suggesting that in gill epithelium, ASIC4 protein is mainly expressed in MRCs. SEM analysis of the gill filament demonstrated that MRCs are clearly distinguished on the surface of the epithelium and have a broad apical convex opening to the environment (Figure 2.7A; arrowhead). The generated 3D reconstructions of the staining immunoreactivity pattern for ASIC4 and NKA proteins revealed that ASIC4 and NKA were present in the same cells, but in distinct regions of cell. NKA was present on the basolateral membrane (arrows; green staining), while ASIC4 was localized to the broad apical surface of the cell (arrowhead; red staining). Figure 2.7B shows a generated image with a top view, while Figure 2.7C is the same cell as viewed from the side.

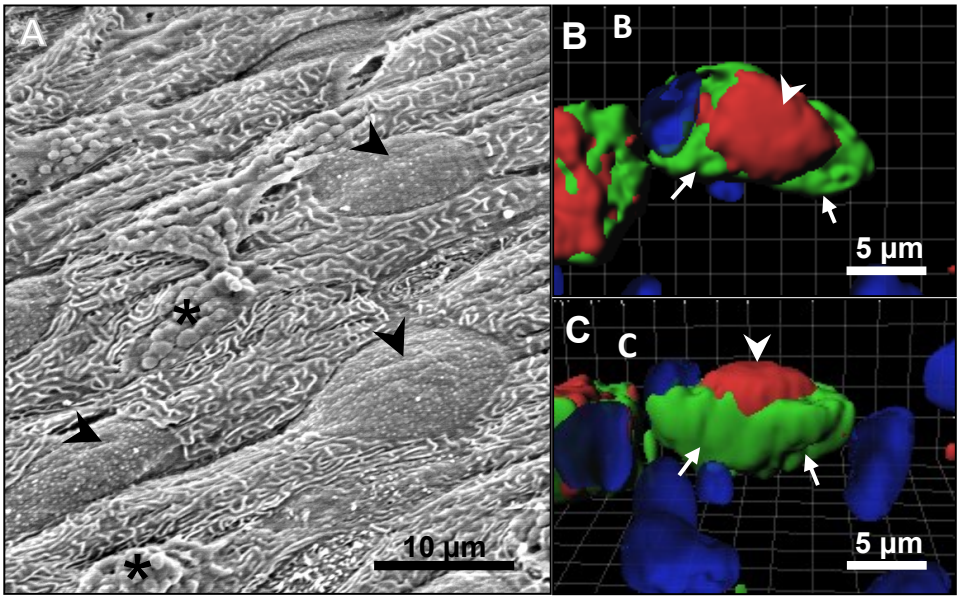

Figure 2.7. Three-dimensional (3D) views of freshwater rainbow trout MRCs. A) Scanning electron micrograph of freshwater rainbow trout gill epithelium showing broad apical openings of MRCs (arrowheads) and mucous cells (*). (*B-C*) 3D reconstruction of Z-stack images showing apical localization of ASIC4 protein (red; arrowhead) and basolateral localization of NKA (green; arrow). B) Top view. C) Side view.

Discussion

The existence of an apical Na^+ channel electrochemically coupled to a VHA mediating Na^+ uptake from dilute freshwaters has been postulated on theoretical thermodynamic grounds for a number of decades (Avella and Bornancin, 1989; Parks et al., 2010; Perry, 1997). However, an inability to determine the molecular identity of the Na^+ channel has been a major drawback in the general acceptance of the model. Using a combination of pharmacological blockade, isotopic fluxes, immunocytochemistry and molecular biology, we propose that an ASIC family member is potentially the long sought after apical Na^+ channel responsible for Na^+ uptake by rainbow trout acclimatized to water with low Na^+ and low pH. This study provides the first evidence for a non-neuronal role for ASICs in any vertebrate, whereby in freshwater fishes gill, ASICs are associated with the MRCs and tASIC4 localizes to the apical membrane of NKA positive cells.

ASICs are a broad family of Na^+ specific ion channels that have been extensively studied in mammalian models (Kellenberger, 2008; Kellenberger and Schild, 2015), with only a few studies performed in any fish species (Springauf and Grunder, 2010; Paukert et al., 2008; Vina et al., 2013). To date, ASICs had primarily been associated with neuronal tissues, with studies focusing on a neuronal function for ASICs (Kellenberger and Schild, 2015). In this study, *asic1* and *asic4* were cloned in rainbow trout using PCR and they were expressed in a variety of tissues, both neuronal and non-neuronal in origin (Figure 2.5). Importantly, *tasic1* gene was present in all five investigated tissues, including whole blood. It appears that *tasic4* gene has a more defined tissue distribution than *tasic1*, with expression in both the ionoregulatory tissues (trunk kidney and perfused gill) and the brain. Unlike *tasic1*, there was no apparent

expression of *tasic4* in the head kidney or the blood. Therefore *tasic4* expression in tissues like MRCs and perfused gill could not be attributed to blood contamination.

Both *tasic1* and *tasic4* genes were expressed in the gill epithelium, and more specifically they were present in the MRCs of rainbow trout gills. It is believed that, similar to ENaCs, functional ASIC channels are trimers (Jasti et al., 2007) although their configuration has not yet been resolved. It has been demonstrated that with a few exceptions ASICs function as either homomers (forming channels of identical subunits) or heteromers (forming channels with other ASIC subunits) (Chen et al., 2007, Kellenberger and Schild, 2015). Currently, ASICs have been characterized by using oocyte expression in both zebrafish (Paukert et al., 2004; Chen et al., 2007) and dogfish shark (ASIC 1b only; Springauf and Grunder, 2010). It has been found that co-expression of zASIC4.1 with zASIC1.3 in *Xenopus* oocytes increased the current amplitude and abundance (~15-fold) of the channel at the cell surface indicating that these two ASIC subunits form a functional channel (Chen et al., 2010). Moreover, this ASIC4.1/1.3 heteromeric channel was more efficiently trafficked to the plasma membrane and had increased affinity for H^+. Additionally, zASIC 4.1, when heterologously expressed in Xenopus oocytes, has also been shown to be gated open by decreases in extracellular Ca^{2+}. The signal responsible for gating of zASIC 4.2 was unable to be determined in that study (Chen et al., 2010). It is therefore possible that tASIC1 and tASIC4 form a heteromeric channel in MRCs but this cannot be determined at this time, and would require confirmation by immunohistochemistry with an anti-ASIC1 antibody that is immunoreactive for rainbow trout. It is also possible that other ASIC subunits and/or regulatory elements may be involved in the function of ASICs in

the freshwater trout gill. A full characterization of tASIC4 by oocyte expression and electrophysiology is required to understand the mechanisms of gating in low Na^+, low Ca^{2+} waters.

In our study, ASIC4 protein was co-localized with NKA, and was present on the apical surface of cells, suggesting that it is found primarily in MRCs (Figure 2.6D,E). Previous studies on ASICs in fishes have suggested that they are primarily associated with neuronal tissue and sensory cells (Springauf and Grunder, 2010; Paukert et al., 2004; Levanti et al., 2011; Vina et al., 2013). Morphological studies of adult and developing zebrafish using confocal immunofluorescence techniques demonstrated that gill MRCs come into direct contact with nerve fibers in the basolateral region (Jonz and Nurse, 2006; Jonz and Nurse, 2008). However, in our study, ASIC4 protein was clearly localized to the apical region of the MRCs as demonstrated by 3D reconstruction of confocal images. ASIC4 immunoreactivity did not overlap with the standard basolateral immunoreactive pattern associated with NKA (Figure 2.7B,C). Therefore, we conclude that neuronally-derived tissues cannot account for the expression of ASIC4 protein in MRCs. We also corroborate the ASIC4 staining pattern with the MRC external morphology which shows that in freshwater rainbow trout raised in Edmonton tap water (Na^+=~ 800 μM), the MRCs have wide apical openings (Figure 2.7A). This apical localization of ASIC4 protein in the cells of a transporting epithelium is the first evidence for a non-neuronal function for any ASIC member and suggests that ASIC4, as a Na^+ channel, may be responsible for apical uptake of Na^+ in freshwater fish.

Pharmacological profiling has long been used to differentiate the mechanisms of ion transport across epithelial tissues. For Na^+ transport, classical analysis has usually

involved amiloride and its substituted derivatives (e.g. EIPA, MIBA, phenamil) as a means to differentiate between the involvement of NHE isoforms and ENaC in Na^+ transport (Kleyman and Cragoe, 1988). We investigated two newly described ASIC specific inhibitors, diminazene and DAPI (Chen et al., 2010), for their potency in inhibiting unidirectional Na^+ uptake in fish. Both diminazene and DAPI exhibited a dose-dependent inhibitory relationship and both were very effective at low concentrations (Figure 2.1). Na^+ uptake in rainbow trout acclimatized to low ionic strength, acidic water was clearly inhibited by these diarylamidines at concentrations similar to those reported by a previous study in cultured rat hippocampal neurons (Chen et al., 2010). However, in our study, DAPI proved to be more effective than diminazene, which is in contrast to what was observed in rat neurons. The inhibition of $^{22}Na^+$ uptake by DAPI and diminazene was also compared to other common Na^+ transport inhibitors: amiloride and phenamil. Amiloride was observed to be an effective inhibitor of Na^+ uptake in rainbow trout but only at relatively high concentrations (500 μM), which is consistent with previous studies (e.g. Perry and Randall, 1981; Boisen et al., 2003). Recently, amiloride has also been demonstrated to completely block ASIC mediated currents (Paukert et al., 2004; Springauf and Grunder, 2010; Chen et al., 2010), however, it is also known to block many other Na^+ transporters including NHE and ENaC (Kleyman and Cragoe, 1988). Amiloride, therefore, cannot be used as a distinguishing pharmacological agent.

While DAPI, diminazene and amiloride almost completely blocked Na^+ transport in the present study, phenamil had no significant effect on Na^+ flux in rainbow trout. This suggests that phenamil is a poor inhibitor of Na^+ uptake in trout exposed to low

ionic water (Na^+ =30 μM). There have been inconsistent results in past studies that have examined the effects of phenamil on Na^+ uptake in a variety of freshwater fishes. For example, in neon tetras acclimatized to low Na^+ (50 μM), phenamil had no effect on Na^+ transport (Preest et al., 2005), whereas it caused over 70% reduction in Na^+ influx in *Cyprinidon variegatus hubbsi* (Na^+=100 μM) and 60% reduction in goldfish (Na^+=300 μM) (Boisen et al., 2003; Preest et al., 2005). These conflicting results from various phenamil studies suggest that sensitivity to phenamil might be species and/or environment specific. Collectively, the pharmacological analysis suggests that the observed Na^+ uptake in freshwater rainbow trout is most likely not mediated by ENaC, given the lack of inhibition by phenamil, but may be attributed to ASIC, since Na^+ uptake was almost completely blocked by DAPI and diminazene, both of which inhibit ASICs but not ENaC.

In our Na^+ flux study with various pharmacological agents we made an interesting observation that inhibition of $^{22}Na^+$ uptake was less pronounced for all tested inhibitors during the second consecutive measurement (90-180 min) (Figure 2. 2). We are unaware of any previous study on fish reporting this phenomenon, where efficacy of the tested drug diminishes over time. This observation may be explained by either a decreased stability of the tested pharmacological agents in aqueous media, metabolism of the drug by the animal, or activation of compensatory Na^+ uptake mechanisms not sensitive to amiloride, DAPI, or diminazene. We believe that the observed decrease of the efficacy of amiloride, DAPI and diminazene over time demonstrates the importance of proper experimental design and choice of period of study when examining ion fluxes using pharmacological inhibitors.

While the two novel ASIC inhibitors have been tested for their potency in inhibiting ASICs and ENaC in neurons (Chen et al., 2010), they have not previously been tested for their potential effects on other sodium transporters implicated in Na^+ uptake in fishes, most notably, the NHEs. To verify that the Na^+ uptake inhibition caused by DAPI and diminazene in rainbow trout was due to inhibition of ASICs directly rather than NHEs, we tested the effect of DAPI on MRCs isolated from the rainbow trout gill epithelium. Our laboratory has previously shown that rainbow trout possess two populations of MRCs: PNA positive (PNA^+) and PNA negative (PNA^-) MRCs (Galvez et al., 2002). It has been demonstrated that NHE3 and NHE2 are both expressed in PNA^+ cells isolated from branchial epithelium of freshwater rainbow trout (Ivanis et al., 2008). Therefore, we investigated the effect of DAPI on PNA^+ cells and compared it to the effect of EIPA, a potent and highly selective inhibitor of NHE (Kleyman and Cragoe, 1988). Earlier studies in our lab using cell imaging determined that PNA^+ cells undergo NHE-dependant alkalinization (Parks et al., 2007; 2010). Here we demonstrate that while EIPA was effective at inhibiting NHE function in PNA^+ cells (Figure 2.3A), there was no effect of high concentrations of DAPI on Na^+-dependent pH_i elevation, demonstrating that NHE was not inhibited by DAPI (Figure 2.3B). Therefore, the measured inhibition of Na^+ uptake by DAPI that we see in whole animals (Figure 2.1) cannot be attributed to inhibition of NHE.

Based on the mRNA expression of tASIC1 and tASIC4 genes in the gill epithelium and isolated MRCs, localization of ASIC4 protein to the apical region of the MRCs, and pharmacological blockade of Na^+ influx by ASIC inhibitors in adult rainbow trout, we propose a revised model for transepithelial Na^+ uptake in freshwater rainbow

trout gills (Figure 2.8), whereby one apical mode of Na^+ entry is via an ASIC4 mediated mechanism.

A number of recent studies on Na^+ uptake in freshwater fishes have demonstrated the presence of the NHE/Rh metabolon in the gills of various species (e.g. Nakada et al., 2007; Nawata et al., 2007, Hung et al., 2007). As mentioned previously, we specifically targeted the rainbow trout as a model for this study as it is native to oligotrophic, Na^+-poor mountain streams with low buffering capacity. This type of environment presents key thermodynamic challenges to the NHE/Rh metabolon as Na^+ restrictions cannot be alleviated by the presence of an Rh protein (see Chapter 1). Moreover, searches of rainbow trout genomes and transcriptomes have failed to identify any ENaC subunits (alpha, beta and gamma), despite the fact that rainbow trout are known to actively take up Na^+ from water with Na^+ concentrations below 50 μM (Wood and Randall, 1973). Furthermore, other studies have suggested and demonstrated an apical localization of the VHA in the gills of rainbow trout (Sullivan et al., 1996; Wilson et al., 2000) and bafilomycin, a VHA specific inhibitor, has been demonstrated to reduce Na^+ uptake in zebrafish (Boisen et al., 2003), tilapia and carp (Fenwick et al., 1999). Previous studies have proposed VHA to be a part of the NHE/Rh metabolon (Wright and Wood, 2009; Shih et al., 2012), however the placement of an apically oriented VHA is counterintuitive to the function of an NHE as it would exacerbate the noted thermodynamic constraints. Placement of a VHA in concert with an apical ASIC is more plausible since it would not only facilitate Na^+ uptake from very low ionic strength water but could also provide a mechanism for gating of ASIC mediated Na^+ conductance.

It still remains to be determined if ASIC and VHA proteins co-localize to the same type of MRCs.

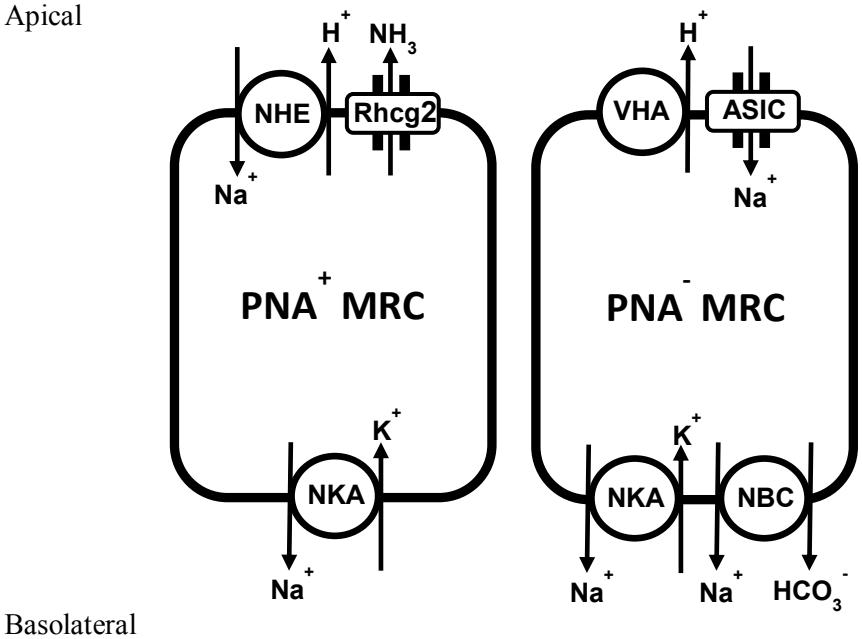

Figure 2.8. Model for Na^+ uptake in PNA^+ and PNA^- MRCs in the gill of rainbow trout showing placement of proposed ASIC mediated Na^+ uptake mechanisms.

Chapter 3:
The role of acid-sensing ion channels (ASICs) in epithelial Na^+ uptake in adult zebrafish, *Danio rerio*

A version of this chapter has been published previously.

Dymowska, A. K., Boyle, D., Schultz, A. G., Goss, G. G. 2015.The role of acid-sensing ion channels (ASICs) in epithelial Na^+ uptake in adult zebrafish (*Danio rerio*). *Journal of Experimental Biology.*218, 1244-1251.

Introduction

In the previous Chapter 2, *asic1* and *asic4* were cloned from the gill cDNA of the adult rainbow trout, and using immunohistochemistry ASIC4 was apically localized to MRCs rich in NKA. Additionally, ASIC-specific inhibitors DAPI and diminazene (Chen et al., 2010), were demonstrated to decrease Na^+ uptake in a dose-dependent manner in juvenile rainbow trout acclimated to a low Na^+ (~50 μM) environment (Chapter 2).

In this Chapter of my thesis, I investigated whether ASICs are involved in branchial Na^+ transport in another model organism used for ion transport research, the zebrafish (*Danio rerio*). Zebrafish are stenohaline freshwater cyprinoids that inhabit rivers in India (Briggs, 2002). In recent years, it has become one of the most intensively studied model organisms in the field of integrative physiology. Research on ion transport in zebrafish has greatly benefited from these fish being amongst the earliest teleost species to have their genome fully sequenced and relatively well annotated. Moreover, the ease of husbandry, rapid generation time, well-defined development and the availability of advanced molecular manipulations (e.g. reverse genetics) have allowed the elucidation of ion transport mechanisms to proceed rapidly. Currently, zebrafish is the most popular model organism to for use in studies of freshwater fish ionoregulation (e.g.,Boisen et al., 2003; Hwang, 2009; Kumai and Perry, 2011; Shih et al., 2012; Yan et al., 2007). Moreover, zebrafish are the only fish species in which ASICs have been extensively studied and characterized. To date, six subunits have been cloned from embryonic zebrafish brain and eye (ASIC 1.1, 1.2, 1.3, 2, 4.1, and 4.2) and each subunit is encoded by a different gene (Grunder et al., 2000; Paukert et al., 2004; Sakai et al., 1999; Waldmann and Lazdunski, 1998).

The first objective of the study presented in this Chapter was to verify that ASICs are present in the gills of the adult zebrafish. Unlike rainbow trout, which have two distinct MRC sub-types, zebrafish have been demonstrated to have at least four types of MRC in the gill and skin epithelia: VHA-rich cells (HR cells), NKA-rich cells (NaR cells), cells expressing Na^+/Cl^- co-transporter (NCC cells), and K^+-secreting cells (KS cells), with HR cells proposed to be the main site of Na^+ uptake (see Chapter 1). The current model for Na^+ uptake in zebrafish proposes two Na^+ transporters on the apical side of HR MRCs: NHE and an unidentified epithelial Na^+ channel (see Chapter 1). Based on the previous findings in rainbow trout (Chapter 2), we hypothesized that the role of the epithelial Na^+ channel in adult zebrafish gill is assumed by proteins from the ASIC family.

The second objective of this study was to determine whether ASICs are involved in Na^+ uptake at the whole animal level using flux experiments. To achieve this objective, I measured Na^+ uptake using radiotracer ($^{22}Na^+$) analysis in zebrafish exposed to ultra-low (Na^+~50μM; pH=6) and low (Na^+~500μM, pH=8.5) Na^+- containing media in the presence and absence of common Na^+ uptake pharmacological inhibitors, including DAPI. Na^+ concentrations in both exposure media were chosen to span the theoretical limits of the NHE model (Parks et al., 2008). Expression levels of mRNA of different *asic* subunits were evaluated in the ultra-low, low, and high Na^+ (Na^+~1400μM; pH=7) exposures to examine changes in expression associated with a change in environment.

Materials and methods

Animals

Adult zebrafish (*Danio rerio* wild type strain A/B) were obtained from the University of Alberta Aquatic Facility where they were maintained in 30l flow-through tanks supplied with aerated and de-chlorinated conditioned reverse osmosis (RO) water (high Na^+ water Table 3.1; temp. 28°C). Fish were fed twice daily with live brine shrimp (*Artemia salina*; INVE Aquaculture Nutrition) and trout chow (O.S.I. Marine Lab Inc.) and were kept on a 14h light: 10h dark photoperiod. All animals used in the experiments were males due to variability in mass in females caused by the egg mass. The experiments were conducted in compliance with University of Alberta Animal Care protocol AUP00000072.

Exposure to ultra-low and low Na^+ media

For acclimation experiments zebrafish were transferred to temperature controlled (temp. 28°C) 20 l glass tanks containing either ultra-low or low Na^+ media (Table 3.1) for 1 week prior to $^{22}Na^+$ uptake experiments. To prepare ultra-low Na^+ water, ions were added from stock solutions (1M NaCl, 10M $CaSO_4$, 10mM $MgSO_4$) to reverse osmosis (de-ionized) water, followed by addition of KOH or H_2SO_4 to obtain the desired pH level of 6. Alternatively, for low Na^+ water, City of Edmonton de-chlorinated tap water was used. For all exposures approximately 1/2 of the water volume was changed daily to prevent accumulation of nitrogenous waste. Fish were not fed for the duration of the acclimation. Water ion concentrations were monitored daily using atomic absorption spectrophotometery (Perkin Elmer, Model 3300, CT, USA).

Pharmacological inhibition of Na^+ uptake

Sodium uptake in zebrafish acclimated to ultra-low or low Na^+ water was measured in 600 ml, aerated flux chambers using radiolabelled $^{22}Na^+$ as described previously (Goss and Wood, 1990). Briefly, fish (n=6 per treatment) were transferred from the acclimation tank to the flux chamber 1h prior to the measurement to enable chamber acclimation. Radiolabelled $^{22}Na^+$ (either 8 µCi/l or 19 µCi/l as appropriate) was then added to each chamber and allowed to mix for 10 min. For experiments involving pharmacological treatment, pharmacological agents were added 10 minutes prior to $^{22}Na^+$ addition. After 10 minutes of mixing of $^{22}Na^+$, an initial 3 ml water sample was collected while a final flux sample was taken after 90 min of exposure. Zebrafish were then euthanized by overdose with MS-222, removed from the flux chambers, rinsed 3 times in 300 mM NaCl solution, blotted dry, weighed and individually analysed for $^{22}Na^+$ activity by gamma counter (Packard Cobra II, Auto Gamma, Model 5010, Perkin Elmer, MA, USA). Unidirectional $^{22}Na^+$ influx JNa^+_{in} (nmol g^{-1} h^{-1}) was calculated as:

$$JNa^+_{in} = \frac{CPM}{SA \cdot t \cdot M}$$

where CPM (counts per minute) is the total radioactivity of one fish (n=1), SA is the specific media activity (CPM μmol^{-1}), t is the time lapsed (h), and M is the mass of the fish (g).

The first series of fluxes investigated concentration dependent effects of 4',6-diamidino-2-phenylindole (DAPI) at 0, 0.01, 0.1, 1, 10, and 100 µM on Na^+ uptake.

Since DAPI had not been used in adult zebrafish previously, we needed to determine the effective dose. The dose-response study was performed only in zebrafish acclimated to low Na^+ medium, since preliminary Na^+ flux experiments showed insensitivity to DAPI in zebrafish acclimated to ultra-low Na^+ medium. The second series of fluxes investigated the effect of amiloride (200 μM), an inhibitor of NHE, ENaC and ASICs (Kleyman and Cragoe, 1988; Paukert et al., 2004), ethyl-iso-propyl-amiloride (EIPA; 100 μM), an inhibitor with high affinity for NHE but not Na^+ channels (Kleyman and Cragoe, 1988), and 4',6-diamidino-2-phenylindole (DAPI; 10 μM) an inhibitor of ASICs but not ENaCs (Chen et al., 2010) on Na^+ uptake in zebrafish acclimated to either ultra-low or low Na^+ water. All pharmacological agents were dissolved in 0.1% dimethyl sulfoxide (DMSO) and for the control group only 0.1% DMSO was used.

Immunoprecipitation and Western blot

An anti-zebrafish ASIC4.2 antibody was generated as described previously (Chapter 2). Immunoreactivity of anti-ASIC4.2 antibody in zebrafish was validated using IP technique according to the protocol used in Chapter 2. Briefly, whole gill baskets were dissected out of adult zebrafish, washed in ice-cold PBS, and cells lysed in 1ml of IP buffer containing 1% Triton-X for 30 min. The whole lysate was incubated with 4 μl of anti-ASIC4.2 antibody at 4°C over night with agitation. Following the incubation, 60 μl of pre-swelled and pre-blocked protein A-Sepharose CL4b beads (Sigma Chemical Co., St. Louis, MO) were added to the lysate and incubated for 6h on a rotator. After that, the samples were briefly centrifuged, and the supernatant was removed and the beads were washed 3 times with 1ml of the IP buffer. Washed beads

were incubated with 35µl Laemmli buffer for 15 min at 65°C, centrifuged and the supernatant retained for Western blot analysis as described previously in Chapter 2. Briefly, the samples were separated on a 7.5% polyacrylamide mini-gel, transferred to a nitrocellulose membrane, blocked in 5% skim milk in Tris-buffered saline containing Triton X-100 (0.2%) (TBST) and incubated with anti-ASIC4.2 antibody (1:1000) on a rocker at 4°C overnight. Subsequently, the membrane was washed, blocked again with 5% skim milk in TBST and incubated for 1h at room temperature with a secondary horseradish peroxidase-conjugated goat anti-rabbit antibody (1:10,000; Santa Cruz Biotechnology, Dallas, TX). Finally, the membrane was washed and immunoreactive bands were visualized with SuperSignal West Pico Chemiluminescence Substrate kit (Thermoscientific) according to the manufacturer's protocol.

Immunohistochemistry

Gills of zebrafish acclimatized to high Na^+ (Table 3.1) were examined for the presence of ASIC4.2, V-type H^+-ATPase (VHA), and Na^+/K^+-ATPase. Zebrafish were euthanized by an overdose of MS-222 (1g/l), and the second and third gill arches were removed from the gill basket, fixed in 4% paraformaldehyde in PBS (pH=7.4) overnight at 4°, embedded in paraffin blocks, and processed for immunochemistry as described previously in Chapter 2. Briefly, serial sections (4µm) were cut, rehydrated and incubated for 1h in 10 mM citrate buffer at 70°C for epitope retrieval. For co-localization of ASIC4.2 and NKA, sections were incubated with the anti-ASIC4.2 polyclonal antibody (1:250) and anti-NKA monoclonal antibody (1:250; Developmental Studies Hybridoma Bank, University of Iowa) over night, followed by 1h incubation

with TRITC conjugated anti-rabbit (1:500; Invitrogen, Oregon, USA) and FITC conjugated anti-mouse (1:500; Invitrogen, Oregon, USA) secondary antibodies. To analyse co-localization of ASIC4.2 with VHA, consecutive sections were incubated over night with either anti-ASIC4.2 antibody as described above or anti-VHA antibody (1:300; kindly donated by Dr. Steve Perry, University of Ottawa), since both polyclonal antibodies were raised in the same host. Subsequently, sections were incubated for 1h with secondary TRITC conjugated anti-rabbit antibody (1:500; Invitrogen, Oregon, USA) and sections stained with anti-ASIC4.2 were compared with consecutive sections stained with anti-VHA in order to determine co-localization. All slides were analysed with a laser scanning confocal microscope (Zeiss LSM 710, Germany) at the Cross Cancer Institute Cell Imaging Facility, Edmonton, Alberta. Obtained images were processed with LSM Image Browser (v. 4.2.0.121; Carl Zeiss) and Adobe Photoshop software.

Reverse-transcription polymerase chain reaction (RT-PCR)

Total RNA was isolated from zebrafish gill tissues using TRIzol® reagent (Invitrogen, Carlsbad, CA, USA) according to the manufacturer's instructions. Following the isolation, RNA was treated with DNase I (Ambion, Austin, TX, USA) in order to remove genomic DNA and further purified with an on-column cleanup using RNeasy Mini Kit (Qiagen, Mississauga, ON, Canada). The quality of the RNA was then assessed by visualization on a formaldehyde gel and the concentration was measured with a NanoDrop® ND-1000 UV-vis Spectrophotometer (NanoDrop Technologies, Rockland, DE, USA). First strand cDNA was synthesized from 1µg of RNA using SuperScript III Reverse Transcriptase (Invitrogen) according to protocols provided by the manufacturer.

Table 3.1. Ion composition and pH of the exposure media

	Concentration (μM)			
	Na^+	Cl^-	Ca^{2+}	pH
Ultra-low Na^+	49.5±0.5	64±1	308±15	6
Low Na^+ (tap water)	511±25	304±32.5	1179±30	8.5
High Na^+	1420±28	1051±35.5	425±31	7

Gene specific primers for zebrafish *asic1.1*, *1.2*, *1.3*, *2*, *4.1*, and *4.2* were designed with PrimerQuest (Table 3.2). PCR was performed with Phusion polymerase (New England Biolabs, MA, USA) under the following conditions: 98°C for 1 min of initial denaturation followed by 35 cycles of denaturation at 98°C for 10s, annealing at 63°C for 30s, elongation at 72°C for 40s, and with a final elongation at 72°C for 10 min. PCR products were visualized by 1% agarose gel electrophoresis followed by ethidium bromide staining.

Statistical analysis

Data are reported as means ± S.E.M. For Na^+ flux data one-way ANOVA and post-hoc comparison with Tukey test was performed (SigmaPlot version 11, Systat, Chicago, IL, USA).

Table 3.2. Gene specific primers used for RT-PCR

Gene	Primer sequence (5'-3')	Accession number	Amplicon (bp)
asic1.1	F: AACCCAGACGTCAAAGGAACGCTA R: AAGACAGTTTCGAGCCGTCGCTAT	AJ609615	264
asic1.2	F: TCATTGGAGCCAGTATTCTTACC R: GAGAGAGAACAACCACGAGATG	AJ609616	312
asic1.3	F: CACACCTGAGCAGTACAAAGA R: CCACCGATATCACCAAGTAACC	AJ609617	300
asic2	F: GGAAAGCAGATGCTTGTGGACCT R: AGCAGCCAATTGAGATGCGGAAAC	AJ609618	339
asic4.1	F: AACACCATCCTCCCGAATCACCAT R: AGTCCTGCGAAAGGAGTTGGGAAA	AJ609619	305
asic4.2	F: CCAGGAACAGAGGCTAACATA R: CCATAGAGAGCTCTTTCCCATAC	AJ609619	305
elf1α1	F: GGGTCTGTCCGTTCTTGGAG R: TTCTCAGGCTGACTGTGCTG	NM_131263	83

Results

Pharmacological inhibition of Na^+ uptake

To determine if DAPI, an ASIC selective inhibitor (Chen et al., 2010) displayed a similar dose-response inhibition effect on Na^+ uptake in zebrafish to that of rainbow trout, flux experiments using $^{22}Na^+$ were performed on adult zebrafish exposed to low-Na^+ media (~500 μM Na^+; Table 3.1). After 90 min zebrafish showed reduced Na^+ uptake with increasing concentration of DAPI (Figure 3.1). The maximal (but not complete) inhibition of Na^+ uptake rate was observed at 10 μM of DAPI and was equal to 59% of control Na^+ uptake. Increasing DAPI concentration to 100 μM did not result in further decreases in Na^+ uptake.

To determine the relative involvement of Na^+ transporters in Na^+ uptake, DAPI and two other Na^+ inhibitors EIPA, which has a high selectivity for NHE (Ito et al., 2014; Kleyman and Cragoe, 1988), and amiloride, which inhibits both NHE and Na^+ channels (Kleyman and Cragoe, 1988), were tested at low-Na^+ (511±25 μM) and ultra-low Na^+ (49.5 ± 0.5 μM) conditions (Figure 3.2). Zebrafish acclimated to low-Na^+ media exhibited a 55% decrease in Na^+ uptake in the presence of DAPI (10 μM) (Figure 3.2A), which was in agreement with the dose-response experiment (Figure 3.1). Amiloride (200 μM), also reduced Na^+ uptake by 55%, whereas EIPA (100 μM) had no significant effect, although a consistent trend towards increase in Na^+ uptake was noted (Figure 3.2B). In contrast, when zebrafish were acclimated to ultra-low Na^+ media, the control rate of flux was reduced by ~50% (Figure 3.2A), and the effect of the pharmacological agents on Na^+ uptake was no longer observed.

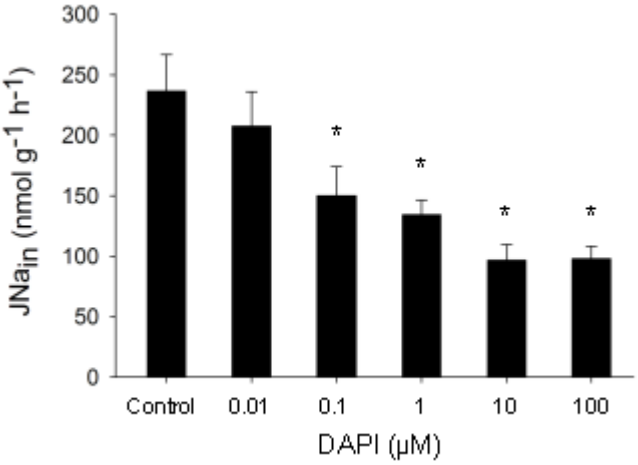

Figure 3.1. The effect of DAPI on Na^+ uptake rates in adult zebrafish acclimated to low Na^+ medium (~500 μM). Values are mean ± S.E.M. (n=6). * Significantly different from the control group (*P<0.05*).

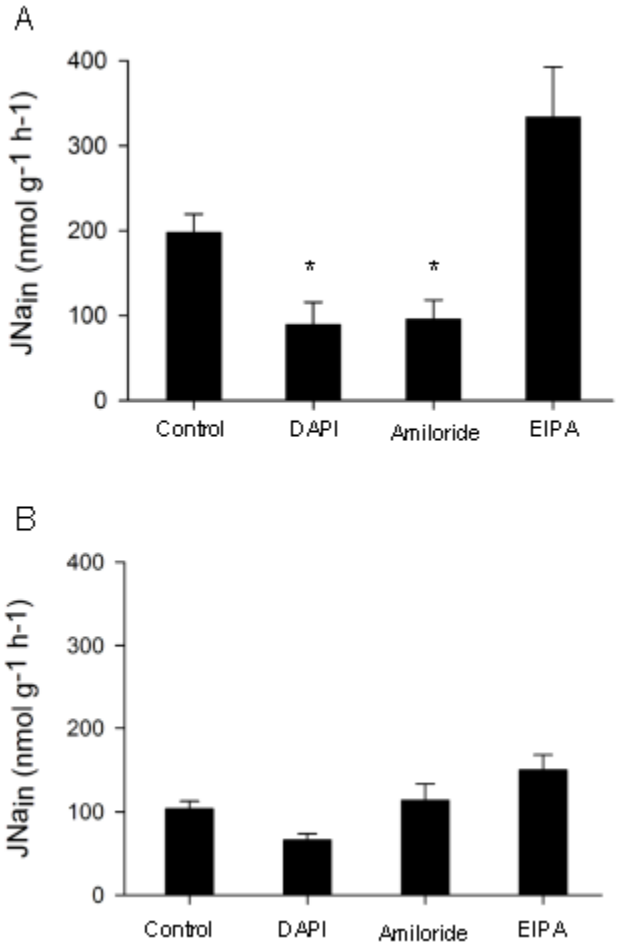

Figure 3.2. The effect of DAPI, amiloride, and EIPA on Na^+ uptake rates in adult zebrafish acclimated to low and ultra-low Na^+ media. Na^+ uptake rates were measured in A) low Na^+ (~500 μM) medium, and B) ultra-low Na^+ (~50 μM) medium. Values are mean ± S.E.M. (n=6). * Significantly different from the control group (*P<0.05*).

ASICs mRNA expression in the gills

The expression pattern of different *asic* subunits (*asic1.1*, *1.2*, *1.3*, *2*, *4.1*, and *4.2*) mRNAs in the gill tissue of zebrafish acclimated to high-, low- and ultra-low-Na^+ water was examined by RT-PCR. Elongation factor 1α1 (*ef1α1* was used as an internal control (primers used are shown in Table 3.2). All 6 *asic* subunits mRNAs were present in the zebrafish gill tissue regardless of the acclimation media (Figure 3.3).

Immunolocalization of ASIC4.2 in zebrafish gills

With the use of a custom made anti-zebrafish ASIC4.2 antibody, we verified the expression of ASIC4.2 in the gills of zebrafish by IP and a single band corresponding to ~65 kDa (predicted size 62.8 kDa) was identified in the gills of multiple independent animals (Figure 3.4). Immunohistological analysis with the anti-ASIC4.2 antibody demonstrated that ASIC4.2 was present in the gills of the adult zebrafish (Figure 3.5B, 3.6B). To determine the cell type to which ASIC4.2 localizes, gills were initially double stained with anti-ASIC4.2 and anti-NKA, a marker of the NaR MRC type in zebrafish (Hwang and Lee, 2007). Cells positive for anti-ASIC4.2 and anti-NKA were observed in the lamellae and interlamellar region of the gills (Figure 3.5B,C), however, ASIC4.2 and NKA did not co-localize, which suggests that the ASIC4.2 transporter is not present in NaR MRCs (Figure 3.5D). To determine if ASIC4.2 co-localizes with other transporting proteins, gills were also stained with ASIC4.2 and VHA, a marker for HR type MRC. Since both the anti-ASIC4.2 and anti-VHA antibodies were raised in rabbit, staining was carried out on consecutive 4 μm sections, to avoid cross-reactivity. Comparison of staining patterns in both sections revealed that many cells positive for anti-ASIC4.2

were also positive for anti-VHA (Figure 3.6D), suggesting that ASIC4.2 protein is localized to HR-type MRCs.

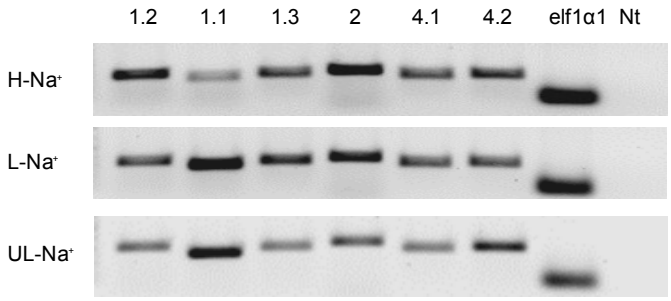

Figure 3.3. RT-PCR analysis of the expression of ASIC family subunits in the gills of adult zebrafish acclimated to high Na^+ (~1200 μM), low Na^+ (~500 μM), and ultra-low Na^+ media (~50 μM). elf1α1 – zebrafish elongation factor used as a positive control, Nt – no template.

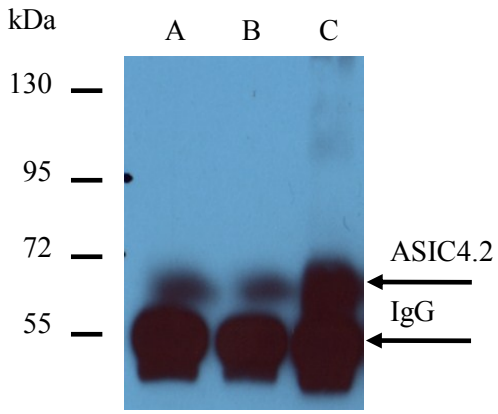

Figure 3.4. Western blot analysis with anti-zASIC4.2 antibody of whole gill homogenates from zebrafish acclimated to high Na^+ medium (~1200 µM). Lanes A and B are gill homogenates from one individual fish, lane C is pooled sample of gill homogenates from two fish. IgG – rabbit immunoglobulin G.

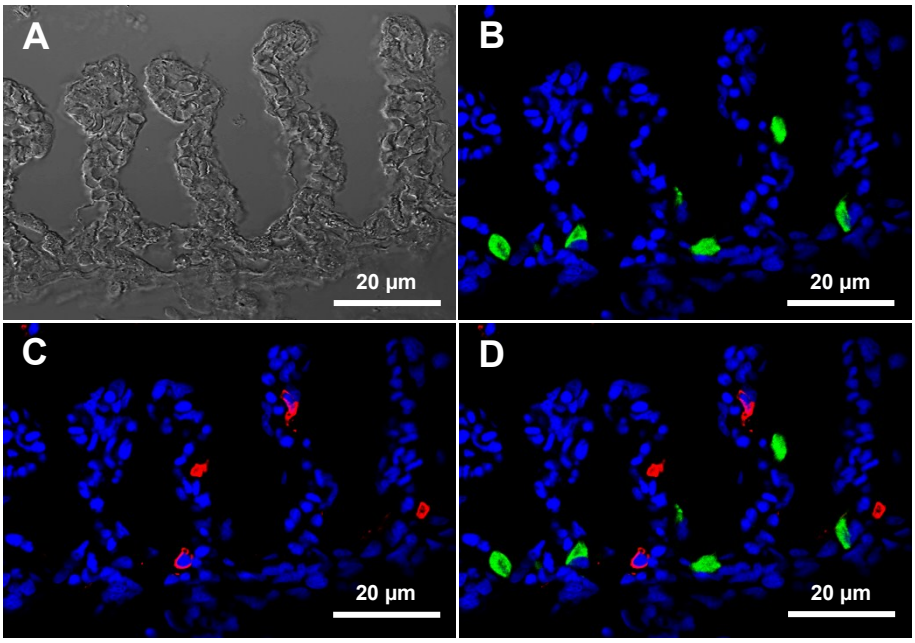

Figure 3.5. Double immunostaining with anti-Na^+/K^+-ATPase (α5) antibody and anti-ASIC4.2 antibody in zebrafish gill. A) Bright field, B) anti-Na^+/K^+-ATPase (green), C) anti-ASIC4.2 (red), D) merged image of B) and C).

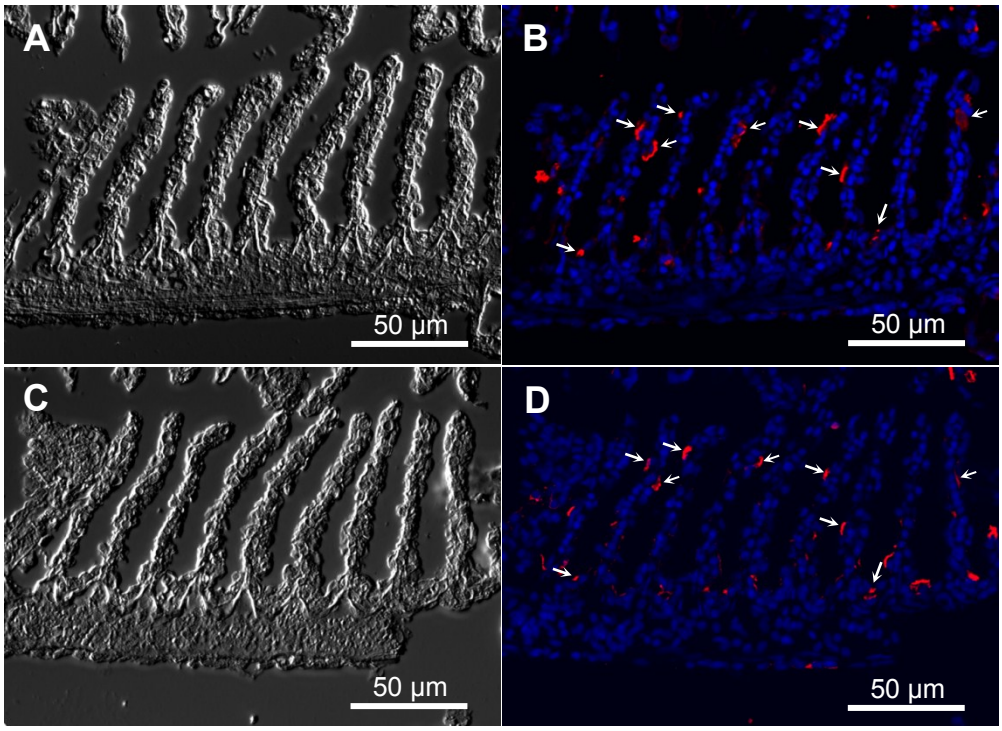

Figure 3.6. Immunostaining with anti-ASIC4.2 antibody and anti-V-H^+-ATPase (VHA) antibody in consecutive sections of zebrafish gill. A) and C) Bright field, B) anti-ASIC4.2 , D) anti-VHA. Arrows indicate cells displaying co-localization of ASIC4.2 and VHA.

Discussion

The objective of the present study was to verify whether ASICs are expressed in the gill tissue of the adult zebrafish, and if they are involved in branchial Na^+ uptake as was shown recently for rainbow trout (Chapter 2). Previous studies on ASICs in zebrafish have demonstrated their widespread expression in the central and peripheral nervous systems, specifically in brain, retina, intestine and taste buds, where they have been suggested to be involved in nerve transduction and neural communication (Levanti et al., 2011; Paukert et al., 2004; Vina et al., 2013). However, their presence and function in the gill epithelium of zebrafish has never before been tested. The present study demonstrates that multiple subunits of *asics* are expressed in the zebrafish gill tissue at the mRNA level, and that ASIC4.2 protein localizes to the MRCs. Pharmacological blockade of Na^+ uptake with ASIC specific inhibitors revealed that ASICs are involved in Na^+ regulation at the whole animal level. Based on the findings in the present study we propose that ASICs play a role in branchial Na^+ uptake in adult zebrafish.

In Chapter 2, *asic4* and *asic1* genes have been demonstrated to be expressed in the MRCs from the gill tissue of rainbow trout. Moreover, ASIC4 protein has been found to co-localize with the NKA, a classic marker for the MRCs in rainbow trout, and expressed in the apical region of the cell. In the present study, I observed that similar to rainbow trout, ASIC4.2 was present in the lamellar and interlamellar region of the adult zebrafish gill. However, staining with anti-ASIC4.2, anti-VHA, and anti-NKA antibodies revealed that in zebrafish gill epithelium ASIC4.2 protein co-localized to the cells expressing VHA, but not to the cells that express NKA. Therefore, I infer that in zebrafish gills, ASIC4.2 protein is present in the HR type of ionocytes. Previous studies

using *in situ* hybridization and immunohistochemistry techniques have demonstrated that HR ionocytes of zebrafish are abundant in NHE3b, and VHA, but in contrast to rainbow trout, they are not characterized by high abundance of NKA (Dymowska et al., 2012; Esaki et al., 2007; Lin et al., 2006; Yan et al., 2007; Chapter 1). Our finding could be further corroborated by co-localization of ASIC4 with NHE3b, however this remains be determined.

In zebrafish, HR cells are suggested to be the primary site for Na^+ uptake and H^+ secretion. This was determined by measurement of H^+ fluxes in the vicinity of HR cells using scanning ion-selective electrode technique (SIET) (Lin et al., 2006). Currently, the most favoured model for Na^+ uptake in freshwater fish, including zebrafish, incorporates an electroneutral NHE since a Na^+ epithelial channel that could alternatively perform that function in the freshwater gill epithelium had never previously been identified. However, previous studies in zebrafish adults and larvae demonstrated that bafilomycin, a specific VHA inhibitor, caused a substantial reduction of Na^+ uptake rates (i.e.,Boisen et al., 2003; Kumai and Perry, 2011; Kwong and Perry, 2013). Moreover, knockdown of VHA subunit A (*atp6v1a*) in zebrafish larvae caused a decrease in whole body Na^+ content in morphants (Horng et al., 2007). Therefore, it is likely that in zebrafish, there exists a secondary, VHA-dependent mechanism for Na^+ transport. The mechanism by which VHA activity promotes Na^+ uptake is not yet known, however two alternatives may exist: firstly VHA charges the apical membrane potential thereby increasing the electrochemical gradient for Na^+ to enter in the cell through ASIC, and secondly that VHA provides a gating signal to ASIC by acidification of the boundary layer, since ASICs are gated by extracellular H^+ ions that activate several amino acid residues

located in different extracellular domains (Bonifacio et al., 2014; Paukert et al., 2008). One complicating factor is that ASIC4.2 was demonstrated to be insensitive to extracellular H^+ (Chen et al., 2007). However, there is evidence that ASICs assemble into homo- or heteromeric trimers (Jasti et al., 2007), therefore it is possible that ASIC4.2 forms a channel with other ASIC subunits that show extracellular H^+ gating. Given that we have demonstrated by PCR the presence of all known isoforms of ASIC in the gill of zebrafish, this may be a scenario by which a heteromeric ASIC channel could mediate Na^+ transport in conjunction with the VHA.

In the present study, use of the ASIC-specific inhibitor DAPI, verified involvement of ASICs in Na^+ uptake in adult zebrafish. DAPI is a diarylamidine, a class of drugs that have been recently shown to block ASIC Na^+ currents in cultured mice hippocampal neurons, but do not block other epithelial Na^+ channels, such as ENaCs (Chen et al., 2010). Recently, DAPI has also been demonstrated to inhibit Na^+ uptake in rainbow trout exposed to ultra-low ionic strength/low pH water (Chapter 2). Moreover, DAPI did not affect the NHE-mediated alkalinisation in isolated NHE-expressing (PNA^+) MR cells from rainbow trout gill, indicating lack of inhibitory effect of DAPI on the trout NHEs (Chapter 2). Since DAPI had not been previously employed in Na^+ transport studies in zebrafish, we demonstrated a dose-dependent inhibitory effect on Na^+ uptake rate in animals acclimated to low ionic strength water. However, unlike in rainbow trout, where DAPI almost completely (>90%) inhibited Na^+ uptake (Chapter 2), in zebrafish the maximal inhibition of Na^+ uptake was ~ 59%, and further increases in DAPI concentration did not cause any further reduction in Na^+ uptake. This result suggests that

other DAPI insensitive mechanism(s) for Na^+ transport exists in the zebrafish gill that could account for the remaining 41% of Na^+ transport capacity (see below).

Given the thermodynamic limitations of various transport systems at low and ultra-low Na^+ concentrations, we combined the use of pharmacological agents inhibiting different Na^+ transporters with acclimation media varying in Na^+ concentration. Our results revealed that the effect of the inhibitors on Na^+ uptake differed significantly between the exposure media at the different Na^+ concentrations examined. Zebrafish acclimated to low-Na^+ water showed a significant reduction in Na^+ uptake rates in the presence of DAPI and amiloride, while fish exposed to ultra-low Na^+ media were insensitive to the presence of DAPI, amiloride, or EIPA. These results suggest the existence of another mechanism for Na^+ uptake in adult zebrafish that is insensitive to any of the inhibitors used in this study.

It should be noted that our experimental protocol included changes in H^+ and Ca^{2+} concentration in the exposure media. For the ultra-low Na^+ medium, the lower pH (pH=6) was chosen specifically to impose thermodynamic constraints on the NHE function. In regard to ASICs, it has been previously shown in toadfish that increase of the external H^+ concentration resulted in activation and opening of more channels (Zhang et al., 2006). Similarly, extracellular Ca^{2+} can modulate ASIC dependence on pH, whereby an increase in external Ca^{2+} concentration shifts the pH required for activation of mammalian ASIC1 and ASIC3 to more acidic values (Babini et al., 2002; Immke and McCleskey, 2003). Additionally, one study demonstrated that a decrease in external Ca^{2+} resulted in increased number of open ASIC1 channels in toadfish (Zhang et al., 2006). Based on these findings, it has been suggested that Ca^{2+} and H^+ compete for the

same binding site (Kellenberger and Schild, 2015). In our study, we observed reduced Na^+ uptake together with insensitivity to ASIC inhibitor in the ultra-low Na^+ exposure media when compared to low Na^+ conditions, which in our case suggests no apparent stimulatory effects of increases in external H^+ and/or decreased (~4 fold) Ca^{2+} on ASIC4 mediated Na^+ uptake.

Previous studies using amiloride and EIPA inhibitors in zebrafish have reported conflicting results. Similar to our findings, Boisen and colleagues (2003) demonstrated no effect of either amiloride or EIPA on Na^+ uptake in adult zebrafish acclimated to ultra-low ionic strength water (Na^+ ~35 μM) (Boisen et al., 2003), while other studies (i.e., Kumai and Perry, 2011; Shih et al., 2012) have demonstrated an effect of EIPA on Na^+ transport in zebrafish larvae. Kumai and Perry (2010), reported a significant reduction in Na^+ uptake by EIPA in 4dpf zebrafish larvae reared in acidic water, while Shih et al. (2012) observed supressed Na^+ gradients (as measured with a SIET electrode) in larvae acclimated to water with very low Na^+ concentration (Na^+ ~50 μM). Therefore, it is possible that amiloride and EIPA sensitivity of Na^+ uptake in ultra-low Na^+ environments is highly variable between zebrafish developmental stages (embryos to adults).

As mentioned above, the results from fluxes in low and ultra-low Na^+ media with DAPI, amiloride and EIPA suggested the involvement of an alternative Na^+ uptake mechanism to NHE and ASIC. One apparent candidate for this alternative Na^+ uptake mechanism is the Na^+/Cl^- co-transporter (SLC12A10.2) that has been demonstrated to be apically expressed in the NCC sub-type of MRCs in zebrafish gill and embryonic skin (Hwang and Lee, 2007; Hwang et al., 2011). Translational knockdown of either *nhe3b*

or *gcm2*, the latter being a transcription factor that controls differentiation into HR cells (Chang et al., 2009) in zebrafish larvae, resulted in a substantial increase in the number of NCC type of MRCs in the morphants, which also coincided with an increased Na^+ content in the *gcm2* morphants (Chang et al., 2013). However, the function of an electroneutral NCC operating as currently described, with 1:1 inwardly directed co-transport of Na^+ and Cl^- is highly questionable to be able to transport Na^+ from a low or ultra-low environment, based on the thermodynamics principles (Hwang et al., 2011; Dymowska et al, 2012).

In conclusion, I have demonstrated the presence of ASIC4.2 in the HR cells located on the zebrafish gill epithelium. Further, using pharmacological blockade with DAPI and amiloride, we demonstrated the involvement of ASIC channels in Na^+ uptake in zebrafish acclimated to low Na^+ media. Additionally, I demonstrated that Na^+ transport in low and ultra-low waters are controlled by a number of different transport systems, and that in ultra-low Na^+ water, Na^+ uptake is insensitive to NHE and ASIC specific inhibitors, suggesting that an alternative mechanism is working at this Na^+ level.

Chapter 4:
ASIC4.2 is involved in Na^+ uptake in zebrafish (*Danio rerio*) larvae

Introduction

In the recent years, the yolk sac of zebrafish larvae has been used as a surrogate model in studies on ion regulation and acid-base balance in freshwater fish (e.g. Lin et al., 2006; Bayaa et al., 2009; Kumai et al., 2014). Similar to the adult zebrafish gill epithelium, zebrafish larvae yolk sac comprises at least four types of MRCs: HR cells, NaR cells, NCC cells and KS cells, with Na^+ uptake occurring on HR cells via NHE and/or Na^+ channel proteins (see Chapter 1). It has been also proposed that NCC may play a minor role in Na^+ balance in adult and larval zebrafish (Hwang and Lee, 2007), however the functional characteristic of this transporter remains to be determined (see Chapter 1). In Chapter 3, I demonstrated that epithelial Na^+ channel ASIC4.2 is expressed in the HR type of MRCs in the gill epithelium of adult zebrafish and using a coupled pharmacology and radiotracer approach to measure Na^+ fluxes demonstrated that ASICs are involved in Na^+ acquisition in these fish. The weakness of the previous approach, however, is an inability to distinguish a specific role for ASIC4.2 as the drug DAPI does not display enough differentiation between the different ASIC subunits. In this Chapter, I applied a loss-of-function approach with the use of the antisense morpholino oligonucleotide (MO) technique, to further investigate the specific role that ASIC4.2 plays in Na^+ uptake in zebrafish,.

MOs, first developed by Summerton (1997) for in vivo inhibition of RNA transcripts, are currently one of the most advanced, reliable and widely used knock down techniques in zebrafish (Eisen and Smith, 2008). MOs are synthetic oligonucleotides designed to inhibit translation of the coding region of the gene of interest, or prevent its proper splicing (Ekker, 2000; Draper et al., 2001; Bill et al., 2009). MOs are delivered to an embryo by direct microinjection into the center of the yolk. Due to the fact that MOs

have a morpholine ring instead of a ribose ring, they are more resistant to nucleases and have been demonstrated to be effective in zebrafish larvae up to 5 days post-fertilization (Kimmel et al., 2003; Bill et al., 2009). In zebrafish, the MO technique has been predominately employed in developmental research studying organogenesis and genetic disorders (e.g., Draper et al., 2001; Kimmel et al., 2003; Bill et al., 2008; 2009). However recently, it has also been effectively applied to studies of ion transport in zebrafish larvae, where morphants have been produced with translational or splice-site knockdown of *ncc* (Chang et al., 2013; Wang et al., 2009), *nhe3b* (Chang et al., 2013), *rhcg1* (Kumai et al., 2011, 2012, Shih et al., 2012), *slc26* (Cl^-/HCO_3^- exchanger; Bayaa et al., 2009), and *apt6v1a* (VHA subunit A; Horng et al., 2007).

The objective of the present study was to expand and verify the results of Chapter 3 by investigating the specific role of ASIC4.2 in transport of Na^+ using the splice-site targeted MO knockdown technique. I chose this mode of MO action over the translational knockdown, as non-functional shortened transcripts may be directly detected by PCR. Morphant larvae were also reared in media with varying levels of Na^+ concentration and pH below and above the thermodynamic limits of the NHE/Rh metabolon model (see Chapter 1) to verify in which conditions ASICs play a predominant role in Na^+ uptake. In parallel, we assessed the sensitivity of Na^+ uptake to DAPI as an indication of involvement of ASICs in Na^+ uptake in zebrafish larvae. Finally, we performed immunocytochemical analysis in order to determine localization of ASIC4.2 in the zebrafish larvae yolk sac.

Materials and methods

Animal holding

Adult zebrafish (*Danio rerio*) were obtained from Big Al's Aquarium Services (Ottawa, ON Canada) and maintained at the University of Ottawa Aquatic Care Facility. Fish were kept in flow-through tanks supplied with aerated and dechlorinated City of Ottawa water at 28°C and under a 14h light: 10h dark photoperiod. Fish were fed daily with No. 1 crumble sourced from Zeigler (Aquatic Habitats, Apopka, FL) to satiation. Animals were bred and embryos collected according to a routine standardised protocol (Westerfield, 2009). Briefly, fish were transferred to grid-bottom breeding tanks at a ratio of 2 females to 1 male per tank and left overnight. The following morning and after fish had spawned at first light, embryos were collected into 50 ml Petri dishes, and picked over to remove non-fertilized eggs.

Embryos were reared in three acclimation media, all supplemented with 0.05% methylene blue to prevent bacterial and fungal growth at 28.5°C. All acclimation media were prepared by adding ions from stock solutions (1 M NaCl, 10 mM $CaSO_4$, 100 mM $MgSO_4$) to distilled water and pH adjusted by addition of KOH or H_2SO_4. Nominal ion concentrations were: control water (Na^+=600 μM, Ca^{2+}=200 μM, Mg^{2+}=200 μM, pH=8), low pH water (Na^+=600 μM, Ca^{2+}=200 μM, Mg^{2+}=200 μM, pH=4), and low Na^+/low pH water (Na^+=50 μM, Ca^{2+}=200 μM, Mg^{2+}=200 μM, pH=6). Dead embryos and debris were removed, and water changed daily. All flux experiments were performed when larvae were 96 hpf. The experiments were performed in compliance with the Canadian Council of Animal Care and under the protocol BL-226 approved by the University of Ottawa.

Antisense knock-down of ASIC4.2

All morpholino antisense oligonucleotides used in this study were designed and synthesized by GeneTools, LLC (Philomath, OR). The zebrafish ASIC4.2 (gene accession no: AJ609619) morpholino was designed to splice out exon 2 of the pre-mRNA transcript (5'-AAACCTGCAGACCAATCACAAGCAT-3'). The morpholino oligonucleotide was delivered to one-cell stage zebrafish embryos at a dose of 2 ng/embryo using a microinjection method described previously by Kumai and Perry (2011). Briefly, the morpholino was diluted to a final concentration of 4 ng/nl with Danieau buffer (58 mM NaCl, 0.7 mM KCl, 0.4 mM $MgSO_4$, 0.6 mM $Ca(NO_3)_2$, 5 mM HEPES, pH=7.6) and supplemented with 0.05% phenol red for visualization. Morpholino solution was then injected into embryos with a microinjection system (IM 300, Narishige, Long Island NY). To control for the effect of microinjection, a group of embryos were injected with a standard control morpholino (5'-CCTCTTACCTCAGTTACAATTTATA-3') (control morphants) as provided by Genetools. After injection, embryos were reared in control, low pH, or low Na^+/low pH medium as described in the previous *Animal holding* section. Both ASIC4.2 and control morpholino oligonucleotides were labelled with carboxyfluorescein, and at 24 hpf embryos were screened for successful morpholino delivery with a fluorescent dissecting microscope (Nikon SMZ1500, Nikon Instruments, Melville, NY). Only embryos with homogenous distribution of carboxyfluorescein throughout the cells were used in subsequent experiments (Figure 4.1).

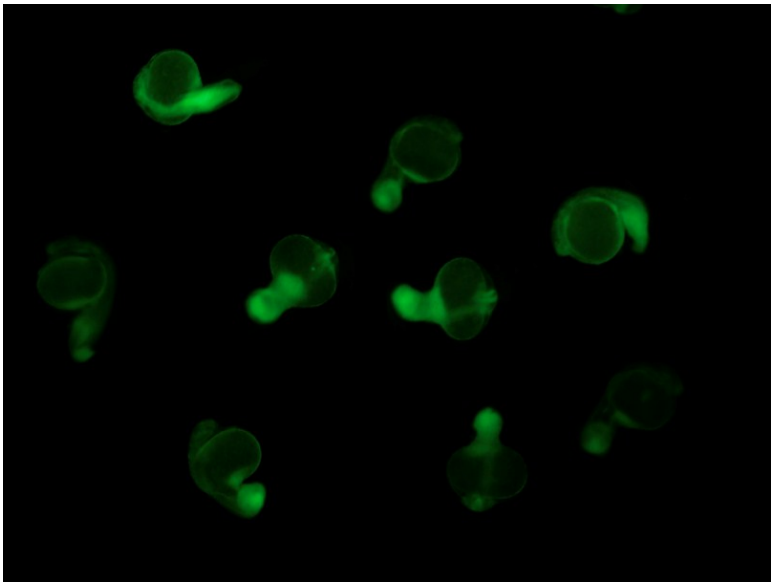

Figure 4.1. Zebrafish morphant larvae (24 hpf) exhibiting homogenous distribution of carboxyfluorescein.

Na^+ uptake and effects of DAPI

Sodium uptake rates in wild type (non-injected), morphant and control embryos reared in either control, low pH, or low Na^+/low pH medium were measured at 96 hpf as described previously (Kumai and Perry, 2011). Briefly, 12 zebrafish larvae (n=6) were transferred to a 2 ml microcentrifuge tube filled with 1.5 ml of the rearing medium and maintained at the temperature of 28.5°C. Radiolabelled $^{22}Na^+$ (0.3 μCi/ml; Perkin Elmer, Woodbridge, ON, Canada) was added to each tube and mixed gently by pipetting. Water samples (50 μl each) were collected at the beginning (at 5 min) and at the end of the 90 min flux period to measure specific activity of the flux media. At the end of the flux, zebrafish larvae were euthanized with an overdose of MS-222 and rinsed 3 times in isotope-free media containing 300 mM NaCl to remove $^{22}Na^+$ loosely adsorbed to larvae. Larvae were then digested in the tissue solubilizer Solvable (Perkin Elmer) for 12 h at 65°C. Scintillation cocktail (Biosafe-II, RPI Corp, Mt. Prospect, IL) was added to water samples (5 ml) and digests (10 ml), and samples with digested larvae were additionally neutralized with 450 μl of glacial acetic acid. Activity of $^{22}Na^+$ in all samples was measured with a scintillation counter (Beckman Coulter LS 6500 Liquid Scintillation Counter, Mississauga, ON) and background corrected by the scintillation counting program. The rate of Na^+ uptake JNa^+_{in} (pmol larva^{-1} h^{-1}) was calculated as:

$$JNa^+_{in} = \frac{DPM}{SA \cdot t \cdot n}$$

where DPM (disintegration per minute) is the total incorporated radioactivity, SA is the specific media activity (DPM $pmol^{-1}$), t is the time lapsed (h), and n is number of larvae (typically two).

To further investigate involvement of ASIC4.2 in Na^+ uptake in zebrafish larvae, animals were exposed to the ASIC inhibitor 4',6-diamidino-2-phenylindole (DAPI) (Chen et al., 2010) and $^{22}Na^+$ uptake rate was measured. Wild type larvae reared either in control, low pH, or low Na^+/low pH medium were subjected to 0.001, 0.01, 0.1, 1, and 10 μM DAPI dissolved in 0.1% dimethyl sulfide (DMSO) at 96 hpf in order to determine effective dose. Additionally, ASIC4.2 morphants reared in low pH medium were exposed to a blocking dose of DAPI (10 μM). DAPI was dissolved in 0.1% dimethyl sulfide (DMSO). Control wild type larvae and control morphants were fluxed in 0.1% DMSO only. DAPI was added to flux tubes at least 5 min prior to addition of the radioisotope.

Reverse-transcription polymerase chain reaction (RT-PCR)

To confirm and quantify the level of effectiveness of the morpholino knockdown, RT-PCR was performed using total RNA. Total RNA was extracted from 96 hpf ASIC4.2 morphants reared in either control, low Na^+, or low pH medium using TRIZOL (Invitrogen, Carlsbad, CA, USA) and according to the manufacturer's protocol. Following extraction, RNA was treated with DNase I (Invitrogen, Carlsbad, CA, USA) for genomic DNA removal, and first strand cDNA was synthesized from 1 μg of RNA using RevertAid M-MNuLV reverse transcriptase (Fermentas, Burligton, ON, Canada) according to the manufacturer's instructions. PCR amplification was carried out using

primers designed with PrimerQuest, located in the splice site boundaries flanking exon 2: forward 5' – GCCGAAGGAAGGATCAGAATA- 3', reverse: 5' – TTCCCATACCGGGTCAAATTAC- 3', using Phusion polymerase (New England Biolabs, MA, USA) in the following conditions: 98°C for 1 min of initial denaturation followed by 35 cycles of denaturation at 98°C for 10 s, annealing at 60°C for 30 s, elongation at 72°C for 90 s, with a final elongation at 72°C for 10 min. PCR products were visualized by 1% agarose gel electrophoresis followed by ethidium bromide staining.

Immunohistochemistry

To determine localization of ASIC4.2 on the zebrafish larvae yolk sac, live 96 hpf larvae were incubated with a medium containing 50 μg l^{-1} of Alexa-633 conjugated ConA (Invitrogen, Burlington, ON, Canada) for 30 min. ConA has been demonstrated by previous studies to work as a marker for HR cells on zebrafish larvae yolk sac (Esaki et al., 2007; Lin et al., 2006; Kumai et al., 2012). Following the incubation with ConA, larvae were euthanized by an overdose of MS-222, washed briefly in PBS and fixed overnight at 4°C in 4% paraformaldehyde in PBS (pH=7.4). After fixation, zebrafish larvae were rinsed in PBS, transferred to 100% ethanol and stored at -20°C. On the day of the immuno-staining, larvae were rehydrated through graded washes with ethanol in PBS and subjected to epitope retrieval by incubating in 150 mM Tris buffer (pH=9) at 65°C for 10 min. Subsequently, larvae were washed several times in PBS with 5% Triton-X (PBST), blocked with 2% goat serum and 2% bovine serum albumin in PBST, and incubated with zebrafish anti-ASIC4.2 antibody that previously have been

successfully used in the rainbow trout (Chapter 2) and adult zebrafish (Chapter 3; dilution 1:100). Simultaneously, anti-Na^+/K^+-ATPase (NKA: dilution 1:250; anti-chicken α5 subunit; Developmental Studies Hybridoma Bank, University of Iowa) antibody was used as a marker for NaR type of MRCs in zebrafish (Hwang and Lee, 2007) at 4°C overnight. The next day, larvae were washed several times in PBST and incubated simultaneously with Alexa-488 conjugated anti-rabbit (dilution 1:500; Invitrogen, Burlington, ON) and Alexa-546 conjugated anti-mouse (dilution 1:500; Invitrogen, Burlington, ON) secondary antibodies for 2 h at 37°C. After incubation, larvae were washed several times in PBST with a final wash in PBS and mounted onto a glass slide. Samples were observed and analyzed using scanning confocal microscope (Leica ZM-510) and images were processed with Zen software (Carl Zeiss).

Statistical analysis

Statistical analyses were performed with SigmaPlot (version 13.0, Systat, Chicago, IL, USA). Data are reported as the mean ± SEM. All Na^+ flux data were analysed with one-way ANOVA and if significant differences ($P \leq 0.05$) were found, a post-hoc Holm-Sidak test was applied.

Results

Pharmacological inhibition of Na^+ uptake by DAPI in wild-type larvae

Exposing zebrafish larvae to increasing concentrations of DAPI did not alter Na^+ uptake rate in animals reared in control medium (Figure 4.2A). However, larvae reared in water with the same ion concentration as the control water, but with a lower pH (pH=4.0), exhibited a ~ 42% decrease in Na^+ uptake rate at DAPI concentration of 0.01 μM, when compared to the control group (Figure 4.2B; 665.4 ± 62.1 and 1146 ± 129.6 pmol $larva^{-1}$ h^{-1}). Further increases in DAPI concentration to 10 μM did not result in further decrease of Na^+ uptake (Figure 4.2B). In larvae reared in low Na^+/low pH medium, Na^+ uptake rate was reduced (by ~51%) only at DAPI concentration of 10 μM (Figure 4.3), when compared to the control group (213 ± 24 and 427.6 ± 12.4 pmol $larva^{-1}$ h^{-1}). Lower concentrations of DAPI were ineffective in this test media.

Na^+ uptake rates were significantly higher in control groups of larvae reared in low pH (Figure 4.2B; 1146 ± 129.6,) and low Na^+/low pH (Figure 4.3; 427.6 ± 12.4) media, than in the control medium (Figure 4.2A:127.7 ± 18.4 pmol $larva^{-1}$ h^{-1}).

The effect of ASIC4.2 knockdown on Na^+ uptake

Knockdown of ASIC4.2 with antisense morpholino oligonucleotide was verified in 96 hpf morphants with the use of RT-PCR. There was a shift of the amplicon size from 1201bp (the predicted size) to ~1055bp confirming successful splicing out of exon 2 (Figure 4.5A). There were no significant differences in Na^+ uptake rate between control morphants and ASIC4.2 morphants reared in a control medium (Figure 4.4A; 165 ±35 *vs.* 135 ± 29.3 pmol $larva^{-1}$ h^{-1}). However, knockdown of ASIC4.2 reduced Na^+ uptake rate

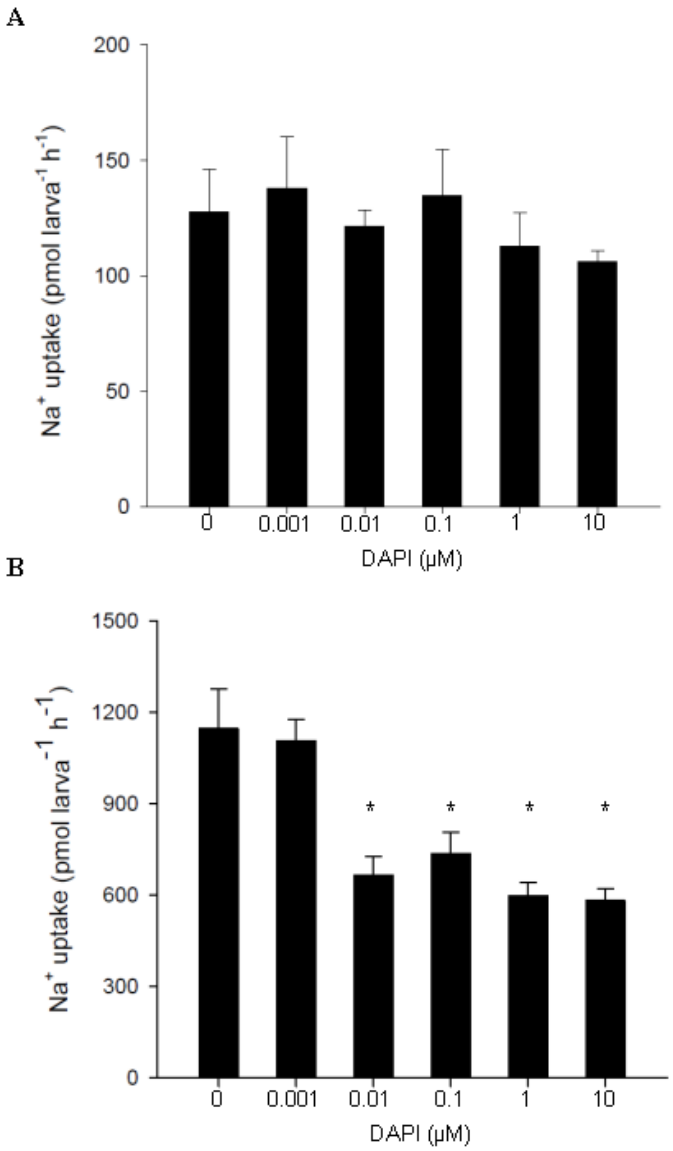

Figure 4.2. The effect of increasing concentrations of DAPI on Na^+ uptake rates in wild-type zebrafish larvae. Larvae were reared in A) control (Na^+=~600 μM; pH=8.0), and B) low pH (Na^+=~600 μM; pH=4.0) media. Na^+ uptake rates were measured in the respective acclimation media. Values are means ± S.E.M (n=6). * Significantly different from the control group ($P < 0.05$).

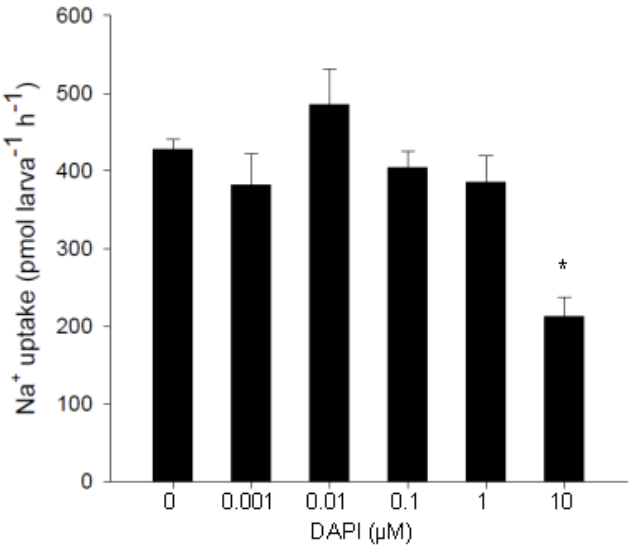

Figure 4.3. The effect of increasing concentrations of DAPI on Na^+ uptake rates in zebrafish larvae reared in low Na^+/low pH medium (Na^+=~50 μM; pH=6.0). Values are means ± S.E.M. (n=6). * Significantly different from the control group ($P < 0.05$).

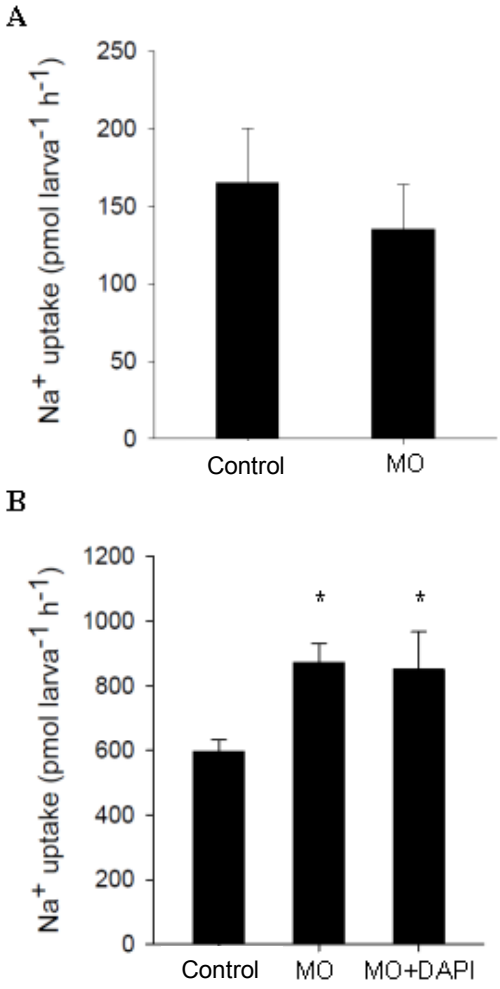

Figure 4.4. The effect of ASIC4.2 knockdown on Na^+ uptake rates in zebrafish larvae. Larvae were reared in A) control (Na^+=~600 µM; pH=8.0) and B) low pH (Na^+=~600 µM; pH=4.0) media. Control- control morphants; MO- ASIC4.2 morphants. B) DAPI treatment did not inhibit Na^+ in ASIC4.2 morphants reared in low pH medium. Values are means ± S.E.M. (n=7-12). * Significantly different from the control group ($P < 0.05$).

in larvae reared in low Na^+/ low pH media by 65% (Figure 4.5B; from 563.9 ± 33.7 pmol $larva^{-1}$ h^{-1} in control to 199.7 ±32 pmol $larva^{-1}$ h^{-1} in ASIC 4.2 morphants). In morphants reared in low pH medium, there was an observed 46% increase in Na^+ uptake in ASIC 4.2 morphants (from 596.7 ± 35.2 pmol $larva^{-1}$ h^{-1} in controls to 872.1 ± 58.9 pmol $larva^{-1}$ h^{-1}; Figure 4.4B). To verify whether other ASIC subunits may account for this increase in Na^+ uptake rate, morphants were additionally subjected to a blocking dose (10 μmol l^{-1}) of DAPI in 0.1% DMSO. DAPI had no effect on Na^+ uptake rate in the ASIC 4.2 morphants. Morphants examined either with or without DMSO (0.1%) did not show any difference in uptake rate and were therefore combined. As in wild type (non-injected larvae), the control rate of Na^+ uptake was significantly higher in larvae reared in both low pH/low Na^+ and low pH media compared to the control media.

Immunostaining with anti-ASIC4.2 antibody

Immunohistological analysis of the 96 hpf wild type zebrafish larvae yolk sac with zebrafish anti-ASIC4.2 antibody revealed the presence of ASIC4.2 protein in a large number of cells present on the yolk sac membrane (Figure 4.6B). Triple staining of ASIC 4.2 with the MRC sub-type markers ConA (Figure 4.6A), and anti-NKA antibody (Figure 4.6C), revealed co-localization of ASIC4.2 with ConA positive cells (Figure 4.6D; arrows), but not with cells staining positive for NKA (Figure 4.6D). To examine the cellular localization of ASCI4.2 within the ConA positive cells, z-stack analysis of the staining profile of ASIC 4.2 and ConA was performed in a representative MRC (Figure 4.7C, C1). ConA staining (Figure 4.7B, B1) was localized to the apical crypt of

the analysed cell, while ASIC4.2 staining revealed more of a punctate pattern (Figure 4.7A) that was localized to the apical region of the cell (Figure 4.7A, A1).

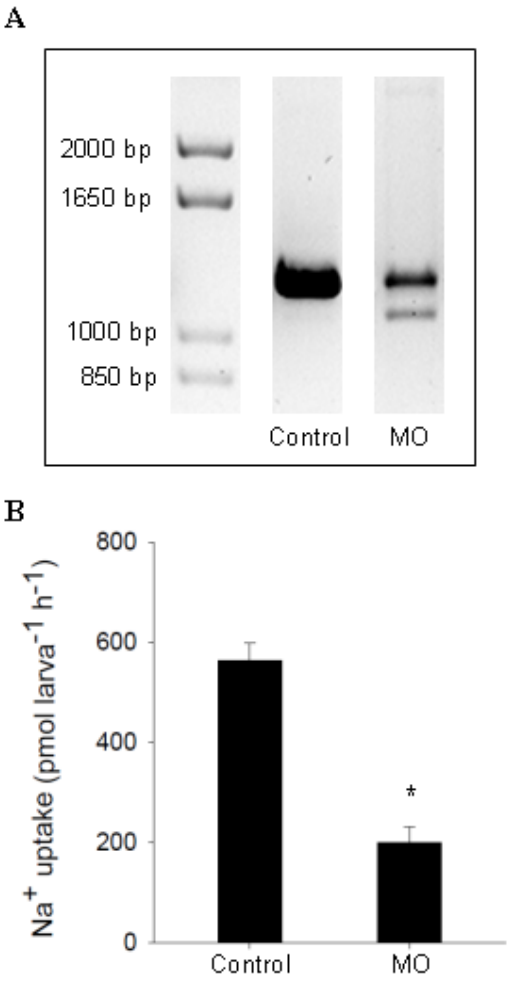

Figure 4.5. The effect of ASIC4.2 knockdown on Na^+ uptake rates in zebrafish larvae reared in low Na^+/low pH medium (Na^+=~50 µM; pH=6.0) . Control- control morphants; MO- ASIC4.2 morphants. A) ASIC4.2 morphants (MO) exhibited effectively removed exon 2 of the target, B) Na^+ uptake rate was significantly decreased in ASIC4.2 morphants. Values are means ± S.E.M. (n=6). * Significantly different from the control group ($P < 0.01$).

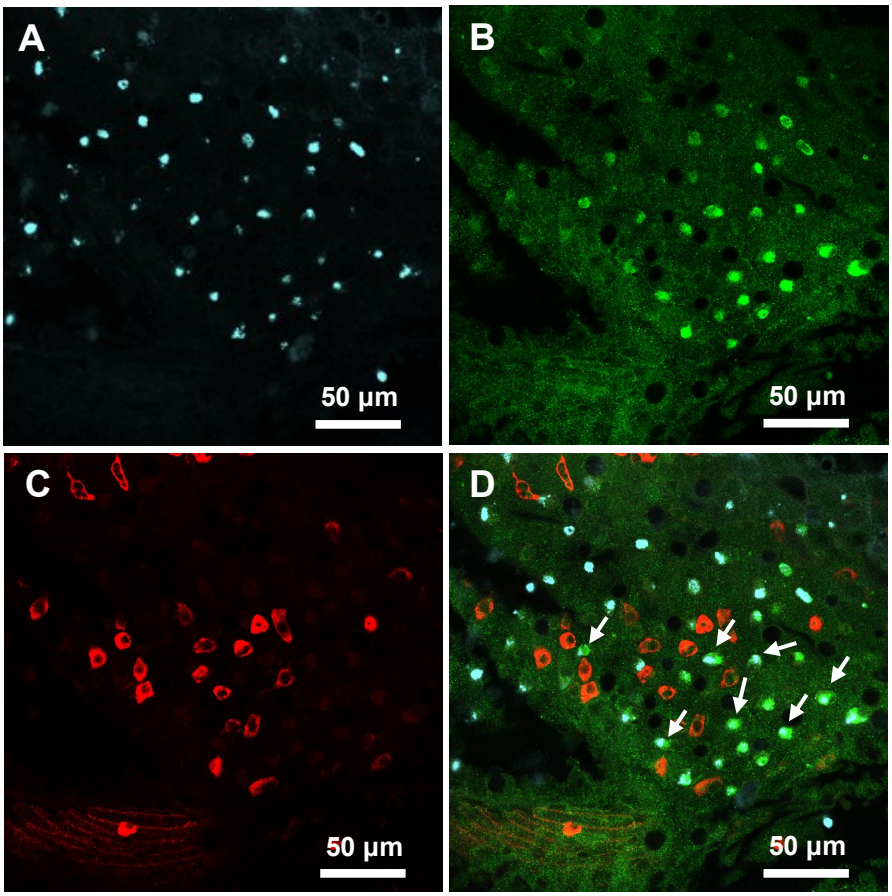

Figure 4.6. Triple immunostaining in wild-type larvae yolk sac with Concanavalin A, anti-ASIC4.2, and anti-Na^+/K^+-ATPase (NKA) antibody. A) Concanavalin A (light blue), B) anti-ASIC4.2 antibody (green), and C) anti-NKA antibody (red). D) is a merged image of A, B, and C. Arrows indicate co-localization of ASIC4.2 and Concanavalin A.

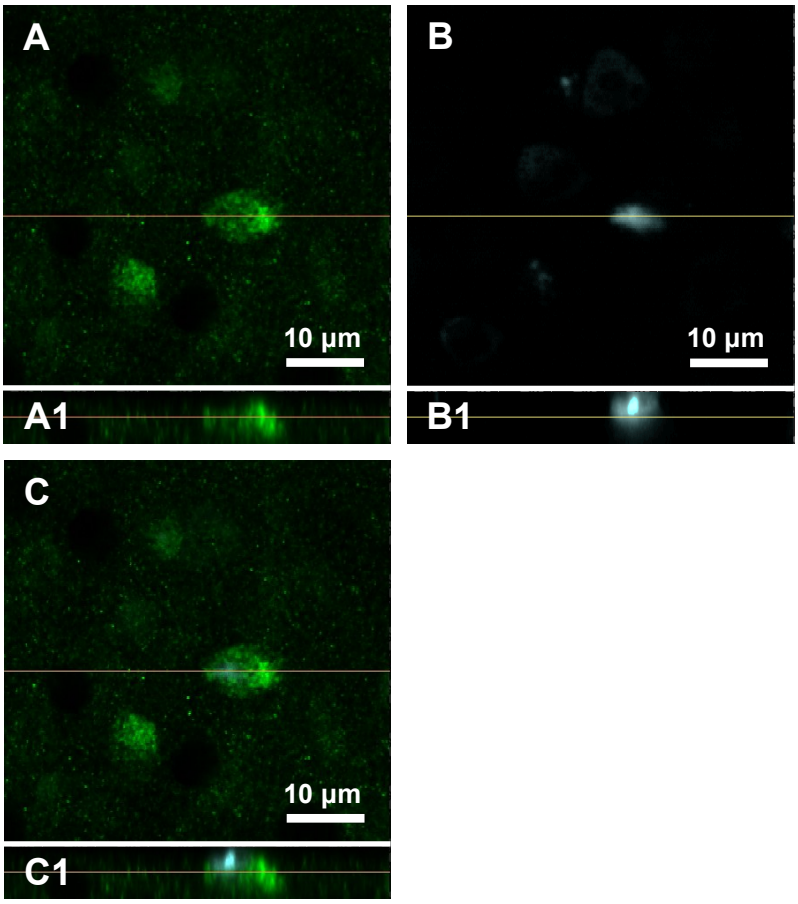

Figure 4.7. Immunostaining with Concanavalin A and anti-ASIC4.2 antibody showing co-localization to the same cell. A) and A1) anti-ASIC4.2 antibody (green) and B) and B1) Concanavalin A (light blue). C) A and B merged, C1) A1 and B1 merged. A, B, C – x, y plane. A1, B1, C1 - z plane.

Discussion

Data presented in the current study confirms and extends findings from the previous Chapter 3 that ASICs play a role in uptake of Na^+ in zebrafish. In the previous Chapter 3, I demonstrated through RT-PCR the expression of multiple *asic* subunits in the gill epithelium of the adult zebrafish. The current study has extended that finding to demonstrate, as investigated by loss-of-function approach, that the ASIC4.2 subunit specifically is crucial for transport of Na^+ in low Na^+/low pH conditions, and may also play a role in low pH media.

Immunohistochemical analysis revealed that ASIC4.2 subunit is expressed on the yolk sac membrane of the zebrafish larvae, validating the use of these animals as a surrogate model system for investigation of the role of ASIC4.2. It has been demonstrated by multiple studies that zebrafish larvae utilize their yolk sac membrane in ionoregulation and that the sub-types of MRCs present on the yolk sac membrane correspond to the MRC sub-types found on gill epithelium (Lin et al., 2006; Horn et al., 2006; Esaki, et al., 2006; Hwang). In the present study, triple staining with anti-ASIC4.2, anti-NKA antibodies and ConA, revealed that ASIC4.2 co-localizes to the HR subtype of the MRCs, in agreement with what was observed in the adult zebrafish gills (Chapter 3). These findings support the proposed model for Na^+ uptake in zebrafish gill/skin, which places a putative epithelial Na^+ channel on the apical surface of the HR cells together with other proteins involved in Na^+ transport such as NHE, Rhcg1, and V-ATPase (Dymowska et al., 2012; Hwang et al., 2011). Moreover, the results show that in zebrafish larvae, ASIC4.2 appears to be localized to the apical and sub-apical region of the HR cell, which is similar to the apical localization observed in the rainbow trout MRCs (Chapter 2). Nevertheless, a more detailed analysis of the staining pattern by co-

localization with subcellular markers and/or immunogold analysis are required for more definite localization of the ASIC4.2 staining to the apical and/or particular subcellular components (e.g. recycling plasma membrane vesicles).

Similar to Chapter 2 and 3, in this study we used the novel inhibitor DAPI to verify involvement of ASICs in Na^+ uptake in zebrafish larvae. Additionally, larvae were reared and Na^+ fluxes measured in media with various levels of Na^+ and pH in order to examine the effect of these environmental parameters on DAPI sensitivity. Wild type zebrafish larvae reared in control medium displayed no sensitivity to DAPI (Na^+=~600 μM and pH=8). This finding is secondarily supported by the lack of effect of ASIC4.2 knockdown on Na^+ uptake rates in the control water. It has been previously proposed that at environmental pH=8 and above, NHE should not be constrained thermodynamically if the external concentration of Na^+ is greater than ~500 μM (Kirschner, 2004; Parks et al., 2008). Therefore, it is possible that ASICs do not play a major role in Na^+ uptake in these circumneutral pH environments with relatively high external Na^+ concentration, since in these conditions NHE function would theoretically be favourable.

However, wild type larvae reared under similar environmental Na^+ concentrations as the control water (Na^+=600 μM) but with lowered pH (pH=4) demonstrated significant sensitivity to DAPI at concentrations as low as 10 nM. However, the observed reduction of Na^+ uptake was incomplete (only ~42% maximum inhibition) and Na^+ uptake was refractory to increasing DAPI concentrations in this media. Previously, Kumai et al. (2011b) studying Na^+ uptake in larval zebrafish exposed to acidic water revealed that there are at least two mechanisms responsible for Na^+

transport in these conditions: NHE3b linked to Rhcg1 protein, and VHA potentially linked to an unknown epithelial Na^+ channel. In our study, it is possible that a NHE3b/Rh protein metabolon could perform this residual Na^+ uptake. The presence of an Rh protein in combination with the NHE3b would allow for an elevation of the pH in the boundary layer and removal of the exofacial pH inhibition of NHE3b. We believe that in freshwater fish multiple mechanisms may be used to acquire Na^+ from the external environment and that the type of the used mechanism depends greatly on the environmental conditions. However, it should be noted that in one study (Chang et al., 2013), NHE3b mRNA expression and protein abundance in the HR cells in the gills of adult zebrafish was shown to be down regulated in very similar conditions (pH=4 and Na^+ = 500 μM.). These appear to be opposite responses to what would be predicted, and clearly more research on the regulation of expression and activity of NHE3b in Na^+ transport is warranted.

In our study, knockdown of ASIC4.2 in larvae reared in the low pH water resulted in substantial elevation of Na^+ uptake. This response, although unexpected, was similar to the responses observed in *gcm2* zebrafish morphants, where translational knockdown of the HR cells differentiation factor, *gcm2*, and *slc12a10.2* (NCC), another transporter involved in Na^+ uptake in zebrafish, resulted in a significant increase in Na^+ uptake (Chang et al., 2009, 2013; Wang et al., 2009). The abovementioned studies together with the results from the current study demonstrate that in developing zebrafish, there is likely a functional redundancy of Na^+ uptake mechanisms, whereby the loss of one of the Na^+ uptake mechanisms is compensated for by up regulation of another one. It is therefore likely that the observed augmentation of Na^+ uptake in ASIC4.2

morphants is caused by increased expression and/or activation of other Na^+ transporting pathways.

It has been demonstrated that a functional ASIC channel is a trimer and may comprise multiple ASIC subunits (Jasti et al., 2007). We know that all six identified ASIC subunits are expressed in adult zebrafish gill (including ASIC4.2 –see Chapter 3). To exclude the possibility that the observed increase in Na^+ uptake resulted from up regulation of other ASIC subunits, ASIC4.2 morphants were treated with a blocking concentration of DAPI. There was no further decrease in Na^+ uptake in ASIC 4.2 morphants compared to the control group suggesting that other ASIC subunits were not involved in the up regulation of Na^+ transport. This suggests the involvement of other Na^+ transporting mechanisms in the low pH induced compensation. Future studies using a broader panel of pharmacological inhibitors including metolazone, a specific inhibitor of NCC (Wang et al., 2009), EIPA, a specific NHE inhibitor (Ito et al., 2014) and DAPI in concert is needed to uncover the mechanisms underlying these complex responses.

In this study, a role for ASICs in low Na^+/low pH media was also investigated. Zebrafish larvae reared in these conditions did not display substantial sensitivity to DAPI until relatively higher concentrations (10 μM) were applied. Our previous study in adult zebrafish (Chapter 3) acclimatized to low Na^+/low pH water show no effect of DAPI on Na^+ uptake rates in these media. Nevertheless, knockdown of ASIC 4.2 resulted in a reduced Na^+ uptake rate (~ 67%) in larvae reared in these conditions. The reason for this discrepancy is unknown and to investigate the complex relative roles that both NHE/Rh and ASICs play in Na^+ uptake under different pH and Na^+ conditions, a full multifactorial design is required.

Overall, results from this study demonstrate that ASIC4.2 is expressed on the transporting epithelium of the zebrafish larvae. Moreover, splice-out knockdown using MOs provided evidence for direct involvement of ASIC4.2 in Na^+ uptake in zebrafish larvae exposed to moderately low pH and to low environmental Na^+ conditions. However, there is a complex dynamic whereby the interaction of environmental pH and Na^+ levels, along with a functional redundancy of the mechanisms available for Na^+ transport result in multiple solutions to achieve Na^+ homeostasis in this model species. Future research focusing on unraveling these interactions will aid our understanding of the relationship between organism and environment needed to achieve Na^+ homeostasis.

Chapter 5:
General Discussion

General summary

The mechanisms used by freshwater fish to actively take up Na^+ from the dilute environments they inhabit have been a focus of numerous studies in the past 70 years. However, the precise mechanisms used still remain the subject of a lively debate among fish physiologists. Two models of apical Na^+ uptake have been proposed - the first model is where Na^+ ions enter the cell in exchange for a H^+ counter ion *via* electroneutral NHE, whereas the second model proposed that Na^+ is acquired from the media by means of an epithelial Na^+ channel. Based on the mechanism of Na^+ uptake that occurs in frog skin (Harvey, 1992), the Na^+ channel responsible for the branchial Na^+ uptake in freshwater fish was proposed to be an ENaC homologue. At the beginning of my PhD, the NHE model had gained substantial support from both functional studies in various freshwater fish species using NHE specific pharmacological blockers, and later from immunochemical analysis with NHE specific antibodies that localized NHE to the apical surface of the MRCs in the gill epithelium. As a result, the NHE model became the most favoured model. The ENaC model, on the other hand, remained controversial due to the lack of functional or molecular evidence for its existence. Regardless, at very low environmental Na^+ concentrations and very low water pH, the ability of NHE to function was questioned on thermodynamic grounds (Parks et al, 2007; see Chapter 1).

In my PhD thesis, I demonstrated that ASIC, a close relative to ENaC, is the long sought-after Na^+ channel involved in Na^+ uptake in freshwater fish. I not only demonstrated that ASICs are present in the gill epithelium of freshwater rainbow trout and zebrafish at the molecular and protein level, but with the use of novel ASIC specific pharmacological inhibitors, I also demonstrated that ASICs play an important role in

Na^+ uptake in these two model species. My thesis is the first detailed report providing evidence for existence of an epithelial Na^+ channel in fish gill tissue, and thus validating the Na^+ channel model for branchial Na^+ uptake in freshwater fish. Moreover, I have initiated investigations into the roles that both ASICS and NHEs potentially play in uptake of Na^+ from freshwater and consequent regulation of whole body Na^+ homeostasis.

In addition to this contribution to the field of fish transport physiology, my thesis is the first report to document a non-neuronal function of ASICs in any vertebrate. This has implications not only within my field of comparative fish physiology, but it opens up an entirely new avenue for functional studies of ASIC in a broad variety of other organisms, including humans. In this final Chapter of my thesis, I will summarize findings from the previous Chapters, highlight the similarities and differences in ASICs expression and function in the investigated two fish species - rainbow trout and zebrafish, and point out future directions for researchers interested in this area of study.

Localization of ASICs in the fish gill/yolk sac epithelium

In Chapters 2, 3, and 4, I have demonstrated using both RT-PCR and zebrafish anti-ASIC4.2 antibody that ASICs are present in the gill epithelium of both adult rainbow trout and zebrafish, and in the yolk sac epithelium of the zebrafish larvae. In Chapter 2, using RACE, I obtained one full and one partial sequence of the RNA transcripts for two *asic* homologues in the rainbow trout gill tissue. Further bioinformatics and phylogenetic analyses revealed that the full length clone was an *asic4* subunit homologue, whereas the partial clone belonged to the *asic1* subunit group. I was,

however, unable to detect any of the other *asic* subunits in the rainbow trout gill and it is not known at the moment if other ASIC subunits are expressed. Tissue distribution analysis *via* RT-PCR demonstrated that in rainbow trout, *asic4* and *asic1* are also present in kidney, and brain. Interestingly, *asic1* was also identified in blood, which is a novel finding since previous studies in mammals and fish have associated ASICs exclusively with the central and peripheral nervous system (see Chapter 1). In contrast to rainbow trout, in Chapter 3 I demonstrated that in zebrafish all six known *asic* subunits: *asic1.1*, *1.2*, *1.3*, *2*, *4.1*, and *4.2* were expressed in the gill. The potential involvement of each subunit in Na^+ uptake remains to be determined (see future directions section below), since it is possible that *asics* are expressed and have a function in cells other than MRCs (i.e., neurons, neuroepithelial cells, pavement cells and others).

The location of ASICs within the gill epithelium was further determined using immunohistochemical analysis with our custom made zebrafish anti-ASIC4.2 antibody. After validation of cross-species reactivity of the anti-ASIC4.2 antibody using immunoprecipitation, and Western blotting, I was able to use this antibody in rainbow trout, zebrafish adults and zebrafish larvae. As described in Chapter 2, I observed immunoreactivity in the cells located in the lamellae and the interlamellar region of rainbow trout gills. The majority of these cells also co-stained with the NKA antibody suggesting that in rainbow trout epithelium, ASIC4 is present in the MRCs.

Following this, I then demonstrated localization of ASIC4.2 in the adult zebrafish gill and in the yolk sac membrane of zebrafish larvae. In Chapter 3, using a double staining technique involving both anti-NKA and anti-VHA antibodies I showed that in zebrafish gill ASIC4.2 is present in the HR MRCs, an ionocyte sub-type

previously demonstrated to be involved in Na^+ transport in zebrafish (Lin et al., 2006). A similar and supporting result was found in the yolk sac membrane of the zebrafish larvae in Chapter 4, where triple staining with anti-ASIC4.2, anti-NKA antibodies, and ConcavalinA revealed that ASIC4.2 is localized to HR MRCs. Additionally, using confocal microscopy, I was able to identify ASIC4 in rainbow trout and ASIC4.2 in zebrafish in close proximity to the cellular membrane. Taken together, my results from Chapters 2, 3, and 4 present strong evidence for expression of ASIC4 in MRCs of both rainbow trout and zebrafish.

Functional analysis of ASIC involvement in Na^+ uptake

In my thesis, I investigated the involvement of ASICs in Na^+ uptake of rainbow trout and zebrafish using novel pharmacological ASIC specific inhibitors, DAPI and diminazene, that were discovered and characterized in rat hippocampal neurons by Chen et al. (2010). In Chapter 2, I demonstrated that in rainbow trout DAPI and diminazene decreased Na^+ uptake in a dose-dependent manner and were effective at very low concentrations. These findings validated the effectiveness of these novel inhibitors for use in freshwater fish. Furthermore, both DAPI and diminazene almost completely blocked Na^+ uptake in rainbow trout acclimated to low Na^+ (~50μM) and low pH (~6.0), suggesting that under these environmental conditions, ASICs play an important role in Na^+ uptake. I then utilized DAPI, as described in Chapter 3, to investigate the involvement of ASICs in adult zebrafish Na^+ uptake. In this study I used two different acclimation media with varied Na^+ concentrations and pHs that spanned the theoretical thermodynamic limits of NHE function. One medium had the same parameters as those

used in the rainbow trout study presented in Chapter 2, whereas the second medium had a higher concentration of Na^+ and a higher pH. The results from this study were more complex and more difficult to interpret than the results from the rainbow trout study. In zebrafish acclimated to the same conditions as the rainbow trout (Na^+ =~50μM, pH =~6.0) DAPI had no effect on Na^+ uptake. Interestingly, I also found that other pharmacological agents such as the general Na^+ uptake inhibitor amiloride and NHE specific inhibitor EIPA did not reduce the uptake on Na^+ in zebrafish exposed to these environmental conditions. I propose that there at least are two possible explanations for this result. The first possibility is that at a very low environmental Na^+ concentration and low pH, zebrafish acquire Na^+ with the use of mechanisms alternative to either ASICs or NHE. Alternatively, in zebrafish, a combination of external low Na^+ and low pH alters the molecular structure of both ASICs and NHE, thus rendering them insensitive to the pharmacological agents used in the study. The understanding of the variability in pharamacological response remains to be established by future studies (see future directions below).

At higher concentrations of Na^+ and higher pH, ASICs seemed to play a role in Na^+ uptake in zebrafish. In these conditions, Na^+ uptake rate was inhibited by DAPI, and also by amiloride. However, for both agents, the inhibition was not complete, even at high doses. This suggests that in zebrafish the mechanism, which accounts for the residual Na^+ transport is DAPI and amiloride-insensitive.

Together, my findings from Chapter 2 and 3 demonstrate that involvement of ASICs in Na^+ uptake differ significantly between adult rainbow trout and zebrafish. This should not be surprising taking into account that teleost fish are the most diverse group

of vertebrates (>25,000 species identified) and have successfully established populations in almost every aquatic environment on earth. Given the substantial evolutionary distance between salmonids and cyprinids, it is not unexpected that both zebrafish and rainbow trout evolved different strategies for ionoregulation, whereby each species possess different ionocyte sub-types with a specific set of transporters.

In Chapter 4, I further examined the role of ASIC4.2 in uptake of Na^+ using pharmacology and a loss-of-function approach in zebrafish larvae. I demonstrated that, similar to adults, Na^+ uptake rates are inhibited by DAPI. However, the responses in larvae reared in media with varying Na^+ concentrations and pH were different from the responses described for adults in Chapter 3. Obviously, there are significant complexities with regard to both environmental responses and developmental processes that will need to be examined. Knockdown of ASIC4.2 significantly reduced Na^+ uptake in larvae reared in low Na^+ and low pH medium, pointing to the involvement of this ASIC subunit in transport of Na^+ in zebrafish.

New model for Na^+ uptake in freshwater fish

Based on my findings from Chapter 2, 3, and 4, I would like to propose a new model for Na^+ uptake in rainbow trout and zebrafish, whereby acquisition of Na^+ can be mediated by ASICs (Figure 5.1). In rainbow trout, I propose that ASIC4 is present on the apical side of the MRCs. The current model of MRCs in rainbow trout places an unidentified Na^+ channel on the apical surface of the PNA^- ionocyte (Figure 1.1). However, in this thesis I was unable to further identify to which MRC sub-type ASIC4

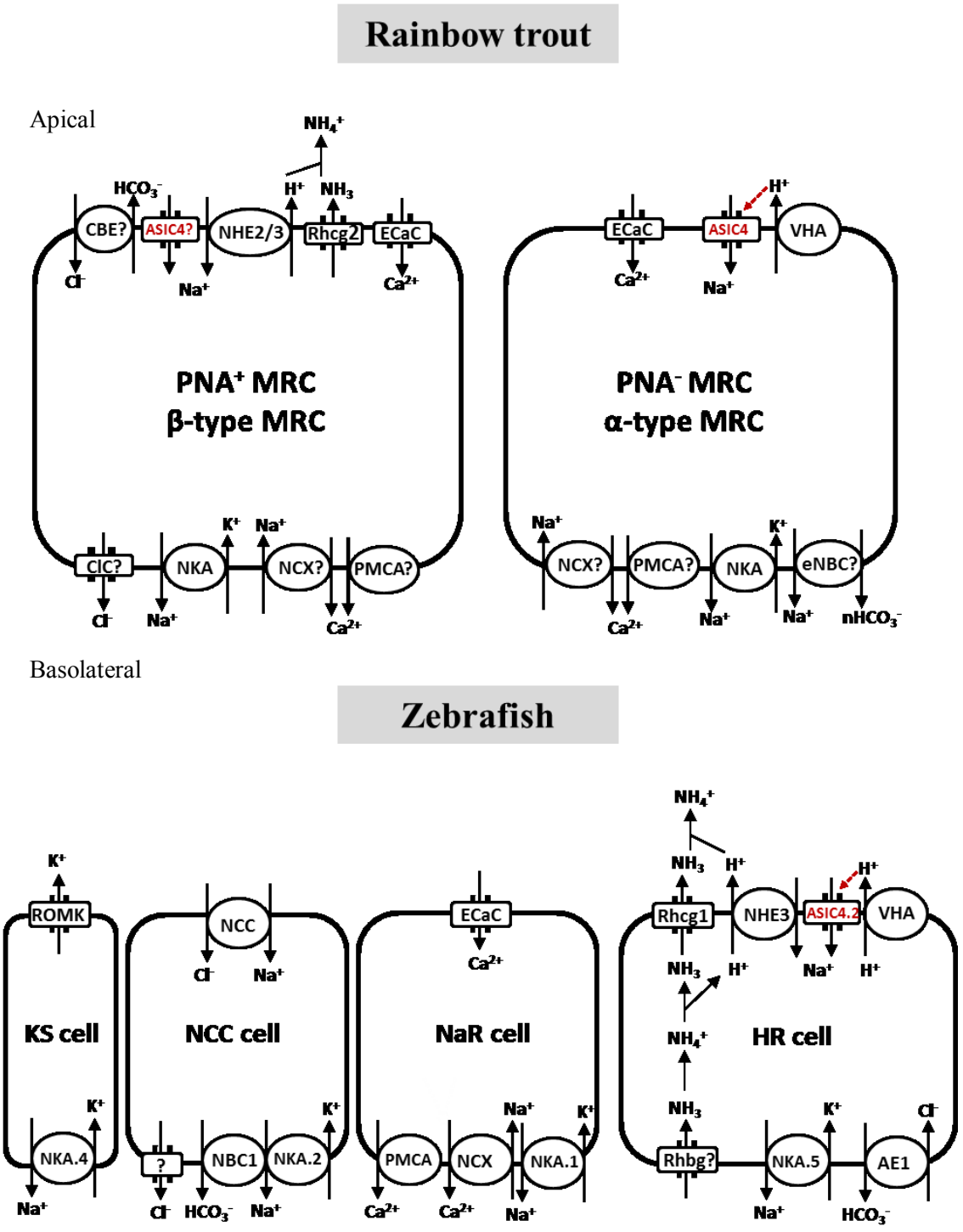

Figure 5.1. Proposed new model for Na^+ uptake in rainbow trout and zebrafish. See General Summary section for details.

localizes. In zebrafish, I have clearly demonstrated that ASIC4.2 is present in HR MRCs, where it is co-expressed with VHA and NHE (Figure 5.1).

This new proposed model for Na^+ uptake provides an attractive solution to the debate surrounding the thermodynamic limitations of the other proposed Na^+ transport mechanisms, and resolves the conundrum of the role of an apical VHA in Na^+ transport. This study has profound implications whereby it demonstrates for the first time in 70+ years the existence of a channel in freshwater gill epithelium that can serve as a mechanism for sodium uptake from the water. I believe that my findings will have a significant impact on future research in gill transport physiology and open new avenues for research into the variable role(s) that this channel plays in different environments and different species.

Future directions

While the demonstration of ASIC as a functional channel in the gill of both rainbow trout and zebrafish is a significant advancement in the field of fish ionoregulation, there remain many questions that require future research effort. Below, I outline some of the ideas that need investigation to help guide future researchers interested in this topic.

What is the involvement of other ASIC subunits in fish Na+ uptake?

In Chapter 4, I demonstrated using morpholino knockdown technique that the specific *asic4.2* gene product is involved in branchial Na^+ uptake in zebrafish larvae. However, the potential role of other ASIC subunits in freshwater Na^+ uptake has not been established. As mentioned in this thesis, six *asic* subunits coded by six different

genes have been identified in zebrafish (Grunder et al., 2009; Paukert et al., 2004) and published in GenBank. In Chapter 3, I demonstrated that all six of these ASIC subunits are expressed in the zebrafish gill tissue at the mRNA level raising the possibility that the functional channel is heteromeric, with the functional channel being comprised of multiple subunits. Therefore, it is strongly recommended to investigate the role that different *asic* subunits may play in Na^+ uptake. To achieve this objective, the knockdown or knockout of individual and/or multiple subunits (by MO, CRISPr or other technologies) in combination with Na^+ uptake rate measurements and pharmacological inhibitors is recommended. One potential concern is that the complexity of Na^+ transport which often involves other transport systems (e.g. NHE, NCC) may result in rescue/up regulation of these other transporters. Therefore, a careful experimental protocol and cautious interpretation is recommended.

A second method to examine the potential role of other subunits is to investigate the subunit composition of the functional Na^+ channel at the protein level. It has been previously demonstrated that in mammals ASICs are homo- or heteromeric trimers (Jasti et al., 2007). In Chapter 3 and 4, I demonstrated that ASIC4.2 is expressed in the HR MRCs in adult zebrafish gill and larval yolk sac membrane, but this does not inform us of the potential role of other subunits. Future studies should determine whether in zebrafish transporting epithelium, ASIC4.2 subunit occurs as either a homomeric or a heteromeric channel, or both. One method to resolve this question is by use of a co-immunoprecipitation technique whereby the functional unit is identified through the use of antibodies specific for each unit component. However, such study would require a set

of antibodies specific for all ASIC subunits, and these are not commercially available at the moment.

In my thesis, I cloned both *asic4* and *asic1* from the rainbow trout gill epithelium and demonstrated expression (by immunocytochemistry) of ASIC4 on the apical surface of ionocytes. However, based on the fact that zebrafish express all ASIC isoforms in the gill, and on the fact that other fish species express multiple ASIC subunit homologs (sequences for *asic* isoforms are available in GenBank and Ensembl), it is very likely that other ASIC subunits are also present and functional in rainbow trout gills, and this should be further determined.

What are the functional properties of ASIC subunits in rainbow trout?

The properties of the rainbow trout ASIC subunits should be investigated through functional expression studies. Similar studies on each of the zebrafish ASIC subunit have been performed (Paukert et al., 2004; Chen et al., 2007) and results demonstrated functional differences between the subunits. Furthermore, it has been demonstrated through co-expression studies that the functions of heteromeric ASIC channels display different properties than those of the homomers (Chen et al., 2007). Therefore, in order to fully understand the functional role, pharmacology, and characteristics of trout ASICs, I propose measurement of Na^+ transport kinetics and pharmacology to be conducted using electrophysiological characterization in a heterologous expression system, such as *Xenopus* oocytes or cell lines.

Is there a functional association between ASIC and VHA?

In the previous Chapters, using immunohistochemistry I have shown that in zebrafish adults and larvae ASIC4.2 protein is expressed in the MRCs that also express apical VHA. As I mentioned in Chapter 1, in freshwater fish there is a proposed connection between Na^+ uptake and the activity of VHA. ASICs are Na^+ channels gated by external H^+ (see Chapter 1) and in the peripheral nervous system, where they are mostly expressed, ASICs are gated open by a drop in extracellular pH. In zebrafish and rainbow trout gill MRCs, ASIC4 is localized to the apical side of the epithelial cell (see Chapter 2 and 4). This raises an intriguing possibility that the gating signal comes from the environment the fish is exposed to. In the previous Chapters of this thesis, I proposed that in fish gills Na^+ uptake *via* ASICs may be regulated by VHA, which provides the protons necessary to gate open ASICs. If ASIC and VHA indeed work in concert, potentially they should be located on the cell membrane in a close proximity to each other. This hypothesis could be tested with a use of a fluorescence resonance energy transfer technique, which is a relatively sensitive and simple method to detect spatial extension of multicomponent structures such as proteins, lipids, and carbohydrates (Clegg, 1995).

To what MRC sub-type do ASICs in rainbow trout localize?

It is of great importance to determine the MRC type to which ASIC localizes in rainbow trout. In Chapter 2, I demonstrated that ASIC4 in rainbow trout co-localizes with NKA. However, due to the lack of species-specific antibodies that can serve as distinct cellular markers for MRC subtypes, I was unable to localize ASIC4 to either

PNA^+ or PNA^- MRC subtype. Localization to the MRC sub-type could be easily achieved through immunohistochemical analysis and double staining with our zebrafish anti-ASIC4.2 antibody and specific anti- NHE and anti-VHA antibodies. The current model for freshwater rainbow trout gill predicts a Na^+ channel on the PNA^- cell. If this is the case for ASIC4, cells staining positive with the zebrafish anti-ASIC4.2 antibody should also stain positive for the VHA, but negative for the NHE. If all the antibodies are raised in the same species as the zebrafish anti-ASIC4.2 antibody, staining could be performed on consecutive sections (see Chapter 3). Otherwise, one of the antibodies could be labelled by biotin using a biotinylation kit.

What are the implication of environmental Na^+ and pH levels on ASIC expression and function?

Results from the pharmacological inhibition study in Chapter 2, show that ASICs play an important role in Na^+ uptake in rainbow trout acclimatized to low Na^+/low pH water, whereas in zebrafish, the expression and function at low Na^+ and low pH was more complex. Future research should investigate whether ASICs are also involved in Na^+ uptake at higher environmental Na^+ and/or pH conditions, in which NHE would not be thermodynamically constrained. This could be achieved with the use of ASIC pharmacological inhibitors, DAPI and diminazene, combined with Na^+ fluxes using radiotraces. A full multifactorial design involving various Na^+ concentrations and pHs would help to determine which Na^+ transporter, ASICs or NHE, plays a more important role in specific environmental conditions. It would also be interesting to see whether environmental Na^+ and pH concentrations have an influence on the expression of a

particular ASIC subunit. This could be investigated using quantitative RT-PCR and western blotting.

Are ASICs expressed in other freshwater fish species?

My thesis demonstrated that ASICs play a role in Na^+ uptake in rainbow trout and zebrafish, however future research should investigate, whether ASICs are involved in Na^+ uptake in other freshwater fish species, especially those that inhabit low Na^+/low pH environments. Fish inhabiting Rio Negro of the Amazon River system could serve as model organisms for this study. Although waters of Rio Negro are characterized by very low ionic strength with Na^+ concentrations of only ~ 10 μmol l^{-1} and pH varying from 4.5 to 5.1, the river is successfully inhabited by more than 1000 fish species (Gonzalez et al., 2002). Unidirectional fluxes with radiolabelled $^{22}Na^+$ revealed that despite these unfavourable conditions for the NHE to function, these fish were able to uptake Na^+ in these extreme conditions (Gonzales et al., 2002). This suggests that a Na^+ uptake mechanism alternative to NHE, such as ASICs, exists in these species.

Another potential species worth investigating is the freshwater Tilapia, *Oreochromis sp.*. These fish have been extensively used in ionoregulation and acid/base balance studies and their MRCs and gill function have well characterized (for review see Hwang et al., 2011; Dymowska et al., 2012). This provides a strong background of physiological studies for comparison. Moreover, a sequence for *asic4* in the Nile tilapia, *Oreochromis niloticus*, is available in GenBank (see Chapter 2, Figure 2.4), and expression in the gill epithelium could be determined by RT-PCR. However, it should be noted that currently the model of Na^+ uptake in freshwater tilapia does not predict the

presence of a Na^+ channel on any MRC subtype and the limits of low pH/low environmental Na^+ concentrations for this species are not as robust as either trout or zebrafish in withstanding low ionic strength waters.

General Conclusion

The amazing diversity of fish species and their solutions to the problems of ion and acid-base regulation allows the application of the Krogh principal where "for such a large number of problems there will be some animal of choice, or a few such animals, on which it can be most conveniently studied". This field continues to provide researchers with countless challenges and allow new research directions, new models and new environmental conditions to be explored.

References

Abbas, L., Hajihashemi, S., Stead, L.F., Cooper, G.J., Ware, T.L., Munsey, T.S., Whitfield, T.T., White, S.J., 2011. Functional and developmental expression of a zebrafish Kir1.1 (ROMK) potassium channel homologue Kcnj1. *Journal of Physiology* 589, 1489-1503.

Alper, S.L., Sharma, A.K., 2013. The SLC26 gene family of anion transporters and channels. *Molecular Aspects of Medicine* 34, 494 – 515.

Avella, M., Bornancin, M., 1989. A new analysis of ammonia and sodium transport through the gills of the freshwater rainbow trout (*Salmo gairdneri*). *Journal of Experimental Biology* 142, 155-175.

Babini, E., Paukert, M., Geisler, H. S., Grunder, S., 2002. Alternative splicing and interaction with di- and polyvalent cations control the dynamic range of acid-sensing ion channel 1 (ASIC1). *Journal of Biological Chemistry* 277, 41597-41603.

Bartoi, T., Augustinowski, K., Polleichtner, G., Grunder, S., Ulbrich, M.H., 2014. Acid-sensing ion channel (ASIC) 1a/2a heteromers have a flexible 2:1/1:2 stochiometry. *Proceedings of the National Academy of Science* 11, 8281-8286.

Bayaa, M.B., Vulsevic, A., Esbaugh, M., Braun, M.E., Ekker, M., Perry, S.F., 2009. The involvement of SLC26 anion transporters in chloride uptake in zebrafish (*Danio rerio*) larvae. *Journal of Experimental Biology* 212, 3283-3295.

Bill, B.R., Balciunas, D., McCarra, J.A., Young, E.D., Xiong, T., Spahn, A.M., Garcia-Lecea, M., Korzh, V., Ekker, S.C., Schimmenti, L.A., 2008. Development and Notch signalling requirements of the zebrafish choroid plexus. *PLoS One 3*, e3114.

Bill, B. R., Perzold, A.M., Clark, K.J., Schimmenti, L.A., Ekker, S.C., 2009. A primer for morpholino use in zebrafish. *Zebrafish* 6, 69-77.

Boisen, A.M.Z., Amstrap, J., Novak, I., Grosell, M., 2003. Sodium and chloride transport in soft water and hard water acclimated zebrafish (*Danio rerio*). *Biochemica et Biophysica Acta (BBA)– Biomembranes* 1618, 207-218.

Bond, C.E., 1996. Biology of fishes. Saunders College Publishing.

Bonifacio, G., Lelli, C. I. S., Kellenberger, S., 2014. Protonation controls ASIC1a activity via coordinated movements in multiple domains. *Journal of General Physiology* 143, 105-118.

Boyle, D., Clifford, A. M., Orr, E., Chamot, D., Goss, G.G., 2014. Mechanisms of Cl^- uptake in rainbow trout: cloning and expression of slc26a6, a prospective Cl^-/HCO_3^- exchanger. *Comparative Biochemistry and Physiology Part A* 180, 43-50.

Bradshaw, J.C., Kumai, Y., Perry, S.F., 2012. The effects of gill remodeling on transepithelial sodium fluxes and the distribution of presumptive sodium-transporting ionocytes in goldfish (*Carassius auratus*). *Journal of Comparative Physiology B* 182, 351-366.

Briggs, J.P., 2002. The zebrafish, a new model organism for integrative physiology. *American Journal of Physiology – Regulatory, Integrative and Comparative Physiology* 282, R3-R9.

Brix, K.V., Grosell, M., 2012**.** Comparative characterization of Na^+ transport in C*yprinodon variegatus variegatus* and *Cyprinodon variegatus hubbsi*: a model species complex for studying teleost invasion of freshwater. *The Journal Experimental Biology* 215: 1199-1209.

Burnett, K.G., Bain, L.J., Baldwin, W.S., Callard, G.V., Cohen, S., Di Giulio, R.T., Evans, D.H.,Gomez-Chiarri, M., Hahn, M.E., Hoover, C.A., Karchner, S.I., Katoh, F., MacLatchy, D.L., Marshall, W.S., Meyer, J.W., Nacci, D.E., Oleksiak, M.F., Rees, B.B., Singer, T.D., Stegeman, J.J., Towle, D.W., Van Veld, P.A., Vogelbein, W.F., Whitehead, A., Winn, R.N., Crawford, D.L., 2007. *Fundulus* as the

premier teleost model in environmenral biology: Opportunities for new insights using genomics. *Comparative Bioochemistry and Physiology Part D: Genomics and Proteomics* 2, 257-286.

Burns, J., Copeland, D.E., 1950. Chloride excretion in the head region of *Fundulus heteroclitus*. *The Biological Bulletin* 99, 381-385.

Bury, N., Wood, C.M., 1999. Mechanism of branchial apical silver uptake by rainbow trout is via the proton-couples Na^+ channel. *American Journal of Physiology – Regulatory, Integrative and Comparative Physiology* 277, R1385-R1391.

Carnally, S.M., Dev, H.S., Stewart, A.P., Barrera, N.P., Van Bemmelen, M.X., Schild, L., Henderson, R.M., Edwardson, J.M., 2008. Direct visualization of the trimeric structure of the ASIC1a, using AFM imaging. *Biochemical and Biophysical Research Communications* 372, 752-755.

Chang, I.C., Lee, T.H., Yang, C.H., Wei, Y.W., Chou, F.I., Hwang, P.P., 2001. Morphology and function of gill mitochondria-rich cells in fish acclimated to different environments. *Physiological and Biochemical Zoology* 74, 111-119.

Chang, I.C., Wei, Y.Y., Chou, F.I., Hwang, P.P., 2003. Stimulation of Cl^- uptake and morphological changes in gill mitochondria-rich cells in freshwater tilapia (*Oreochromis mossambicus*). *Physiological and Biochemical Zoology* 76, 544-552.

Chang, W. J., Horng, J. L., Yan, J. J., Hsiao, C. D., Hwang, P. P., 2009. The transcription factor, glial cell missing 2, is involved in differentiation and functional regulation of H^+-ATPase-rich cells in zebrafish (*Danio rerio*). *American Journal of Physiology – Regulatory, Integrative and Comparative Physiology* 296, R1192-201.

Chang, W.J., Hwang, P.P., 2011. Development of zebrafish epidermis. *Birth Defects Research Part C – Embryo Today* 93, 205-214.

Chang, W.J., Wang, Y.F., Hu, H.J., Wang, J.H., Lee, T.H., Hwang, P.P., 2013. Compensatory regulation of Na^+ absorption by Na^+/H^+ exchanger and Na^+-Cl^- cotransporter in zebrafish (*Danio rerio*). *Frontiers in Zoology* 10, 46.

Chasiostis, H., Kolorov, D., Bui, P., Kelly, S.P., 2012. Tight junctions, tight junction proteins and paracellular permeability across the gill epithelium of fishes: a review. *Respiratory Physiology and Neurobiology* 184, 269-281.

Chen, Y.Y., Hwang, P.P., 2003. Comparisons of calcium regulation in fish larvae. *Journal of Experimental Zoology* 295A, 127-135.

Chen X, Polleichtner G, Kadurin I, Grunder S. Zebrafish acid-sensing ion channel (ASIC) 4. Characterization of homo- and heteromeric channels, and identification of regions important for activation by H^+. *The Journal of Biological Chemistry* 282: 30406-30413, 2007.

Chen, X., Qiu, L., Li, M., Durrnagel, S., Orser, B.A., Xiong, Z.G., MacDonald, J.F., 2010. Diarylamidines: High potency inhibitors of acid-sensing ion channels. *Neuropharmacology* 58, 1045 – 1053.

Choi, J.H., Lee, K.M., Inokuchi, M., Kaneko, T., 2010. Acute responses of gill mitochondria-rich cells in Mozambique tilapia *Oreochromis mossambicus* following transfer from normal freshwater to deionized freshwater. *Fisheries Science* 76, 101-109.

Claiborne, J. B., Edwards, S. L., Morrison-Shetlar, A. I., 2002. Acid-base regulation in fishes: Cellular and molecular mechanisms. *Journal of Experimental Zoology* 293, 302-319.

Clegg, R.M., 1995. Fluorescence resonance energy transfer. *Current Opinion in Biotechnology* 6, 103-110**.**

Copeland, D. E., 1948. The Cytological Basis of Chloride Transfer in the Gills of *Fundulus Heteroclitus*. *Journal of Morphology* 82, 201-227.

Coric, T., Zhang, P., Gerstein, M., Canessa, C.M., 2005. Proton sensitivity of ASIC1 appeared with the rise of fishes by changes in residues in the region that follows TM1 in the ectodomain of the channel. *Journal of Physiology* 568, 725-735.

Ditrich, H., 2007. The origin of vertebrates: a hypothesis based on kidney development. *Zoological Journal of the Linnean Society* 150, 435-441.

Donowitz M., Tse M. C., Fuster D., 2013. Slc9/NHE gene family, a plasma membrane and organellar family of Na^+/H^+ exchangers. *Molecular Aspects of Medicine* 34, 236-251.

Doyle, W. H., Gorecki, D., 1961. The so-called chloride cell of the fish gill. *Physiological Zoology* 34, 81-85.

Draper, B.W., Morcos, P.A., Kimmel, C.B., 2001. Inhibition of zebrafish fgf8 pre-mRNA splicing with morpholino oligos: a quantifiable method for gene knockdown. *Genesis* 30, 154-156.

Dymowska, A. K., Hwang, P. P., Goss, G.G., 2012. Structure and function of ionocytes in the freshwater fish gill. *Respiratory Physiology and Neurobiology* 184, 257-268.

Edwards, S.L., Tse, C.M., Toop, T., 1999. Immunolocalization of NHE3-like immunoreactivity in the gills of the rainbow trout (*Oncorhynchus mykiss*) and the blue-throated wrasse (*Pseudolabrus tetrious*). *Journal of Anatomy* 195, 465-469.

Eisen, J. S., and Smith, J. C. 2008., Controlling morpholino experiments: don't stop making antisense. *Development* 135, 1735 – 1743.

Esaki, M., Hoshijima, K., Kobayashi, S., Fukuda, H., Kawakami, K., Hirose, S., 2007. Visualization in zebrafish larvae of Na^+ uptake in mitochondria-rich cells whose differentiation is dependent on foxi3a. *American Journal of Physiology – Regulatory, Integrative and Comparative Physiology* 292, R470-R480.

Evans, D.H., 1968. Measurement of drinking rates in fish. *Comparative Biochemistry and Physiology* 25, 751-753.

Evans, D.H., Piermarini, P.M., Choe K.P., 2005. The multifunctional fish gill: dominant site of gas exchange, osmoregulation, acid-base regulation, and excretion of nitrogenous waste. *Physiological Review* 85, 97-177.

Fenwick, J.C., Bonga, S.E.W., Flik, G., 1999. In vivo bafilomycin-sensitive Na^+ uptake in young freshwater fish. *The Journal Experimental Biology* 202, 3659-3666.

Froese, R., Pauly D., 2012. Fish Base. World Wide Web electronic publication, www.fishbase.org, version 08/2012.

Galvez, F., Reid, S.D., Hawkings, G., Goss, G.G., 2002. Isolation and characterization of mitochondria-rich cell types from the gill of freshwater rainbow trout. *American Journal of Physiology – Regulatory, Integrative and Comparative Physiology* 282, R658-R668.

Galvez, F., Tsui, T., Wood, C.M., 2008. Cultured trout gill epithelia enriched in pavement cells or in mitochondria-rich cells provides insights into Na^+ and Ca^{2+} transport. *In Vitro Cell Development Biology – Animal* 44, 415-425.

Galvez, F., Wong, D., Wood, C.M., 2006. Cadmium and calcium uptake in isolated mitochondria rich cell populations from the gills of the freshwater rainbow trout. *American Journal of Physiology – Regulatory, Integrative and Comparative Physiology* 291, R170-R176.

Garcia-Romeu, F., Maetz J.,1964. The mechanism of sodium and chloride uptake by the gills of freshwater fish, *Carassius auratus*. I. Evidence for an independent uptake of sodium and chloride ions. *Journal of General Physiology* 47, 1195-1207.

Gonzalez, R. J., Wilson, R. W., Wood, C. M., Patrick, M. L., Val, A. L., 2002. Diverse strategies for ion regulation in fish collected from the ion-poor, acidic Rio Negro. *Physiological and Biochemical Zoology* 75, 37-47**.**

Goss, G.G., Adamia, S., Galvez, F., 2001. Peanut lectin binds to a subpopulation of mitochondria-rich cells in the rainbow trout gill epithelium. *American*

Journal of Physiology – Regulatory, Integrative and Comparative Physiology 281, R1718-R1725.

Goss, G., Gilmour, K., Hawkings, G., Brumbach, J.H., Huynh, M., Galvez, F., 2011. Mechanism of sodium uptake in PNA negative MR cells from rainbow trout, *Oncorhynchus mykiss* as revealed by silver and copper inhibition. *Comparative Biochemistry and Physiology A* 159, 234-241.

Goss, G.G., Laurent, P., Perry, S.F., 1992. Evidence for a morphological component in acid-base regulation during environmental hypercapnia in the brown bullhead (*Ictalurus nebulosus*). *Cell and Tissue Research* 268, 539-552.

Goss, G.G., Laurent, P., Perry, S.F., 1994. Gill morphology during hypercapnia in brown bullhead (*Ictalurus nebulosus*) - role of chloride cells and pavement cells in acid-base regulation. *Journal of Fish Biology* 45, 705-718.

Goss, G., Orlowski, J., Grinstein, S., 1996. Coimmunoprecipitation of a 24-kDa protein with NHE1, the ubiquitous isoform of the Na^+/H^+ exchanger. *American Journal Physiology* 270, C1493-502.

Goss, G.G., Orr, E.E., Katoh, F., 2005. Characterization of SLC26 anion exchanger in rainbow trout. *Comparative Biochemistry and Physiology A – Molecuar and Integrative Physiology* 141, S197-S197.

Goss, G.G., Wood, C.M., 1990a. Na^+ and Cl^- uptake kinetics, diffusive effluxes and acidic equivalent fluxes across the gills of rainbow trout. 1. Responses to environmental hyperoxia. *Journal of Experimental Biology* 152, 521-547.

Goss, G.G., Wood, C.M., 1990b. Na^+ and Cl^- uptake kinetics, diffusive effluxes and acidic equivalent fluxes across the gills of rainbow trout. 2. Responses to bicarbonate infusion. *Journal of Experimental Biology* 152, 549-571.

Griffith, R.W., 1974. Environment and salinity tolerance in the genus *Fundulus*. *Copeia* 1974, 319-1331.

Grunder, S., Geissler, H.S., Bassler, E.L., Ruppersberg, J.P., 2000. A new member of acid-sensing ion channels from pituitary gland. *Neuroreport* 11, 1607-1611.

Harvey, B.J., 1992. Energization of sodium absorption by the H^+-ATPase pump in mitochondria-rich cells of frog skin. *Journal of Experimental Biology* 172, 289-309.

Hirata, T., Kaneko, T., Ono, T., Nakazato, T., Furukawa, N., Hasegawa, S., Wakabayashi, S., Shigekawa, M., Chang, M.-H., Romero, M. F., Hirose, S., 2003. Mechanism of acid adaptation of a fish living in a pH 3.5 lake. *American Journal of Physiology - Regulatory Integrative and Comparative Physiology* 284, R1199-R1212.

Hiroi, J., McCormick, S.D., 2012. New insight into gill ionocyte and ion transporter function in euryhaline and diadromous fish. *Respiratory Physiology and Neurobiology* 184: 257-268.

Hiroi, J., McCormick, S.D., Ohtani-Kaneko, R., Kaneko, T., 2005. Functional classification of mitochondrion-rich cells in euryhaline Mozambique tilapia (*Oreochromis mossambicus*) embryos, by means of triple immunofluorescence staining for Na^+/K^+-ATPase, $Na^+/K^+/2Cl(^-)$ cotransporter and CFTR anion channel. *Journal of Experimental Biology* 208, 2023-2036.

Hiroi, J., Yasumasu, S., McCormick, S.D., Hwang, P.P., Kaneko, T., 2008. Evidences for an apical Na^+-Cl^- cotransporter involved in ion uptake in a teleost fish. *Journal of Experimental Biology* 211, 2584-2599.

Hobe, H., Laurent, P., McMahon, B.R., 1984. Whole body calcium flux rate in freshwater teleosts as a function of ambient calcium and pH levels: A comparison between the euryhaline trout, *Salmo gairdneri* and stenohaline bullhead, *Ictalurus nebulosus*. *Journal of Experimental Biology* 113, 237-252.

Holzer, P., 2009. Acid-sensitive ion channels and receptors. *Handbook of Experimental Pharmacology* 194, 283-332.

Hootman, S.R., Philpott, C.W., 1978. Rapid isolation of chloride cells from pinfish gill. *The Anatomical Record: Advances in Integrative Anatomy and Evolutionary Biology* 190, 687-702.

Horng, J.L., Hawng, P.P., Shin, T.H., Wen, Z.H., Lin, C.S., Lin, L.Y., 2009. Chloride transport in mitochondrion-rich cells of euryhaline tilapia (*Oreochromis mossambicus*) larvae. *American Journal of Physiology - Cell Physiology* 297, C845-C854.

Horng, J.L., Lin, L.Y., Huang, C.J., Katoh, F., Kaneko, T., Hwang, P.P., 2007. Knockdown of V-ATPase subunit A (atp6v1a) impairs acid secretion and ion balance in zebrafish (*Danio rerio*). *American Journal of Physiology – Regulatory, Integrative and Comparative Physiology* 292, R2068-R2076.

Hwang, P.P., 2009. Ion uptake and acid secretion in zebrafish (*Danio rerio*). *The Journal of Experimental Biology* 212, 1745-1752.

Hwang, P.P., Lee, T.H., 2007. New insights into fish ion regulation and mitochondrion-rich cells. *Comparative Biochemistry and Physiology A* 148, 479-497.

Hwang, P.P., Lee, T.H., Lin, L. Y., 2011. Ion regulation in fish gills: recent progresses in the cellular and molecular mechanisms. *American Journal of Physiology – Regulatory, Integrative and Comparative Physiology* 301, R28-R47.

Hwang, P.P., Perry, S.F., 2010. Ionic and acid-base regulation. In: Perry, S.F., Ekker, M., Farrell, A.P., Brauner, C.J. (Eds.), Fish Physiology, vol. 29. Zebrafish. Academic Press, San Diego.

Hung, C.Y.C., Tsui, K.N.T., Wilson, J.M., Nawata, C.M., Wood, C.M., Wright, P.A., 2007. Rhesus glycoprotein gene expression in the mangrove killifish *Kryptolebias marmoratus* exposed to elevated environmental ammonia levels and air. *The Journal of Experimental Biology* 210, 2419-2429.

Hyde, H., Perry, S.F., 1987. Acid-base and ionic regulation in the American eel (*Anguilla rostrata*) during and after prolonged aerial exposure: Branchial and renal adjustments. *The Journal of Experimental Biology* 133, 429-437.

Immke, D. C., McCleskey, E. W., 2003. Protons open acid-sensing ion channels by catalyzing relief of Ca^{2+} blockade. *Neuron* 37, 75-84.

Inokuchi, M., Hiroi, J., Watanabe, S., Hwang, P.P., Kaneko, T., 2009. Morphological and functional classification of ion-absorbing mitochondria-rich cells in the gills of Mozambique tilapia. *The Journal of Experimental Biology* 212, 1003-1010.

Inokuchi M., Hiroi, J., Watanabe, S., Lee, K.M., Kaneko, T., 2008.Gene expression and morphological localization of NHE3, NCC and NKCC1a in branchial mitochondria-rich cells of Mozambique tilapia (*Oreochromis mossambicus*) acclimated to a wide range of salinities. *Comparative Biochemistry and Physiology* A 151, 151-158.

Ito, Y., Kato, A., Hirata, T., Hirose, S. and Romero, M. F., 2014. Na^+/H^+ and Na^+/NH_4^+ exchange activities of zebrafish NHE3b expressed in *Xenopus* oocytes. *American Journal Physiology- Regulatory and Integrative Comparative Physiology.* 306, R315-R327.

Ivanis, G., Esbaugh, A J., Perry, S. F., 2008. Branchial expression and localization of SLC9A2 and SLC9A3 sodium/hydrogen exchangers and their possible role in acid-base regulation in freshwater rainbow trout (*Oncorhynchus mykiss*). *The Journal of Experimental Biology* 211, 2467-2477.

Jasti, J., Furukawa, H., Gonzales, E.B., Gouaux, E., 2007. Structure of acid-sensing ion channel 1 at 1.9A resolution and low pH. *Nature* 449, 316-323.

Kasahara, M., 2007. The 2R hypothesis: an update. *Current Opinion in Immunology* 19, 547-552.

Jonz, M.G., Nurse, C.A., 2006. Epithelial mitochondria-rich cells and associated innervation in adult and developing zebrafish. *Journal of Comparative Neurology* 497, 817-832.

Jonz, M.G., Nurse, C.A., 2008. New developments on gill innervation: insights from a model vertebrate. *The Journal of Experimental Biology* 211, 2371-2378.

Katoh, F., Cozzi, R.R.F., Marshall, W.S., Goss, G.G., 2008. Distinct $Na^+/K^+/2Cl^-$ cotransporter localization in kidneys and gills of two euryhaline species, rainbow trout and killifish. *Cell and Tissue Research* 334, 265-281.

Katoh, F., Hasegawa, S., Kita, J., Takagi, Y., Kaneko, T., 2001. Distinct seawater and freshwater types of chloride cells in killifish, *Fundulus heteroclitus*. *Canadian Journal of Zoology* 79, 822-829.

Katoh, F., Hyodo, S., Kaneko, T., 2003. Vacuolar-type proton pump in the basolateral plasma membrane energizes ion uptake in branchial mitochondria-rich cells of killifish Fundulus heteroclitus, adapted to a low ion environment. *The Journal of Experimental Biology* 206, 793-803.

Katoh, F., Kaneko, T., 2003. Short-term transformation and long-term replacement of branchial chloride cell in killifish transferred from seawater to freshwater, revealed by morphofunctional observations and newly established "time-differential double fluorescent staining" technique. *The Journal of Experimental Biology* 206, 4113-4123.

Kellenberger, S., 2008. Epithelial Sodium and Acid-sensing Ion Channels. In: *Sensing with ion channels*. Martinac B: *Springer Series in Biophysics* 11, chapt.11, p. 225-246

Kellenberger, S., Schild, L., 2002. Epithelial sodium channel/degenerin family of ion channels: A variety of functions for a shared structure. *Physiological Reviews* 82, 735-767.

Kellenberger, S., Schild, L., 2015. International Union of Basic and Clinical Pharmacology. XCI. Structure, Function, and Pharmacology of Acid-Sensing Ion Channels and the Epithelial Na^+ Channel. *Pharmacological Reviews* 67, 1-35.

Kerstetter, T.H., Kirschner, L.B., 1972. Active chloride transport by gills of rainbow trout (*Salmo gairdnerii*). *The Journal of Experimental Biology* 56, 263-272.

Kerstetter, T.H., Kirschner, L.B., Rafuse, D.D., 1970. On mechanisms of sodium ion transport by irrigated gills of rainbow trout (*Salmo gairdneri*). *Journal of General Physiology* 56, 342-359.

Keys, A., Willmer, E.N., 1932. "Chloride secreting cells" in the gills of fishes, with special reference to the common eel. *Journal of Physiology - London* 76, 368-378.

Killifish Genome Annotation Workshop and Meeting, 2012. Mount Desert Islands Biological Laboratory (www.mdibl.org/courses/Killifish_Genome_Annotation_Workshop_and_Meeting/439/).

Kim, Y.H., Kwon, T.H., Frische, S., Kim, J., Tisher, C.C., Madsen, K.M., Nielsen, S., 2002. Immunocytochemical localization of pendrin in intercalated cell subtypes in rat and mouse kidney. *American Journal of Physiology – Renal Physiology* 283, F744-F754.

Kimmel, C. B., Ullmann, B., Walker, M., Miller, C. T., Crump, J.G., 2003. Endothelin 1-mediated regulation of pharyngeal bone development in zebrafish. *Development* 130, 1339-1351.

Kirschner, L.B., 2004. The mechanism of sodium chloride uptake in hyperregulating aquatic animals. *The Journal of Experimental Biology* 207, 1439-1452.

Kleyman, T.R., Cragoe, E.J., 1988. Amiloride and its analogs as tools in the study of ion-transport. *Journal of Membrane Biology* 105, 1-21.

Krogh, A., 1938. The active absorption of ions in some freshwater animals. *Zeitschrift fur Vergleichende Physiologie* 25, 335-350.

Kumai, Y., Bernier, N.Y., Perry, S.F., 2014. Angiotensin-II promotes Na^+ uptake in larval zebrafish, *Danio rerio*, in acidic and ion-poor water. *Journal of Endocrinology* 220, 195-205.

Kumai, Y., Bahubeshi, A., Steele, S.L., Perry, S.F., 2011. Strategies for maintaining Na^+ balance in zebrafish (*Danio rerio*) during prolonged exposure to acidic water. *Comparative and Biochemical Physiology A* 160: 52-62.

Kumai, Y., Nesan, D., Vijayan, M.M, Perry, S.F., 2012. Cortisol regulates Na^+ uptake in zebrafish, Danio rerio, larvae via the glucocorticoid receptor. *Molecular and Cellular Endocrinology* 364, 113-125.

Kumai, Y., Perry, S.F., 2011. Ammonia excretion via Rhcg1 facilitates Na^+ uptake in larval zebrafish *Danio rerio*, in acidic water. *American Journal of Physiology –Regulatory, Integrative and Comparative Physiology* 301, R1517–R1528.

Kwong, R.W.M., Perry, S.F.,2013. The tight junction protein claudin-b regulates epithelial permeability and sodium handling in larval zebrafish, *Danio rerio*. *American Journal of Physiology- Regulatory and Integrative Comparative Physiology* 304, R504-R513.

Laurent, P., Chevalier, C., Wood, C.M., 2006. Appearance of cuiboldal cells in relation to salinity in gills of *Fundulus heteroclitus*, a species exhibiting Na^+ but not Cl^- uptake in freshwater. *Cell and Tissue Research* 325, 481-492.

Laurent, P., Dunel, S., 1980. Morphology of gill epithelia in fish. *American Journal of Physiology – Regulatory, Integrative and Comparative Physiology* 238, R147-R159.

Laurent, P., Perry, S.F., 1991. Environmental effects on fish gill morphology. *Physiological Zoology* 64, 4-25.

Lawrence, C., 2011. Advances in Zebrafish Husbandry and Management. *Methods in Cell Biology*. 104, 431-451.

Lee, T.H., Hwang, P.P., Lin, H.C., Huang, F.L., 1996. Mitochondria-rich cells in the branchial epithelium of the teleost, *Oreochromis mossambicus*, acclimated to various hypotonic environments. *Fish Physiology and Biochemistry* 15, 513-523.

Lee, T.H., Hwang, P.P., Shieh, Y.E., Lin, C.H., 2000. The relationship between 'deep-hole' mitochondria-rich cells and salinity adaptation in the euryhaline teleost, *Oreochromis mossambicus*. *Fish Physiology and Biochemistry* 23, 133-140.

Lee, Y.C., Yang, J.J., Cruze, S., Horng, J.L., Hwang, P.P., 2011. Anion exchanger 1b, but not sodium-bicarbonate cotransporter 1b, plays a role in transport functions of zebrafish H^+-ATPase-rich cells. *Americal Journal of Physiology - Cell Physiology* 300, C295-307.

Lehir, M., Kaissling, B., Koeppen, B. M. and Wade, J. B., 1982. Binding of peanut lectin to specific epithelial cell types in kidney. *American Journal of Physiology – Cell Physiology* 242, C117-C120.

Levanti, M.B., Guerrera, M.C., Calavia, M.G., Ciriaco, E., Montalbano, G., Cobo, J., Germana, A., Vega, J.A., 2011. Acid-sensing ion channel 2 (ASIC2) in the intestine of adult zebrafish. *Neuroscience Letters* 494, 24-28.

Liao, B.K., Chen, R.D., Hwang, P.P., 2009. Expression regulation of Na^+-K^+-ATPase alpha1-subunit subtypes in zebrafish gill ionocytes. *American Journal of Physiology – Regulatory, Integrative and Comparative Physiology* 296, R1897-R1906.

Liao, B.K., Deng, A.N., Chen, S.C., Chou, M.Y., Hwang, P.P., 2007. Expression and water calcium dependence of calcium transporter isoforms in zebrafish gill mitochondrion-rich cells. *BMC Genomics* 8, 354.

Lin, H., Randall, D. J., 1990. The effect of varying water pH on the acidification of expired water in rainbow trout. *The Journal of Experimental Biology* 149, 149-160.

Lin, H., Randall, D.J., 1991. Evidence for the presence of an electrogenic proton pump on the trout gill epithelium. *The Journal of Experimental Biology* 161, 119-134.

Lin, L.Y., Horng, J.L., Kunkel, J.G., Hwang, P.P., 2006. Proton pump-rich cell secretes acid in skin of zebrafish larvae. *American Journal of Physiology - Cell Physiology* 290, C371-C378.

Lin, L.Y., Liao, B.K., Horng, J.L., Yan, J.J., Hsiao, C.D., Hwang, P.P., 2008. Carbonic anhydrase 2-like a and 15a are involved in acid-base regulation and Na^+ uptake in zebrafish H^+-ATPase-rich cells. *American Journal of Physiology - Cell Physiology* 294, C1250-C1260.

Maetz, J., Garcia-Romeu F.G., 1964. The mechanism of sodium and chloride uptake by the gills of a fresh-water fish, *Carassius auratus*. *Journal of General Physiology* 47, 1209-1226.

Marshall, W.S., 2002. Na^+, Cl^-, Ca^{2+}, and Zn^{2+} transport by fish gills: retrospective review and prospective synthesis. *Journal of Experimental Zoology* 293, 264-283.

Marshall, W.S., Bryson, S.E., Burghardt, J.S., Verbost, P.M., 1995. Ca^{2+} transport by opercular epithelium of the fish water adapted euryhaline teleost, *Fundulus heteroclitus*. *Journal of Comparative Physiology B: Biochemical, Systemic, and Environmental Physiology* 165, 268-277.

Marshall, W.S., Bryson, S.E., Darling, P., Whitten, C., Patrick, M., Wilkie, M., Wood, C.M., Buckland- Nicks, J., 1997. NaCl transport and ultrustructure of opercular epithelium from freshwater-adapted euryhaline teleost, *Fundulus heteroclitus*. *Journal of Experimental Zoology* 277, 23-37.

McCormick, S.D., Hasegawa, S., Hirano, T., 1992. Calcium uptake in the skin of a freshwater teleost. *Proceedings of the National Academy of Sciences* 89, 3635-3638.

Nakada, T., Hoshijima, K., Esaki, M., Nagayoshi, S., Kawakami, K. and Hirose, S., 2007. Localization of ammonia transporter Rhcg1 in mitochondrion-rich cells of yolk sac, gill, and kidney of zebrafish and its ionic strength-dependent

expression. *American Journal of Physiology – Regulatory, Integrative and Comparative Physiology* 293, R1743-53.

Nawata, C.M., Hung, C.C.Y., Tsui, T.K N., Wilson, J.M., Wright, P.A., Wood, C.M., 2007. Ammonia excretion in rainbow trout (*Oncorhynchus mykiss*): evidence for Rh glycoprotein and H^+-ATPase involvement. *Physiological Genomics* 31, 463-474.

Pan, T.C., Liao, B.K., Huang, C.J., Lin, L.Y., Hwang, P.P., 2005. Epithelial Ca^{2+} channel expression and Ca^{2+} uptake in developing zebrafish. *American Journal of Physiology – Regulatory, Integrative and Comparative Physiology* 289, R1202-R1211.

Panopoulou, G., Poustka, A.J., 2005. Timing and mechanism of acient vertebrate genome duplications – the adventure of a hypothesis. *Trends in Genetics* 21, 559-567.

Parks, S.K., Tresguerres, M., Galvez, F., Goss, G.G., **2010.** Intracellular pH regulation in isolated trout gill mitochondrion-rich (MR) cell subtypes: Evidence for Na^+/H^+ activity. *Comparative Biochemistry Physiology A* 155, 139-145.

Parks, S.K., Tresguerres, M., Goss, G.G., 2007. Interactions between Na^+ channels and Na^+-HCO_3^- cotransporters in the freshwater fish gill MR cell: a model for transepithelial Na^+ uptake. *American Journal of Physiology - Cell Physiology* 292, C935-C944.

Parks, S.K., Tresguerres, M., Goss, G.G., 2008. Theoretical considerations underlying Na^+ uptake mechanisms in freshwater fishes. *Comparative Biochemistry and Physiology C* 148, 411-418.

Patrick, M.L., Part, P., Marshall, W.S., Wood, C.M., 1997. Characterization of ion and acid-base transport in the fresh water adapted mummichog (*Fundulus heteroclitus*). *Journal of Experimental Zoology* 279, 208-219.

Patrick, M.L., Wood C.M., 1999. Ion and acid-base regulation in the freshwater mummichog (*Fundulus heteroclitus*): a departure from the standard model for freshwater teleosts. *Comparative Biochemistry and Physiology* A 122, 445-456.

Paukert, M., Chen, X., Polleichtner G., Schindelin, H., Grunder, S., 2008. Candidate amino acids involved in H^+ gating of acid-sensing ion channel 1a. *Journal of Biological Chemistry* 283, 572-581.

Paukert, M., Sidi, S., Russell, C., Siba, M., Wilson, S.W., 2004. A family of acid-sensing ion channels from zebrafish: widespread expression in the central nervous system suggests a conserved role in neuronal communication. *Journal of Biological Chemistry* 279, 18783-18791.

Payan, P., Mayer-Gostan, N., Pang, P.K.T., 1981. Site of calcium uptake in the fresh water trout gill. *Journal of Experimental Zoology Part A – Ecological Genetics and Physiology* 216, 345-347.

Perry, S.F., 1997. The Chloride Cell: Structure and function in the gill of freshwater fish. *Annual Review of Physiology* 59, 325-347

Perry, S.F., Flick, G., 1988. Characterization of branchial transepithelial calcium fluxes in freshwater trout (*Salmo gairdneri*). *American Journal of Physiology* 254, R491-R498.

Perry, S.F., Goss G.G., 1994. The effects of experimentally altered gill chloride cell - surface area on acid base regulation in rainbow trout during metabolic alkalosis. *Journal of Comparative Physiology* B 164, 327-336.

Perry, S.F., Goss, G.G., Laurent, P., 1992. The interrelationships between gill chloride cell morphology and ionic uptake in four freshwater teleosts. *Canadian Journal of Zoology* 70, 1775-1786.

Perry, S.F., Randall, D.J., 1981. Effects of amiloride and SITS on branchial ion fluxes in rainbow trout, *Salmo gairdneri*. *Journal Experimental Zoology* 215, 225-228.

Perry, S.F., Shahsavarani, A., Georgalis, T., Bayaa, M., Furimsky, M., Thomas, S.L.Y., 2003. Channels, pumps, and exchangers in the gill and kidney of freshwater fishes: Their role in ionic and acid-base regulation. *Journal of Experimental Zoology A* 300, 53-62.

Perry, S.F., Vulesevic, B., Bayaa, M., 2009. Evidence that SLC26 anion transporters mediate branchial chloride uptake in adult zebrafish (*Danio rerio*). *American Journal of Physiology – Regulatory, Integrative and Comparative Physiology* 297, R988-997.

Perry, S.F., Wood, C.M., 1985. Kinetics of branchial calcium uptake in the rainbow trout: effects of acclimation to various external calcium levels. *Journal of Experimental Biology* 116, 411-433.

Pisam, M., Caroff, A., Rambourg, A., 1987. 2 types of chloride cells in the gill epithelium of a fresh water adapted euryhaline fish *Lebistes reticulatus* - their modifications during adaptation to saltwater. *American Journal of Anatomy* 179, 40-50.

Pisam, M., Massa, F., Jammet, C., Prunet, P., 2000. Chronology of the appearance of beta, A, and alpha mitochondria-rich cells in the gill epithelium during ontogenesis of the brown trout (*Salmo trutta*). *The Anatomical Record* 259, 301-311.

Pisam, M., Rambourg, A., 1991. Mitochondria-rich cells in the gill epithelium of teleost fishes - an ultrastructural approach. *International Review of Cytology* 130, 191-232.

Pitts, R. F., 1973. Production and excretion of ammonia in relation to acid–base regulation. In: Handbook of Physiology, Renal Physiology Washington, DC: American Physiology Society. (ed. J. Orloff and R. W. Berliner), 455–496.

Preest, M.R., Gonzales, R.J., Wilson, R.W., 2005. Pharmacological examination of Na^+ and Cl^- transport in two species of freshwater fish. *Physiological and Biochemical Zoology* 78, 259-272.

Reid, S.D., Hawkings, G.S., Galvez, F., Goss, G.G., 2003. Localization and characterization of phenamil-sensitive Na^+ influx in isolated rainbow trout gill epithelial cells. *The Journal of Experimental Biology* 206, 551-559.

Reilly, R.F., Ellison, D.H., 2000. Mammalian distal tubule: physiology, pathophysiology, and molecular anatomy. *Physiological Reviews* 80, 277-313.

Renfro, J.L., 1975. Water and ion transport by the urinary bladder of the teleost *Pseudopleuronectes americanus*. *American Journal of Physiology* 228, 52-61.

Sakai, H., Lingueglia, E., Champigny, G., Mattei, M. G., Lazdunski, M., 1999. Cloning and functional expression of a novel degenerin-line Na^+ gene in mammals. *Journal of Physiology* 519, 323-333.

Scott, G.R., Claiborne, J.B., Edwards, S.L., Schulte, P.M. and Wood, C.M., 2005a. Gene expression after freshwater transfer in gills and opercular epithelia of killifish: insight into divergent mechanisms of ion transport. *The Journal of Experimental Biology* 208, 2719-2729.

Scott, G.R., Keir, K.R., Schulte, P.M., 2005b. Effects of spironolactone on gene expression and cell proliferation after fresh water transfer in the euryhaline killifish. *Journal of Comparative Physiology* B 175, 499-510.

Scott, W.B., Crossman, E.J., 1998. Freshwater fishes of Canada. Galt House Publications Ltd, Oakville, Ontario.

Shahsavarani, A., McNeill, B., Galvez, F., Wood, C.M., Goss, G.G., Hwang, P.P., Perry, S.F., 2006b. Characterization of a branchial epithelial calcium channel (ECaC) in freshwater rainbow trout (*Oncorhynchus mykiss*). *The Journal of Experimental Biology* 209, 1928-1943.

Shahsavarani, A., Perry, S.F., 2006a. Hormonal and environmental regulation of epithelial calcium channel in gill or rainbow trout (Oncorhynchus mykiss). *American Journal of Physiology – Regulative, Integrative and Comparative Physiology* 291, R1490-R1498.

Shih, T.H., Horng, J.L., Hwang, P.P., Lin, L.Y., 2008. Ammonia excretion by the skin of zebrafish (*Danio rerio*) larvae. *American Journal of Physiology – Cell Physiology* 295, C1625-C1632.

Shih, T.H., Horng, J.L., Liu, S.T., Hwang, P.P., Lin, L.Y., 2012. Rhcg1 and NHE3b are involved in ammonium-dependent sodium uptake by zebrafish larvae acclimated to low-sodium water. *American Journal of Physiology - Regulative, Integrative and Comparative Physiology* 302, R84-R93.

Smith, H., 1932. Water regulation and its evolution in fishes. *The Quarterly Review of Biology* 7, 1-26.

Springauf, A., Grunder, S., 2010. An acid-sensing ion channel from shark (*Squalus acanthias*) mediates transient and sustained responses to protons. *Journal of Physiology* 588, 809-820.

Spry, D.J., Wood, C.M., 1985. Ion flux rates, acid-base status, and blood gases in rainbow trout, *Salmo gairdneri*, exposed to toxic zinc in natural soft water. *Canadian Journal of Fisheries and Aquatic Science* 42, 1332-1337.

Sullivan, G.V., Fryer, J.N., Perry, S.F., 1996. Immunolocalization of proton pumps (H^+-ATPase) in pavement cells of rainbow trout gill. *The Journal of Experimental Biology* 198, 2619-2629.

Tresguerres, M., Katoh, F., Orr, E., Parks, S.K., Goss, G.G., 2006. Chloride uptake and base secretion in freshwater fish: A transepithelial ion-transport metabolon? *Physiological and Biochemical Zoology* 79, 981-996.

Tresguerres, M., Parks, S.K., Katoh, F., Goss, G.G., 2006. Microtubule-dependent relocation of branchial V-H^+-ATPase to the basolateral membrane in the Pacific spiny dogfish (*Squalus acanthias*): a role in base secretion. *The Journal Experimental Biology* 209, 599-609.

Tseng, D.Y., Chou, M.Y., Tseng, Y.J., Hsiao, C.D., Huang, C.J., Kaneko, T., Hwang, P.P., 2009. Effects of stanniocalcin 1 on calcium uptake in zebrafish (*Danio*

rerio) embryo. *American Journal of Physiology – Regulative, Integrative and Comparative Physiology* 296, R549-R557.

Vega, G.C., Wiens, J.J., 2012. Why are there so few fish in the sea? *Proceedings of Royale Society B* 279, 2323-2329.

Verbost, P.M., Bryson, S.E., Wendelaar Bonga, S.E., Marshall, W.S., 1997. Na^+-dependent Ca^{2+} uptake in isolated opercular epithelium of *Fundulus heteroclitus*. *Journal of Comparative Physiology B: Biochemical, Systemic, and Environmental Physiology* 167, 205-212.

Vina, E., Parisi, V., Cabo, R., Laura, R., Lopez-Velasco, S., Lopez-Muniz, A., Garcia-Suarez, O., Germana, A., Vega, J.A., 2013. Acid-sensing ion channels (ASICs) in the taste buds of adult zebrafish. *Neuroscience Letters* 536, 35-40.

Wang, Y.F., Tseng, Y C., Yan, J.J., Hiroi, J., Hwang, P.P., 2009. Role of SLC12A10.2, a Na-Cl cotransporter-like protein, in a Cl uptake mechanism in zebrafish (*Danio rerio*). *American Journal of Physiology – Regulative, Integrative and Comparative Physiology* 296, R1650-R1660.

Waldmann, R., Champigny, G., Bassilana, F., Voilley, N., Lazdunski, M., 1995. Molecular cloning and functional expression of a novel amiloride-sensitive Na^+ channel. *Journal of Biological Chemistry* 270, 27411-27414.

Waldmann, R., Lazdunski, M., 1998. H^+-gated cation channels: Neuronal acid sensors in the NaC/DEG family of ion channels. *Current Opinion in Neurobiology* 8, 418-424.

Westerfield, M., 2000. The zebrafish book. A guide for the laboratory use of zebrafish (*Danio rerio*). University of Oregon Press.

Wilson, J.M., Laurent, P., Tufts, B.L., Benos, D. J., Donowitz, M., Vogl, A.W. and Randall, D.J., 2000. NaCl uptake by the branchial epithelium in freshwater teleost fish: An immunological approach to ion-transport protein localization. *The Journal of Experimental Biology* 203, 2279-2296.

Wong, C.K.C., Chan, D.K.O., 1999. Isolation of viable cell types from the gill epithelium of Japanese eel Anguilla japonica. *American Journal of Physiology – Regulatory, Integrative and Comparative Physiology* 276, R363-R372.

Wood, C.M., Laurent, P., 2003. Na^+ versus Cl^- transport in the intact killifish after rapid salinity transfer. *Biochemica et Biophysica Acta (BBA) – Biomembranes* 1618, 106-119.

Wood, C.M., Marshall, W.S., 1994. Ion balance, acid-base regulation, and chloride cell function in the common killifish, *Fundulus heteroclitus*, a euryhaline estuarine teleost. *Estuaries* 17, 34-52.

Wood, C.M., Randall, D.J., 1973. Sodium balance in rainbow-trout (*Salmo-gairdneri*) during extended exercise. *Journal of Comparative Physiology* 82, 235-256.

Wood, C.M., Wheatly, M.G., Hobe, H., 1984. The mechanism of acid-base and ionoregulation in the freshwater rainbow trout during environmental hyperoxia and subsequent normoxia. III. Branchial exchanges. *Respiration Physiology* 55, 175-192.

Wright, P.A., Wood, C.M., 2009. A new paradigm for ammonia excretion in aquatic animals: role of Rhesus (Rh) glycoproteins. *The Journal of Experimental Biology* 212, 2303-2312.

Wu, S.C., Horng, J.L., Liu, S.T., Hwang, P.P., Wen, Z.H., Lin, C.S., Lin, L.Y., 2010. Ammonium-dependent sodium uptake in mitochondrion-rich cells of medaka (*Oryzias latipes*) larvae. *American Journal of Physiology - Cell Physiology* 298, C237–C250.

Yan, J.J., Chou, M.Y., Kaneko, T., Hwang, P.P., 2007. Gene expression of Na^+/H^+ exchanger in zebrafish H^+-ATPase-rich cells during acclimation to low-Na^+ and acidic environments. American Journal of Physiology- Cell Physiology 293, C1814-C1823.

Zhang, P., Sigworth, F. J., Canessa, C. M., 2006. Gating of acid-sensing ion channel-1: release of Ca^{2+} block vs. allosteric mechanism. *Journal of General Physiology* 127, 109-117.